UNDERSTANDING NETWORK DYNAMICS IN FLOODING EMERGENCIES FOR URBAN RESILIENCE

A Dissertation

by

CHAO FAN

Submitted to the Office of Graduate and Professional Studies of
Texas A&M University
in partial fulfillment of the requirements for the degree of

DOCTOR OF PHILOSOPHY

Chair of Committee,	Ali Mostafavi
Committee Members,	John Taylor
	Xia Hu
	Damnjanovic Ivan
	Stephanie Paal
Head of Department,	Robin Autenrieth

December 2020

Major Subject: Civil Engineering

ABSTRACT

Many cities around the world are exposed to extreme flooding events. As a result of rapid population growth and urbanization, cities are also likely to become more vulnerable in the future and subsequently, more disruptions would occur in the face of flooding. Resilience, an ability of strong resistance to and quick recovery from emergencies, has been an emerging and important goal of cities. Uncovering mechanisms of flooding emergencies and developing effective tools to sense, communicate, predict and respond to emergencies is critical to enhancing the resilience of cities. To overcome this challenge, existing studies have attempted to conduct post-disaster surveys, adopt remote sensing technologies, and process news articles in the aftermath of disasters. Despite valuable insights obtained in previous literature, technologies for real-time and predictive situational awareness are still missing. This limitation is mainly due to two barriers. First, existing studies only use conventional data sources, which often suppress the temporal resolution of situational information. Second, models and theories that can capture the real-time situation is limited.

To bridge these gaps, I employ human digital trace data from multiple data sources such as Twitter, Nextdoor, and INTRIX. My study focuses on developing models and theories to expand the capacity of cities in real-time and predictive situational awareness using digital trace data. In the first study, I developed a graph-based method to create networks of information, extract critical messages, and map the evolution of infrastructure disruptions in flooding events from Twitter. My second study proposed and tested an

online network reticulation theory to understand how humans communicate and spread situational information on social media in response to service disruptions. The third study proposed and tested a network percolation-based contagion model to understand how floodwaters spread over urban road networks and the extent to which we can predict the flooding in the next few hours. In the last study, I developed an adaptable reinforcement learning model to leverage human trace data from normal situations and simulate traffic conditions during the flooding. All proposed methods and theories have significant implications and applications in improving the real-time and predictive situational awareness in flooding emergencies.

DEDICATION

This work is dedicated to my family.

ACKNOWLEDGEMENTS

In completing this dissertation, I experienced many challenges such as confusion about the directions of my research, difficulties of learning new knowledge, and helplessness due to paper rejections. I would not have overcome these obstacles and finished my dissertation without the guidance, support and love of my faculty advisors, family, and friends. First and foremost, I would like to deeply thank my Ph.D. advisor, Professor Ali Mostafavi. Ali has been an exceptional advisor and a sincere friend. I have been very grateful to receive his guidance for the three and a half years of my Ph.D. journey. Ali gave me extremely visionary advice, the most generous support, and the most constructive feedback. His research foresight, dedication to high-impact research, and commitment to the students have become the base of my accomplishments and will have a long-term impact on my future academic career.

I would also give my sincere thanks to Professor John Taylor. I met Professor Taylor at the CRC conference in my first year. I was encouraged by him to pursue research in smart city digital twin and submit a paper to HICSS-53. Because of this conversation, I had the chance to learn Professor Taylor's brilliant thinking and professional expertise. Since that, I have had a couple of meetings with Professor Taylor at some conferences and communication on some papers. He offered me invaluable advice and support for my research and academic career development, which is a treasure for me.

I would also thank Professor Xia Hu. I have had an opportunity to work with Professor Hu throughout my Ph.D. He has a wide knowledge of interesting computational

problems and has provided me with very helpful advice on relevant courses and research methodologies. I learned from him how to identify a computational problem and develop a small and nice idea to tackle such a problem. Discussion with Professor Hu often spawned many research sparks.

I would like to appreciate Professor Ivan Damnjanovic and Professor Stephanie Paal. It has been an honor to receive their insightful and constructive comments and feedback on my research. Their enthusiasm for impactful research and profound knowledge greatly motivated me to make my research distinguishable.

I was fortunate to be surrounded by many wonderful and intelligent friends and colleagues inside and outside Texas A&M University. I would like to thank my friends and lab mates in the Urban Resilience.AI lab: Yucheng Jiang, Xiangqi Jiang, Yang Yang, Fangsheng Wu, Bora Oztekin, Ronald Lee, Jiayi Shen, Miguel Esparza, Ramchandani Ankit, Zhang Cheng, Jennifer Dargin, and Wenlin Yao. It was a great pleasure working together with you all. Thanks also go to the department faculty and staff for making my time at Texas A&M University a great experience.

Last but not least, I would give my deep and quiet gratitude to my family, Mom and Dad. I have always been remembering your encouragement and supports, which become my pillars when I had difficulties and even pain. I cannot have my current accomplishments without your love.

CONTRIBUTORS AND FUNDING SOURCES

Contributors

This work was supervised by a dissertation committee consisting of Professors Ali Mostafavi, Ivan Damnjanovic and Stephanie Paal of the Department of Civil and Environmental Engineering, Professor Xia Hu of the Department of Computer Science and Engineering at Texas A&M University, and Professor John Taylor of the School of Civil and Environmental Engineering at Georgia Institute of Technology.

Funding Sources

Graduate study was supported by a graduate research assistantship from Texas A&M University and research funds from National Science Foundation (NSF).

This work was also made possible in part by National Science Foundation under Grant Number IIS-1759537, CMMI-1846069, and CMMI-1832662; and Amazon Web Services (AWS) Machine Learning Award. Its contents are solely the responsibility of the authors and do not necessarily represent the official views of the National Science Foundation and Amazon Web Services.

TABLE OF CONTENTS

LIST OF FIGURES

Page

LIST OF TABLES

Page

CHAPTER I

INTRODUCTION

"Never let a good crisis go to waste."

- Winston Churchill (1940)

1.1 Problem Statement

Globally, over seven hundred thousand people lost their lives, over 1.4 million were injured, and approximately 23 million were made homeless as a result of emergencies in the past ten years (UNISDR, 2015). A critical factor causing human and property loss in emergencies is the large-scale infrastructure disruptions in the built environment (Lu et al., 2018). The National Academy of Engineering (NAE) in the United States has defined a global challenge, "restore and improve urban infrastructure." They aim to globally bring the researchers, engineers, and society to address current innovative and technological challenges worldwide, including effective responses to infrastructure disruptions in emergencies (National Academy of Engineering, 2004). The effectiveness of emergency response not only depends on the resilience of infrastructure systems itself, but also is greatly associated with the performance of humans and existing technologies such as the comprehensiveness of situational awareness, the efficiency of risk communication, and accuracy of situation prediction (Y. Kryvasheyeu et al., 2016).

Situational awareness including the temporal unfolding and geographical distribution of disruptive events can inform the public, first responders, local government

and other stakeholders about the response strategies such as resource allocation and transportation (Sutton et al., 2015). Hence, comprehensive and timely awareness of on-going situations in emergencies is essential for effective emergency response (Department of Homeland Security, 2008). The problem that exists in situational awareness is the difficulties in answering questions such as "where disruptions are occurring" and "how much relief is needed" at the time of an emergency. The problem is usually caused by the rapid evolution of the situation and data scarcity (Kumar et al., 2014). With the wide use of smartphones and social media sites, situational information is often posted and recorded by humans on digital platforms (Rosser et al., 2017). The massive human-generated data provides a unique opportunity for tracking and monitoring the situation in emergencies to inform decision making (Wang and Ye, 2018). Over the past decade, researchers have been attempted to explore the utility and values of human-generated data for situational awareness. However, existing techniques for getting insights from these digital trace data are mainly token-based methods, which investigated the frequency distribution of words and phrases and extracted the events or topics by grouping discrete words together (McMinn et al., 2013). The credibility and meaning of such collections of words are ambiguous and would confuse people who use these techniques. Hence, getting credible and non-ambiguous information is a great challenge in existing studies, especially in the context of unfolding temporal and spatial evolution of emergencies.

In addition to the cyber informatics techniques to get a sense of the situation, online social networks also play an important role in amplifying the transmission of risk information in emergencies. Unlike traditional broadcast information channels such as

radio and television which may be limited by time and space constraints, online social networks allow people to communicate with others from anywhere over the world without time constraints. Hence, risk communication in online social networks enables messages to reach individuals beyond the sender's direct contacts, increasing exposure and potentially leading to lifesaving actions (Sutton et al., 2015). This phenomenon extensively presents in emergencies due to the high demand for information by people at risk for sense making. However, the emergency situation is dynamic and evolving rapidly over time, which may influence the properties and performance of online social networks in risk communication and collective sense-making (Fischer-Preßler et al., 2019). Existing literature is limited to data collected under normal and stationary circumstances, capturing the regular social networks (Bagrow et al., 2011). However, efficient risk communication requires quantitative and dynamic features of the online social networks when the population encounters unfamiliar conditions. This highlights the need of understanding underlying relationships between disruptive events, user activities and network reticulation, with particular attention on social connections and mixing patterns in the networks. Such an understanding can inform evidence-based strategies to improve information communication in online social networks under emergent conditions.

Finally, with the comprehensive awareness of the situation in emergencies, the next critical step is to think ahead and predict the situation in near future. In particular, the urban road network plays an important role in emergency response, provision of essential services, and maintenance of economic well-being (Ganin et al., 2017). Disruptions of road segments will significantly reduce the capabilities of road networks in transporting

relief resources and people evacuation. In times of hurricanes and flooding, urban road networks are susceptible to floodwaters, meaning that flooding tends to spread on road networks over time and space (Paprotny et al., 2018). Developing effective and efficient response strategies essentially relies on the estimation and prediction of flood propagation in road networks. Hence, there is a real need for tools to forecast flood situations in road networks and assist emergency response to road disruptions. Multiple studies (Wang et al., 2019) have been conducted to explore the spatial-temporal properties of floodwaters in urban networks, including hydrodynamic models and machine learning techniques. However, the performance of hydraulic models often relies on various types of hydro-geomorphological monitoring datasets and intensive computation (Guan and Chen, 2018). Due to delay and computational cost, these models may not be able to provide timely and reliable predictions for the spatial-temporal spread of floodwaters in road networks. Although existing machine learning methods requiring fewer types of input data can complement the hydraulic models, these models are limited due to their dependence on large sets of historical data for model training (Tsakiri et al., 2018). In addition, existing machine learning models are designed to capture only the propagation of floodwaters in urban areas. The flood recession process, which is also critical for assessing the resilience of urban networks, is often ignored by existing machine learning models (Mosavi et al., 2018). Hence, bridging this critical methodological gap is to develop a tool that can be simply implemented to provide a timely and fairly accurate prediction of flooding propagation and recession in urban road networks.

1.2 Research Objectives

The overarching goal of this study is to improve urban resilience in coping with flooding emergencies by analyzing human dynamics with integrated human and artificial intelligence. In particular, this study aims to enhance real-time and predictive situational awareness using information retrieval techniques, understanding collective-sense making, and developing prediction tools based on human digital trace data. Through detection and prediction, people at risk can better respond to adverse impacts of flooding. To attain this overarching goal, this research will accomplish three specific objectives:

Objective 1: Develop techniques that can automatically detect and map the situations in the built environment from human digital trace data in emergencies;

Objective 2: Understand the underlying mechanisms of risk communication and collective-sense making in online social networks in the face of service disruptions;

Objective 3: Develop predictive methods that can model and predict physical disruptions and human mobility in emergencies.

1.3 Research Questions

While existing studies have developed tools for detecting flooding situations and unveiled insightful properties of online social networks for information spread, the tools and findings are limited for applications in emergency response and urban resilience. That is because existing tools for situation detection can only generate coarse-grained results using geotagged data that only accounts for a small proportion of the entire dataset. In addition, prior communication theories in existing studies cannot capture the interactions

between the human and physical environment, which do not apply to examine the dynamics of online social networks in emergencies for information spread. Finally, existing predictive methods tend to rely on an extensive set of situational data and take significant computational cost, which may not be able to predict the situation promptly. With these limitations in prior studies, a key research question that has not been addressed with depth is: to what extent do human digital traces can inform, spread and predict the situations in emergencies? Human-generated data on mobile apps during the occurrences of emergencies provides us with an unprecedented opportunity to detect, understand and predict situations in flooding to save human lives and protect properties at risk.

To address the knowledge and methodological gaps raised by the key research question, this research seeks answers for the following three important questions:

Question 1: What situational information can be retrieved from social media for capturing the spatial and temporal evolution of situations in flooding?

Question 2: To what extent do physical disruptions trigger the dynamics of online social networks for risk communication and collective sense-making in service disruption?

Question 3: To what extent can the physical disruptions (e.g., road conditions and human trajectories in emergencies) be predicted using human digital trace data?

1.4 Research Methodology

To address these research questions, my Ph.D. study specifically focuses on the human digital trace data generated during emergencies to retrieve information, understand the patterns, and predict the situations in a short time period. Per these needs, my studies

are in three major directions, aiming to use and develop tools from artificial intelligence, communication theories, and mathematical modeling to explore the capabilities of digital trace data for real-time and predictive situational awareness in flooding emergencies (see Figure 1).

In my first effort, I developed a method to first identify the bursts of the relevant tweets during environmental disruptions. Then, natural language processing techniques such as word embedding are adopted to convert the tweets to vectors. Furthermore, I employed network metrics, weighted degree centrality, from network science to identify the critical tweets in the semantic networks. I defined multiple parameters in the methods and conducted multiple analyses to map and examine the evolution of the situation from social media data in Hurricane Harvey.

My second effort studied the mechanisms of risk communication among affected populations on social media under the context of physical environment disruptions. I adopted the communication theory, network reticulation theory, and further extend the theory to adapt the characteristics of online social networks. This theoretical approach enables us to capture the impacts of environmental disruptions on human behaviors on social media. In addition, I also adopted network metrics including network assortativity to quantify the mixing patterns of online social networks and its evolution over time.

The third effort adopted a mathematical model from epidemiology and applied math to model the flood propagation and recession in urban road networks. The proposed method integrated the differential equation systems and network percolation process that allows us to predict the changes in the magnitude and locations of flooded road segments

efficiently. The predictive approach can be used as an early warning system to inform the public and decision-makers with effective response strategies and policies.

In the final study, I developed an adaptable reinforcement learning model to learn the human mobility patterns from mobile phone data in normal conditions and simulate the traffic condition in emergencies. The proposed model aims to maximize the cumulative rewards by choosing the destination and route that are most closed to the empirical traces. Using the situational data during flooding, the models are allowed to modify the reward table accordingly so that we can expand the capacity of the model to capture the movements of the population in flooding. The application of the model has been demonstrated in a case study of the 2017 Hurricane Harvey. The results from applications show very good performance of the proposed models.

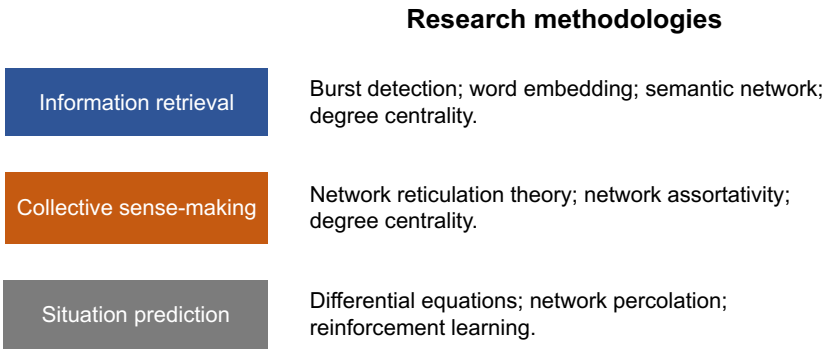

Figure 1 Research methodologies.

1.5 Dissertation Structure

The results presented in this dissertation follow the "four journal paper" format. Chapters 2, 3, 4 and 5 are each crafted to act as a document publishable in a peer-reviewed

academic journal. The structure of this dissertation, the overarching research question that served as the basis for my general academic exploration that corresponds to specific chapters in this dissertation are outlined in Figure 2.

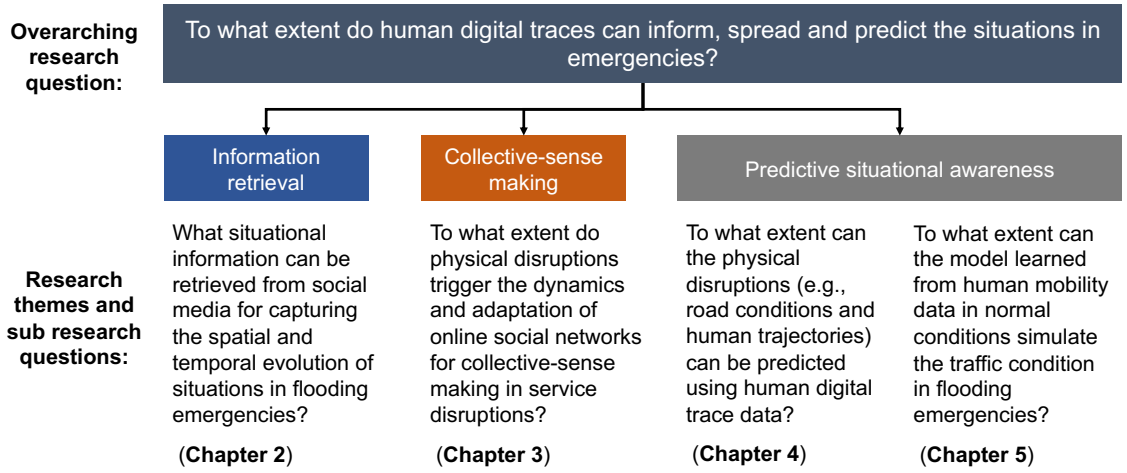

Figure 2 Structure of the dissertation.

In Chapter 2, the first paper presents a graph-based method for detecting disruptions and analyzing evolutions of the situation about critical infrastructure. This chapter includes details about the mathematical definitions and the programming steps, and also presents a case study of Hurricane Harvey in 2017 in Houston. The results highlight the capabilities of the proposed method of detecting credible situational information and capturing the temporal and spatial patterns of infrastructure disruptions. The article was co-authored with Dr. Ali Mostafavi and was published in the *Computer-aided Civil and Infrastructure Engineering* (Fan and Mostafavi, 2019a).

In Chapter 3, I propose a network reticulation theoretical framework to examine the dynamic relationships among triggering events, human activities on social media, and

network reticulation. The results of this study uncover the importance of weak social tiles bridging online communities for collective sense-making in emergencies. The article was co-authored with Dr. Mostafavi and was published in the *Journal of Royal Society Interface* (Chao Fan et al., 2020b).

In Chapter 4, I develop and test a mathematical model for predicting the spatial spread and temporal evolution of the onset and recession of floodwaters in urban road networks. The model captures the situation of flooding with three parameters: propagation rate, incubation rate, and recovery rate. Integrating with the network percolation process, the model can not only predict the temporal evolution of flooding in urban road networks, but also the spatial spread of flooded road segments. The article was co-authored with Dr. Ali Mostafavi and was published in *Scientific Reports* (Chao Fan et al., 2020a).

In Chapter 5, I create and test an adaptive reinforcement learning model that can predict the destinations of movements, estimate the trajectory for each origin and destination pair, and examine the impact of perturbations on humans' decisions related to destinations and movement trajectories. The application of the proposed model in Hurricane Harvey shows that the model can perform very well in predicting traffic patterns and congestions resulting from urban flooding. The article presented in this chapter has been submitted to a peer-reviewed journal and is under-review now.

CHAPTER II

CREDIBLE INFORMATION EXTRACTION FROM SOCIAL MEDIA FOR SITUATIONAL AWARENESS IN DISASTERS[*]

Damages in critical infrastructure occur abruptly, and disruptions evolve with time dynamically. Understanding the situation of critical infrastructure disruptions is essential to effective disaster response and recovery of communities. Although the potential of social media data for situation awareness during disasters has been investigated in recent studies, the application of social sensing in detecting disruptions and analyzing evolutions of the situation about critical infrastructure is limited. To address this limitation, this study developed a graph-based method for detecting credible situation information related to infrastructure disruptions in disasters. The proposed method was composed of data filtering, burst time-frame detection, content similarity calculation, graph analysis, and situation evolution analysis. The application of the proposed method was demonstrated in a case study of Hurricane Harvey in 2017 in Houston. The findings highlighted the capability of the proposed method in detecting credible situational information and capturing the temporal and spatial patterns of critical infrastructure events that occurred in Harvey, including disruptive events and their adverse impacts on communities. The proposed methodology can improve the ability of community members, volunteer

[*] This chapter is reprinted with permission from "A graph-based method for social sensing of infrastructure disruptions in disasters." by Fan, C., and Mostafavi, A., 2019. *Computer-Aided Civil and Infrastructure Engineering*. Dec;34(12):1055-70.

responders, and decision makers to detect and respond to infrastructure disruptions in disasters.

2.1 Introduction

Situational awareness about evolving and life-threatening impacts of natural disasters like hurricanes, wildfires, and earthquakes is crucial for effective disaster response and recovery (Yury Kryvasheyeu et al., 2016; Lu and Brelsford, 2014). A key component of a community is critical infrastructure systems, the damages and failures of which will make severe impacts on human systems (Kadri et al., 2014; Kim et al., 2018) and physical environment (Lu et al., 2018).

The situations of critical infrastructure in disasters change over time due to disruptions and cascading failures. For example, overflow of flood control reservoirs can cause the water level of rivers to rise, and consequently inundate roads and destroy bridges. In response to disasters, first responders and other stakeholders require near real-time situational information as the disaster unfolds (Kim et al., 2018; Troy et al., 2008). Usually, physical and remote sensing techniques (e.g., satellite and unmanned aerial vehicle platforms) are primary approaches for collecting infrastructure data in normal situations and disasters (Chen et al., 2017; Hackl et al., 2018; Jongman et al., 2015). While regional or federal stakeholders may have the access to multiple accurate sources about the status of critical information, local stakeholders such as community members, volunteer responders, relief organizations, residents do not have access to the accurate local data about infrastructure disruptions. In addition, using other sources of information such as

satellite data, decision-makers can examine the spatial distribution of flooding of streets; however, detailed information regarding the local disruptions (e.g., whether a certain road is passible) and also community impacts (e.g., access to critical facilities is disrupted due to flooding of a certain road) cannot be obtained at local level. Besides, satellite data is expensive, only accessible to a few stakeholders, and suitable for regional situation monitoring. Alternatively, humans (as sensors on social media) share information about disaster situations, including critical infrastructure disruptions (Huang et al., 2017; Nik-Bakht and El-diraby, 2016). Hence, the information obtained via social sensing methodology complements the information from physical sensing in three ways: (1) the detected information is free and accessible to the public including relief organizations, volunteer responders, community members, and other various stakeholders; (2) the detected information, such as power outage, road damage, and water release is at local scale and difficult to be detected by physical sensors; and (3) the information obtained via this approach also informs about the impacts of disruptions on communities. Accordingly, this information can help decision-makers and residents better understand the unfolding of events, gather information about the impacts, and respond to the events.

Recent studies (Arthur et al., 2018; Li and Zhang, 2018; Long et al., 2011) have highlighted the importance and applications of social sensing in detecting relevant events and understanding the situation for disaster response and recovery. Social sensing is a technique for collecting and analyzing social posts which deliver online users' observations and sentiments regarding their physical environment. For example, Scollon (2013) developed an analytics method for urban crisis management covering human

emotion mapping and behavior analysis in response to Singapore Haze on social media (Scollon, 2013). Scollon's study only focused on human networks and their mutual communications. Another example of social sensing for disaster response investigated the dynamics of social networks and the formation and evolution of online communities in the 2011 Japanese Earthquake and Tsunami (Lu and Brelsford, 2014). This study processed the content of social posts and provided insights for understanding how patterns of human interaction evolved due to external attacks. Another stream of studies (Fohringer et al., 2015; Yury Kryvasheyeu et al., 2016) related to social sensing focus on flood inundation maps leveraging the geo-coordinates and inundation images in social posts. For example, Fohringer et al. (2015) utilized quantitative data (e.g., water levels and geolocations) derived from images in social posts in disasters to map the inundation area. This approach enables rapid flood mapping, estimation of flood risks, and determination of response actions. However, this approach does not enable detecting events related to infrastructure disruptions (e.g., road closures or power outages) due to flooding.

While the use of social sensing in disasters is growing, little of the existing work focuses on detecting critical infrastructure disruptions. One of the reasons for this limitation is that, in the context of infrastructure disruptions, the output of the methodologies should include the timing and severity of disruptions, effects of disruptions on people, and actions that have been taken to adjust to the disruptions. Thus, to address this methodological limitation, this paper proposed a graph-based method, to detect the situation and corresponding changes of critical infrastructure on social media. A case study related to the situation of critical infrastructure in the Houston area during and after

Hurricane Harvey was conducted to illustrate the feasibility and capability of the proposed method. The application of the proposed method focuses on the functionality of the critical infrastructure such as road closures, power outage, and water supply contamination for communities rather than the structural damages (e.g., road rapture and bridge crack).

2.2 Related Work

Detecting situational information including human activities and physical events on social media in the occurrences of disasters (i.e., event detection) has been investigated in a great number of studies. In a review of the related work, we focused on the approaches that could be applied to large-scale datasets (such as millions of tweets). The existing techniques for event detection include clustering (Alvarez-Melis and Saveski, 2016; Lee et al., 2012), and network analysis (Cordeiro, 2012; Liu et al., 2016; Misra et al., 2017).

Most of the techniques for unspecified event detection from social media data are based on clustering (Becker et al., 2012; Imran et al., 2013). Features such as words and phrases extracted from social posts are the primary objects in the existing clustering processes. For example, Weng and Lee (2011) developed an Event Detection approach which assigns signals to individual words based on their frequencies and applies wavelet analysis on the raw signals to obtain the correlation between the signals (Weng and Lee, 2011). Then, it can cluster the words according to the wavelet-based signals. However, this approach treats each word independently. The identified events are likely to be a group of words associated with different events. Thus, the information related to events detected from this approach cannot be reliable to be used for detecting infrastructure disruptions.

In another study, Pohl, Bouchachia, and Hellwagner (2012) proposed a two-phase clustering approach to identifying individual sub-events within a crisis automatically (Pohl et al., 2012). The first phase uses the geo-referenced data from social posts to locate a sub-event, and then the second phase describes the details of the sub-event by analyzing the images and videos in the social posts. This clustering approach has the potential to detect crisis-related events, but the results are limited to geo-tagged tweets. To detect and categorize significant events, Ritter et al. (2012) developed event categories and classified events based on latent variable models in an open-domain system for Twitter. However, this approach is limited to specific domains (Ritter et al., 2012). Thus, the outcomes of this approach are comparatively generic and cannot identify specific infrastructure disruptions in the context of disasters.

Another stream of the existing studies focuses on event detection on social posts by analyzing graphs or networks (Ahmadlou et al., 2010; Nguyen and Jung, 2017; Palen et al., 2009). However, the majority of the existing graph-based approaches focuses on detecting activities in social networks and did not fully demonstrate the relations between activities of social media users and events. For example, Zhao and Mitra (2007) proposed an approach to detect events by combining text-based clustering, temporal segmentation, and graph cuts in order to construct hierarchical topic clustering and distinguish different events within the same topic (Zhao and Mitra, 2007). The study provided insights into exploring temporal and social information together with text content. However, the results were still token-based, which lacked clear logic among the extracted tokens and failed to comprehensively show the situations. Thus, this approach is limited in improving

situational awareness of specific infrastructure disruptions. Another technique was developed by Wang and Taylor (2018), who explored geographical and semantical dimensions of events from tweets, mapped the semantic network, and ranked the tweets with their importance (Wang and Taylor, 2018). However, the approach can only be applied to geotagged tweets which are very limited in the entire Twitter dataset of a disaster (usually less than 1% of tweets that are geotagged in disasters). In addition, Ipsen et al. (2006) analyzed Google's PageRank which can be used to measure the importance of the nodes. However, this approach did not consider the similarity of the tweets and did not focus on infrastructure situation (Ipsen and Wills, 2006). Another study conducted by Benson (2011) presented a factor-graph model to discover event records from social media feeds (Benson et al., 2011). The output of the model is an event-based clustering of messages, and needs a seed set of example records. As such, it is difficult to explore burst events using this approach without historical data.

Beyond the state-of-the-art event detection techniques, a number of studies (Juffinger et al., 2009; Li and Zhang, 2018) also investigated the credibility of the information retrieved from social media. However, existing approaches for rating credibility of social media posts relied on other sources or labeled data (Castillo et al., 2011). For example, Castillo, Mendoza, and Poblete (2013) proposed a supervised learning approach to determine whether a tweet is credible or not (Castillo et al., 2013). The approach employed crowdsourcing tools to obtain labeled data and then trained the classifier to identify credible tweets. Thus, the approach has limitations in applications with real-time detection and unlabeled data. In another study, Juffinger, Granitzer, and

Lex (2009) compared the quantity structure of a set of blogs to a reference corpus and examined the similarity of each separate blog content with a verified news corpus (Juffinger et al., 2009). Then, a ranking function was derived to sort the blogs by their credibility levels. However, this technique is constrained by the robustness of news corpus.

In summary, existing techniques for event detection on social media data are mainly feature-based methods, which investigated the frequency distribution of words in social media posts and documents and detected the events or topics by grouping discrete words together (McMinn et al., 2013). The credibility and meaning of such collections of words are ambiguous and would confuse people who use these techniques. Hence, getting credible and non-ambiguous information is a great challenge in existing studies, especially in the context of detecting disruptions in critical infrastructure in disasters.

2.3 A Graph-based Method

We propose a Graph-based event detection method as a computational method to identify credible and non-ambiguous situational information regarding infrastructure disruptions on social media. Infrastructure disruptions occur abruptly and evolve over time in disasters. Understanding the situation of critical infrastructure requires time-sensitive and credible information including when disruptions happened, how it affected residents, what caused this disruption and what actions were taken. Twitter as a popular social media platform has 336 million active users and is active in spreading situational information associated with critical infrastructure situation in disasters. In addition, credible information related to high-impact events is often reported and retweeted many times on

Twitter (Yury Kryvasheyeu et al., 2016). Hence, the frequencies of related tweets are supposed to show bursts of events in a short period, and the similarities of a tweet to other tweets can be used to demonstrate the credibility of the situational information in tweets. Accordingly, the underlying premise of the proposed method in this study is to identify and analyze credible tweets that inform us critical infrastructure disruptions and the situational evolutions.

The proposed method includes five steps: data filtering, burst detection, content similarity, critical tweets identification, and infrastructure situational evolution analysis. This study defined critical tweets as the tweets delivering complete and non-ambiguous situational information related to critical infrastructure disruptions in burst time-frames. The input of this method is a complete set of relevant tweets across the entire duration of disasters. One reason for the need of utilizing a complete dataset is that a change in frequency of relevant tweets is a signal indicating infrastructure disruptions because disruptions often result in changes in human behaviors on social media, such as reporting damages and complaining its adverse effects (Weiler et al., 2016; Zhang et al., 2015). In this study, the frequency means the number of relevant tweets posted per hour. Hence, a complete dataset is essential for continuously mapping the frequency change of relevant tweets and identifying signals. The outputs of the graph-based method are critical tweets containing complete situational information about high-impact critical infrastructure disruptions within each detected time-frame. In addition, this method aligns the content of critical tweets with the unfolding of events in disasters to better understand the dynamic

changes in critical infrastructure disruptions and corresponding influences. The details in each step are discussed in the following sections.

2.3.1 Data Filtering and Preprocessing

To understand the situation specific to certain critical infrastructure, the first step is to filter the tweets using specific names of critical infrastructure, or their abbreviations. For example, in the context of Hurricane Harvey in Houston, specific names of infrastructure include "Interstate Highway 10 (1-10 or I10)", "George Bush Airport (IAH)" and "Barker reservoir (Barker)". Relevant tweets will be filtered without any omission, as long as they contain any of those keywords in their texts, no matter the keywords are in hashtags or not, and no matter the tweets are complete or not. This keyword-based searching is implemented to set a strict restriction for data filtering to ensure the completeness of filtered data, which contributes to tagging the tweets and the results with specific infrastructure.

Once the relevant data is filtered, we should preprocess the data before performing content analysis. This is needed since uninformative characters can have adverse effects on the analysis. For example, uninformative characters, such as "is", "I", "!", URL, and "@", if considered elements in tweet vectorization, will lead to an increase in vector dimensions and computational complexity. Such complexity significantly reduces the calculation efficiency and accuracy in content similarity analysis. To alleviate the adverse effects of uninformative words and characters, the filtered data should be preprocessed. The preprocessing approaches that are used commonly in existing studies include lowercase (lower case every letter in the tweet), tokenization (split the tweets as a set of

tokens), stop-words removal (remove some words that commonly appear in other documents), and lemmatization (return the base or dictionary form of a word) (Imran and Castillo, 2015; Zhang et al., 2018). In addition, in this study, we not only use these common preprocessing approaches, but also employ regular expressions to remove the punctuations, URLs, and emojis. After pre-processing is completed, the dataset is ready for graph-based analysis.

2.3.2 Burst Detection of Time-frames

As mentioned earlier, the frequency of relevant tweets indicates the severity and impacts of critical infrastructure disruptions on humans (Buntain et al., 2015). Thus, a burst of frequencies of relevant tweets within a short period can imply a change of situation or a disruption event of critical infrastructure. During a burst period, the frequency of relevant tweets increases significantly, then reaches a peak. Finally, the frequency decreases with the dissipation of adverse effects of a disruption event. High-impact failures of critical infrastructure (such as major road closures, wide-spread power outage, and reservoir overflow) would lead to significant differences in frequencies of associated tweets over time. This step of the proposed method identifies these burst time-frames based on the trend of tweets' frequencies for a specific infrastructure in a disaster.

Prior to a disruption event, the average frequency of relevant tweets related to a specific infrastructure (e.g., a road or bridge) remains within a comparatively low-frequency range. When a disruption occurs, the frequency of tweets related to a specific infrastructure grow abruptly. Based on the understanding of bursts related to certain critical infrastructure on social media, the following equations are derived to calculate a

frequency (Eq. **(1)**) in a certain time period and the average frequency (Eq. **(2)**) prior to a disruption event. The frequency of relevant tweets can be computed as:

$$f(t,S) = \sum_{w \in W} N(w,\ S_t) \quad \textbf{(1)}$$

$$\bar{f}(k,S) = \frac{\sum_{j=1}^{k} f(j,\ S)}{k} \quad \textbf{(2)}$$

where S is a stream of tweets between $t-1$ and t, t is the time slice in hours, w is a relevant tweet, W is a set of relevant tweets, $N(w,\ S_t)$ returns the frequency of token w in the stream S during time slice t. and k is the number of time slices before the events. In Eq. **(2)**, we define the average frequency of relevant tweets $\bar{f}(k,S)$ as the number of relevant tweets in a time slice before the events. This method is an improved extension of an existing technique developed to identify key moments on social media streams from a set of keywords (Buntain et al., 2015). A burst is detected based on the comparison between average frequency and time-slice frequency. Thus, a burst can be identified as:

$$\frac{f(t,\ S)}{\bar{f}(k,\ S)} > \delta \quad \textbf{(3)}$$

where δ is the threshold for burst frequency in social media streams. The value of δ typically ranges from 2 to 15 and is determined by the requirement of precision (Buntain et al., 2015). The larger the value, the more distinguishing the burst frequency in a time slice. There could be cases in which a certain infrastructure component or facility may be rarely or never noticed and discussed on social media, until it is impacted by extreme events causing major disruptions to services. However, the perceived impacts of damage (service disruptions) on users are as important as the damages to components for disaster

response and recovery. For example, the information obtained from social sensing may not inform about damages to a power substation, but rather informs about electricity outages based on impacts on residents (e.g., inability to cook). Hence, the tweets collected and analyzed by the proposed method enable capturing the impacts of service disruptions, as well as damages to infrastructure components and facilities.

In addition, infrastructure disruptions happen abruptly, but the consequent effects tend to take more than one-time slices to dissipate. During that period, people would report a situation (such as power outage) as well as impact information (such as an inability to cook) on social media. Hence, the situation in continuous time slices would be relatively stable (Ebina et al., 2011). To identify the situation and its changes, first, we group the continuous time slices together to form a time-frame. Then, the tweets posted in each time-frame are extracted as a subset. These tweets are considered to describe the same situation for a particular infrastructure disruption (such as inundation of a particular road). The result from this subset can represent the situation in the entire time-frame.

This study filters the relevant tweets within a certain burst time-frame, converts the content of the tweets into vectors, and then calculate the similarity between two vectors as the edge weight. After these steps, the generic graph measures can be implemented on our datasets. While the pace of progression for infrastructure disruption events might be different from generic events, the proposed method enables identifying burst time-frames with unlimited width and numbers, which makes the method fit for different types of events. If an infrastructure disruption event is fast-paced with single burst time-frame, the event is represented by the most critical tweet in the burst time-frame. If the disruptive

event is relatively slower-paced with several burst time-frame, the event is described via several critical tweets in several burst time-frames respectively.

2.3.3 Content Similarity and Graph Mapping

The content in relevant tweets is the key to understand the situation of critical infrastructure disruptions. However, obtaining complete and non-ambiguous information from a large set of tweets is very difficult because of the existence of noise (Atefeh and Khreich, 2013). For example, some tweets only have general and brief descriptions about the situation such as "The road is flooded". Also, some tweets may be spreading misinformation. Hence, to determine credible and complete information, the comparison of contents in tweets is important (Gupta and Kumaraguru, 2012). The similarity of content between tweets posted by different users can indicate the extent of the credibility of the situational information that these tweets deliver (Castillo et al., 2013). To take the credibility of content into account, we integrate content similarity into semantic graphs. The cosine similarity approach can normalize a tweet vector by dividing each of its components by its length. As such, the negative effects of the length of the vector can be eliminated when comparing the similarity of the tweets. The equation for calculating content similarity is computed as (Zhou and Chen, 2014):

$$cos\theta_{ij} = \frac{\overrightarrow{v_i} \cdot \overrightarrow{v_j}}{\|\overrightarrow{v_i}\|\|\overrightarrow{v_j}\|} \quad \textbf{(4)}$$

where $\overrightarrow{v_i}$ and $\overrightarrow{v_j}$ are the vectors of two different tweets. There are multiple well-established methods to convert the list of tokens into vectors. We use one of the most common methods, TF-IDF (i.e., term frequency-inverse document frequency) to obtain numeric

metrics of tweets (Fan et al., 2018). In this study, each tweet is considered as a document, and a tweet is represented based on the frequencies of tokens. The infrastructure-related keywords frequent in each dataset have low weights, while other situation-related words that are not as frequent as infrastructure keywords have high weights in the vector representations. Once vectors of tweets are obtained, we can calculate the content similarity between these tweets using Eq. **(4)**. The results vary from 0 to 1, showing the extent of content similarity between two tweets. The higher the value, the greater the content similarity. Unlike machine learning methods such as recurrent neural networks, cosine similarity does not require massive data for training and tuning parameters.

In semantic graphs, the edges represent the relationships between different nodes. Here, tweets can be considered as nodes, and their content similarity can be exhibited by edges. Thus, we established the undirected weighted semantic graphs G among the tweets. The graph is composed by nodes $v \epsilon V(G)$ and edges $e \epsilon E(G)$. The weights of edges are defined based on the content similarity between two tweets:

$$w(e_k) = \lfloor 10 \times cos\theta_{ij} + 0.5 \rfloor,\ e_k = (v_i, v_j)$$
$$0.2 < cos\theta_{ij} < 0.9 \quad \textbf{(5)}$$

where e_k is one of the edges in graph G, and v_i and v_j are the nodes connected by e_k. $\lfloor x \rfloor$ is the floor function that takes as input a real number x and gives as output the greatest integer less than or equal to x. It should be mentioned that the weights of edges are integers obtained from the integer conversion. As shown in Eq. **(5)**, an edge can be established if the content similarity is greater than 0.2 and smaller than 0.9. If the content similarity is lower than 0.2 between two tweets, it shows that these tweets are quite different, and in

most cases, they are talking about different situations. Therefore, we ignore the relations between these tweets and do not consider the edges between those tweets. In addition, as we discussed earlier, credible tweets tend to be repeated many times by different users. A number of retweets could also be a result of confounding effects of various factors such as credibility, homophily, influence, and novelty (Aral et al., 2009; Vosoughi et al., 2018a). Thus, retweets, the content similarity of which is greater than 0.9, cannot be the unique evidence of the credibility of the tweets. When parsing the retweets, some additional information would be generated automatically in the body of the retweets, such as "RT" showing that it is a retweet, and "@XXX" showing that the retweet is retweeting XXX's tweet. As such, the retweet is not completely same as the original tweets. Based on the results of the experiments, we set the similarity threshold as 0.9. Nevertheless, the retweets can be the supplementary information to show the importance of the information delivered by these tweets. Thus, in the proposed method, we set the weight of the edges between retweets to be the lowest weight (i.e., a value of 2 in our semantic graphs). Once the nodes, edges, and weights are obtained, the semantic graph can be mapped in each time-frame. Such representation provides a simplified model of complex relationships among tweets.

2.3.4 Critical Tweets Identification

Critical tweets are defined as the tweets containing the most complete and non-ambiguous situational information related to certain critical infrastructure disruptions in certain time-frame. In the context of this study, critical tweets have the closest similarity to other tweets. The degree in the semantic graphs represents the similarity of a tweet to other tweets. Thus, a tweet with the highest degree can be considered as the critical tweet.

However, the weights of edges vary depending on the extent of similarity of a tweet to other tweets. A tweet with greater weighted edges should be more critical than a tweet with a few high weighted edges given the same number of low weighted edges. Hence, we defined a weighted degree to take the weights into account:

$$deg_{v_i} = \sum_{e \epsilon v_i \times V} (w(e))^{\alpha} \quad \textbf{(6)}$$

where $v_i \in V(G)$ are the nodes, and α is a parameter that contributes to reducing the impacts of a large number of low weight edges. For example, some tweets contain widely used words (e.g., "flooding", "hurricane", and "help"). Thus, these tweets may connect to many tweets that actually they are talking about totally different situations. To address this issue, the value of α should be greater than 1. Here, the value of α is defined to distinguish the contributions of various weights on the assessment of criticality of the tweets. Through the power operation by α, the edges with high weights would have much larger impacts on the weighted degree of a tweet. As such, the edges with low weights would have fewer impacts on the weighted degree of a tweet. The larger the value of α, the more significant the close similarity between tweets for identifying critical tweets. The definition and implementation of α ensure that the identified critical tweets are more representative than the tweets with a number of low similarities. The semantic comparison and weighted degrees enable the elimination of misinformation (false positive and false negative information) in the results.

It should be noted that there may be multiple discrete components in a semantic graph. It would be possible that a critical tweet is identified from a small component

(rather than a giant component of the network), when a topic is the focus of only a small group of people. To overcome this challenge, we derived an equation by using a weighted degree to identify the giant component in the graph before identifying critical tweets:

$$Max\left\{\Omega(H_k)|\Omega(H_k) = \sum_{v_i \in V(H_k)} deg_{v_i}, H_k \in G\right\} \quad \textbf{(7)}$$

where $H_k \in \{H_1, H_2, \dots, H_n\}$ is a component in the graph G, where the nodes connect to each other within the component and disconnect to the nodes in other components. As shown in Eq. **(7)**, the giant component is obtained from the sum of weighted degrees in a component rather than the size of a component. The weighted degree is the representation of content similarity which emphasizes the criticality and credibility of a tweet. Hence, the giant component in the tweets graph is a collection of tweets with critical and credible information. Then, the critical tweet can be identified in the giant component as:

$$Max\{deg_{v_i}|deg_{v_i}, v_i \epsilon V(H_k)\} \quad \textbf{(8)}$$

As shown in Eq. **(8)**, and also in the definition of critical tweets earlier, there could be a case that more than one tweet has the highest weighted degree. The most common example is retweeted tweets which have the same connections to other tweets as the original tweets. Our method enables to detect all the tweets with the highest weighted degrees and convert them to their original tweets.

2.3.5 Situational Evolution of Critical Infrastructure

Mapping the timing of critical infrastructure disruptions provides a temporal dimension of the disaster situation. Combined the geolocation of critical infrastructure, temporal and spatial information enables identification of potential interdependencies and

co-evolution of critical infrastructure. In this step, thus, the proposed method maps critical infrastructure disruptions in a timeline and performs temporal and spatial analysis to understand the situational evolution of critical infrastructure. In the temporal analysis, there are different important cases that need to be investigated. For example, the tweets discussing the situation of two or more critical infrastructure systems might indicate that these critical infrastructure systems are interdependent or affected by the same impacts. In addition, identifying the geographic proximity of infrastructure is important to assess co-location interdependencies. Disruptions of different critical infrastructure systems may happen or be detected at the same time. Such temporal synchronicity might also indicate interdependencies among these critical infrastructure systems. Hence, detecting such temporal and spatial proximity provides insights into interdependencies among multiple critical infrastructure systems in a disaster. Furthermore, the identified interdependencies and co-evolution are important to develop response actions as a disaster unfolds. In addition, this information can convey the story of critical infrastructure through a disaster to inform mitigation planning in the aftermath of disasters.

2.4 Case Study of Hurricane Harvey

To demonstrate the capabilities of the proposed graph-based method, we conducted a case study of Hurricane Harvey in Houston. Hurricane Harvey, a category four tropical storm landed in Texas from August 25 to August 29 in 2017. Harvey caused significant infrastructure disruptions. For example, more than 200 road sections were closed or flooded, all flights were suspended at Houston Intercontinental Airport System,

and the water level in Addicks and Barker reservoirs reached their maximum capacity, which led to water release from the reservoirs (ENR Editors, 2017). After Hurricane Harvey passed, flooding continued in the affected areas and major roads such as sections of Interstate Highway 10 remained closed.

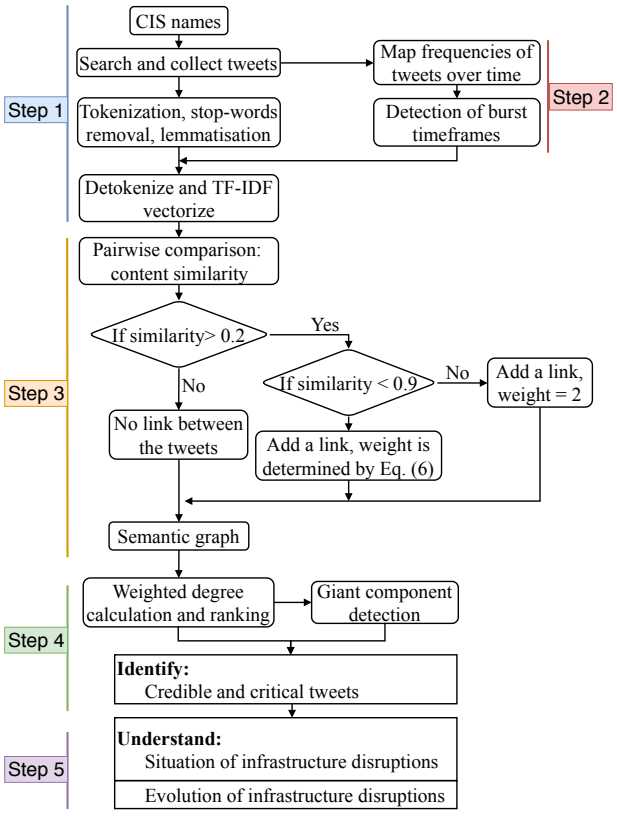

Figure 3 Programming framework for implementation of the graph-based method.

To investigate the impacts of Hurricane Harvey on critical infrastructure in its entire life cycle, we collected around 21 million tweets over the Houston area from August 22 to September 30. This dataset includes all the tweets that posted by users whose profiles have a location of Houston, and the tweets that are geotagged in our predefined bounding

boxes of Houston. People whose profiles mentioned Houston might be in other places. They may or may not comment on the state of infrastructure (e.g., what they learned from news pages or word of mouth). The collection of tweets with localized information about infrastructure is a subset of our total dataset. Hence, the requirement for data collection proposed in this study would need acquiring a complete dataset of tweets with critical situational information and improve the accuracy of our findings.

To implement the graph-based method on this dataset, a programming framework is developed as shown in Figure 3. Once we filter the relevant tweets using relevant keywords, first, we detect the burst time-frames in the dataset based on the temporal information embedded in the tweets and the hourly frequency of the relevant tweets. Then, we tokenize each tweet into a list of separate words and characters, named tokens (Fan and Mostafavi, 2018). Next, we remove some stop-words that are not informative or less than 2 characters and lemmatize the words by grouping together the inflected forms of a word. After that, the remaining words in a tweet will be de-tokenized into a sentence for Term Frequency-Inverse Document Frequency (TF-IDF) vectorization so that computer can compute the similarity of two tweets by comparing the corresponding vectors. Once the similarity between every pair of tweets is calculated, the edges between those tweets can be established and weighted in three conditions using Eq. **(5)**. Finally, we can map the semantic graphs and identify critical tweets using Eq. **(6)**-**(8)**. The output of this method is the critical tweets which contain situational information about the evolution and impacts of critical infrastructure disruptions in disasters, which will be presented in a timeline of the related events (e.g., Figure 7 in the case study).

Table 1 Numbers of collected tweets about each critical infrastructure during investigated period.

Critical infrastructure	Number of tweets
Buffalo Bayou	6595
Addicks and Barker reservoir	14728
Interstate Highway 10	8008
Ben Taub Hospital	1090

2.4.1 Data Filtering and Burst Detection

To understand the performance of critical infrastructure in Harvey, we only need to analyze the data before and during the disaster. Hence, we filter the tweets related to example infrastructure such as Buffalo Bayou, Addicks and Barker reservoirs, Interstate Highway 10 (I10), and Ben Taub Hospital from August 22 to September 4 (because flooding continued until September 4). The numbers of collected tweets associated with each critical infrastructure are listed in Table 1.

Once the relevant datasets are prepared, we could map the frequencies of tweets at the interval of one hour (Figure 4). For example, in Figure 4(b), there is a burst at midnight on August 26 when Hurricane landed in Texas. After that, many bursts appeared on different days because of the rapid changes in the situation of reservoirs and their adverse impacts on nearby residents. In addition, even though different infrastructure (e.g., I10 and reservoirs) in Houston experienced the same extreme weather conditions due to Harvey, the situations and their changes varied. For example, the bursts in frequencies of Interstate

Highway 10 distributed across the entire duration of Hurricane Harvey and subsequent flooding, while Ben Taub Hospital only had bursts at the beginning of Harvey. From the perspective of the magnitude of frequencies, the reservoirs were the most mentioned critical infrastructure because the number of relevant tweets was around 800 per hour. All the bursts shown in Figure 4 were detected by the proposed method. In the following sections, we map the tweets and their relationships into semantic graphs, identify the critical tweets with credible situational information, and further examine how the situation evolved and what potential interdependencies existed between the critical infrastructure detected from our study.

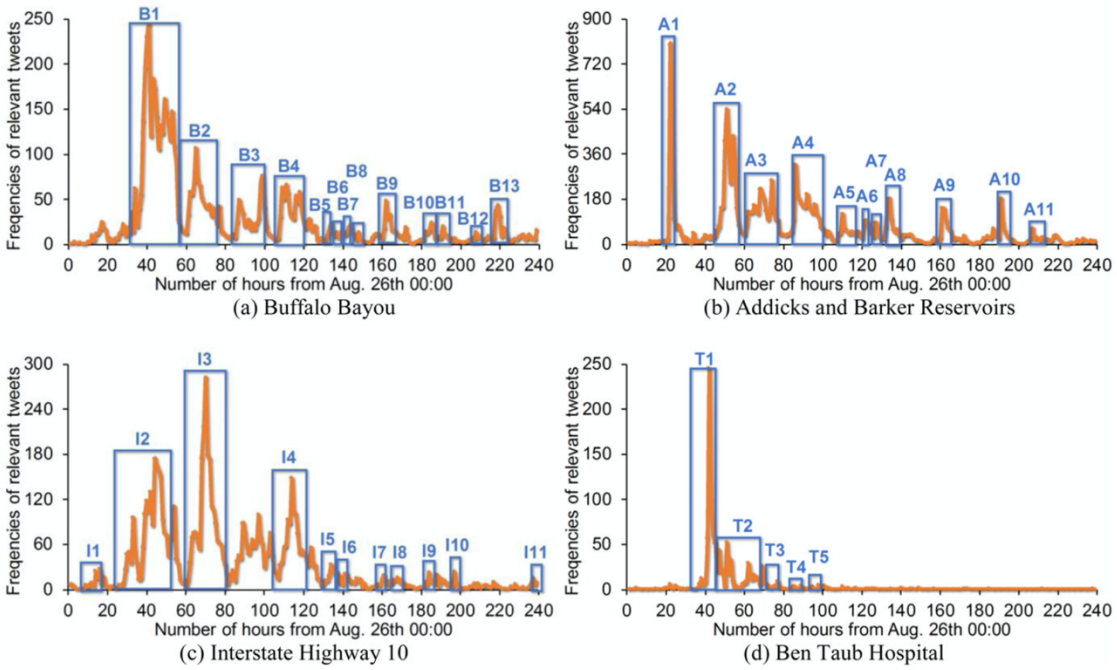

Figure 4 Frequencies of tweets related to investigated critical infrastructure. The horizontal axis is the time point represented by the number of hours from 00:00 on August 26th. The vertical axis is the scale of frequencies.

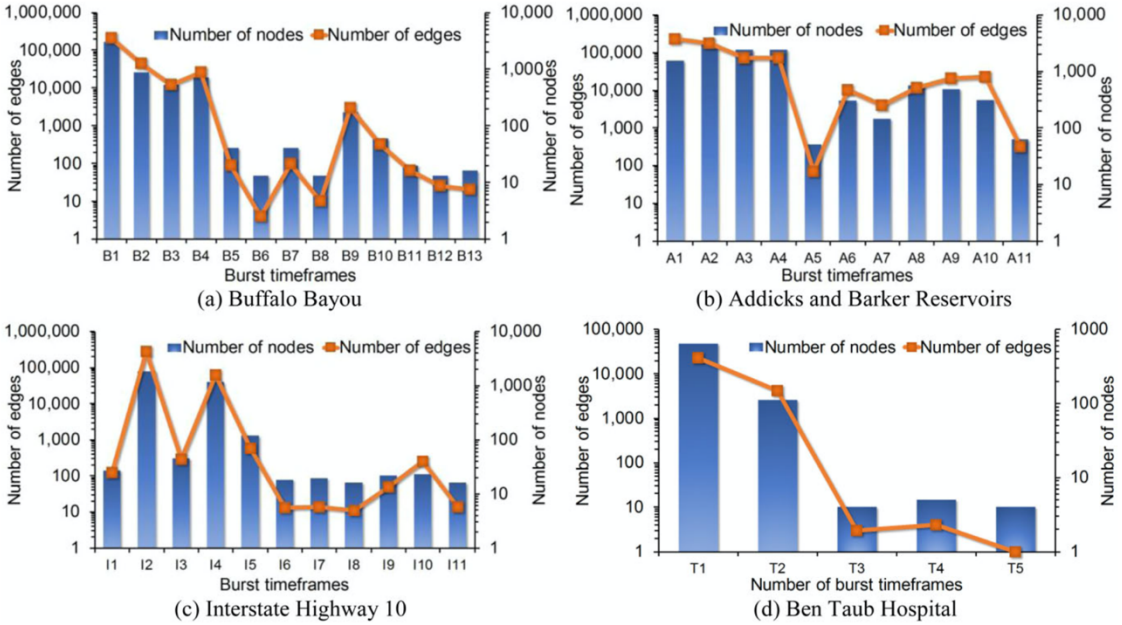

Figure 5 Information about semantic graphs in burst time frames.

2.4.2 Content Similarity and Graph Mapping

The burst time-frames were detected and shown in Figure 5. The spans of the time-frames varied because of the duration of the disruption and the impacts on people. Thus, the numbers of tweets in different time-frames varied as well. For example, the tweets related to Addicks and Barker reservoirs, Buffalo Bayou, and Ben Taub hospital are primarily concentrated in the semantic graphs in the early stage of Hurricane Harvey, while the tweets related to Interstate Highway 10 are primarily concentrated in the semantic graphs in the middle of Hurricane Harvey. Compared to the bursts shown in Figure 4, the detected time-frames were consistent with the crests of the frequencies of relevant tweets.

To implement the content similarity calculation, first, we extracted and grouped the tweets posted in these burst time-frames into clusters. Then, the content similarity calculation was conducted on the vectors of tweets which were converted by TF-IDF. Using Eq. (5), we converted the content similarity to the weights of edges between two tweets. Figure 6 depicts examples of semantic graphs constructed in different burst time-frames related to the four investigated critical infrastructure systems. The weighted degrees vary from 0 to 800, which are distinguished by the intensity of the color and the size of the nodes in all graphs. The coordinates of the nodes are randomly generated by Python code (NetworkX package) and the distance between two connected nodes is only calculated by the number of nodes in a graph ($d = 1/\mathrm{sqrt}(n)$, where n is the number of nodes). Distinctly, there should be only one critical tweet having the closest similarity to other tweets in Figure 6(a), (b), and (c). Meanwhile, a large number of tweets with lower weighted degrees in these graphs can be found as well. These low-degree tweets were associated with the situation of critical infrastructure, but they may not convey informative messages or may not be related to high-impact disruptive events. For example, the content of tweets such as “Reservoir Engineering Technician job at Nearterm Corporation – United States” or “Let's help find man's family guys. He’s at Barker Cypress Rd.” were not recognized as important situational information. Thus, these tweets had low similarities to other tweets and are drawn in small sizes and light colors in our semantic graphs. Furthermore, both Figure 6(a) and (d) have the same pattern that only one or two nodes are significantly larger than other nodes. This finding shows that the situational information in these critical nodes is representative of other nodes, while the information

in other nodes is marginal. However, Figure 6(b) and (c) show a different pattern, the importance of the information in some nodes is very close to the information in the critical nodes. The results indicate that the most important situational information is repeated many times on Twitter. The finding also illustrates the robustness of the proposed method that can capture situational evidence from different patterns on Twitter. The proposed method only extracts the content from the critical node in each graph and map the information based on their temporal stamps in order to provide concise and useful evidence to disaster management teams and other stakeholders.

2.4.3 Critical Tweets Identification and Event Unfolding Analysis

Analyzing temporal and spatial patterns of disruptions is important to understand the evolution of the situation in critical infrastructure. Hence, in this case study, we explore the temporal and spatial patterns from the situational information (Lauw et al., 2005). To this end, we mapped the content of the tweets in a timeline (Figure 7 and Table 2). Based on the detected information, there are two primary patterns of situational evolution for the investigated critical infrastructure during Hurricane Harvey.

One situational evolution pattern among the infrastructure investigated in this study is the interdependency and co-evolution of Buffalo Bayou, Interstate Highway 10, Addicks and Barker reservoirs. According to the identified critical tweets, we deduced the temporal unfolding of events related to Barker and Addicks reservoirs as well as the interaction between reservoirs and other interdependent critical infrastructure. At the beginning of Hurricane Harvey, there was an early warning on social media, which indicated that an extreme weather condition with potential impacts on the reservoirs. Then,

when Harvey landed in Houston, the reservoirs had to release water to eliminate possible breach (dam safety) on August 30. These events led to flooding in nearby neighborhoods (in the downstream of Addicks and Barker reservoirs) and affected other critical infrastructure such as Interstate Highway 10 and Buffalo Bayou. Starting on August 30, Buffalo Bayou continued rising, and the height and flow were updated on Twitter frequently, which indicated the water level increased very fast in Buffalo Bayou during that period. To protect Interstate Highway 10, crews built a temporary dam on this highway on August 31 because water from two reservoirs would swell Buffalo Bayou. Nevertheless, as shown in Figure 7 and Table 2, multiple sections of Highway 10 were closed due to flooding. For example, eastside on Highway 10 in Baytown was closed on August 29. After August 31, Harvey past and water released from reservoirs began to slow down. Water levels in the reservoirs fell, while water levels along Buffalo Bayou were nearly steady or slowly decreasing. Even though mandatory evacuation was still active, some flooded or closed sections on Highway 10 began to reopen. For example, Highway 10 eastbound from Houston to Beaumont was opened on September 2. From the perspective of geographical co-locations, Figure 8 shows the interdependencies among reservoirs, Interstate Highway 10, and Buffalo Bayou. Water released from reservoirs to Buffalo Bayou when the reservoirs reached their capacities. Also, there was uncontrolled outflow from reservoirs affecting nearby neighborhoods and infrastructure (e.g., Highway 10). Then, the water overflowed from Buffalo Bayou and flooded nearby neighborhoods. Such temporal and spatial patterns for the unfolding of events for critical infrastructure systems was detected from our Twitter data using the proposed graph-based method.

Another pattern of situational evolution is the short-term disruption pattern which happen to Ben Taub Hospital during Hurricane Harvey. There might be only one high-impact disruption related to critical infrastructure, and the situation of this disruption may not change significantly over time during the duration of a disaster. For example, in Figure 7 and Table 2, an event that Ben Taub Hospital was flooded and in power outage, was detected on social media on August 27. Patients and staffs in Ben Taub Hospital were evacuated, and the hospital was closed from that moment. In the tweets posted after this event, when people talked about the Ben Taub Hospital, they were discussing the situation in historic flooding and the schedules when the hospital would reopen. Thus, there was only one-time disruption of Ben Taub Hospital. The proposed method is tested in a disaster setting, in which the bursts of the relevant tweets are closely associated with the occurrences of the disruptive events. After disasters pass, the relevant tweets will dissipate subsequently.

Table 2 Situational information about critical infrastructure in disasters (detected on Twitter).

	Situational information from tweets		Situational information from tweets
B1	Buffalo Bayou is out of bank in downtown Houston.	A8	Dams are safe and operating as designed.
B2	More Buffalo Bayou flooding in Houston.	A9	Mayor asking residents w/water in homes to leave.
B3	Buffalo Bayou at Houston TX: Height: 34.11 ft.	A10	Ordering MANDATORY evacuation of West Houston dwellings already flooded.
B4	Buffalo Bayou at Piney Point, TX: Height: 61.98 ft.	A11	Barker is currently at 99.14 ft and falling.
B5	Water from 2 reservoirs will swell Buffalo Bayou; Crews build temporary dam on I-10.	I1	Damage in the Katy area, west of Houston. Along the I-10 feeder between 1463 & Cane Island Parkway.
B6	Buffalo Bayou at Piney Point, TX: Height: 62.81 ft, Flow: 15400 cfs.	I2	Houston Police a viewer in their attic with kids wanted to know if any rescues were planned near I-10 and 59.
B7	Water levels on Buffalo Bayou near Dairy Ashford fluctuationing down a bit.	I3	Closed due to flooding. in #EastSide on I-10 Baytown E Fwy EB between Lockwood and The E Lp.
B8	On Buffalo Bayou, water was in the second floor of the house. We need the releases to slow. Water is still on the 1st floor.	I4	This was I-10 before Harvey. Now it looks like an ocean.
B9	US Army Corps of Engineers says water releases into Buffalo Bayou on west side necessary to avoid larger catastrophe in next rain.	I5	Closed due to flooding. in #WestSide on W Sam Houston Tollway Frontage Rd NB between Westheimer and The I-10 Katy Fwy.
B10	Water levels along Buffalo Bayou nearly steady or slowly falling.	I6	Closed due to flooding. in #Baytown on I-10 Baytown E Fwy Outbound between Sjolander and Hwy 146.
B11	Mandatory evacuation ordered for west Houston residents along Buffalo Bayou, have water in homes by 7am Sunday.	I7	I-10 WB at San Jacinto River is expected to open at some point today,but EB lanes likely to remain closed for now.
B12	Why hasn't the city installed pumps along the Buffalo Bayou to relieve water levels in West Houston.	I8	Road re-opened. frontage roads still closed in #Baytown on I-10 Baytown E Fwy Inbound between Crosby Lynchburg and Magnolia.
B13	Crew has replaced the Buffalo Bayou at Milam Gage, fully operational again… had to replace everything.	I9	I10 eastbound from Houston to Beaumont NOW OPEN!
A1	A possible tornado was reported.	I10	Residents who live between HWY 6 and Gessner, and I10 and Briar Forest ∗with a flooded home∗ are required to evacuate at 7 a.m. Sunday
A2	The release of water from reservoirs has started.	I11	Avoid I-10 W #HOUTraffic. You'll be stuck 25 m longer than usual.
A3	Many shelters have reached capacity.	T1	BREAKING: Ben Taub Hospital being evacuated due to flooding and power outages.
A4	Addicks and Barker dams have NOT breached.	T2	Drone footage shows extensive flooding near Texas Medical Center in Houston.
A5	Crews are getting creative along I-10 to dam up rising water from the Addicks and Barker Reservoir releases.	T3	Memorial Hermann Sugar Land evacuating, Ben Taub plan finally in place #Harvey.
A6	Dams are completely safe and are NOT in danger of failing.	T4	Texas Medical Center hospitals remain operational during historic flooding.
A7	New Mandatory Evacuation for Barker Reservoir Area Communities.	T5	Schedules for Ben Taub, Quentin Mease & LBJ hospitals & all ACS primary care clinics will be decided & announced Wed., Aug. 30.

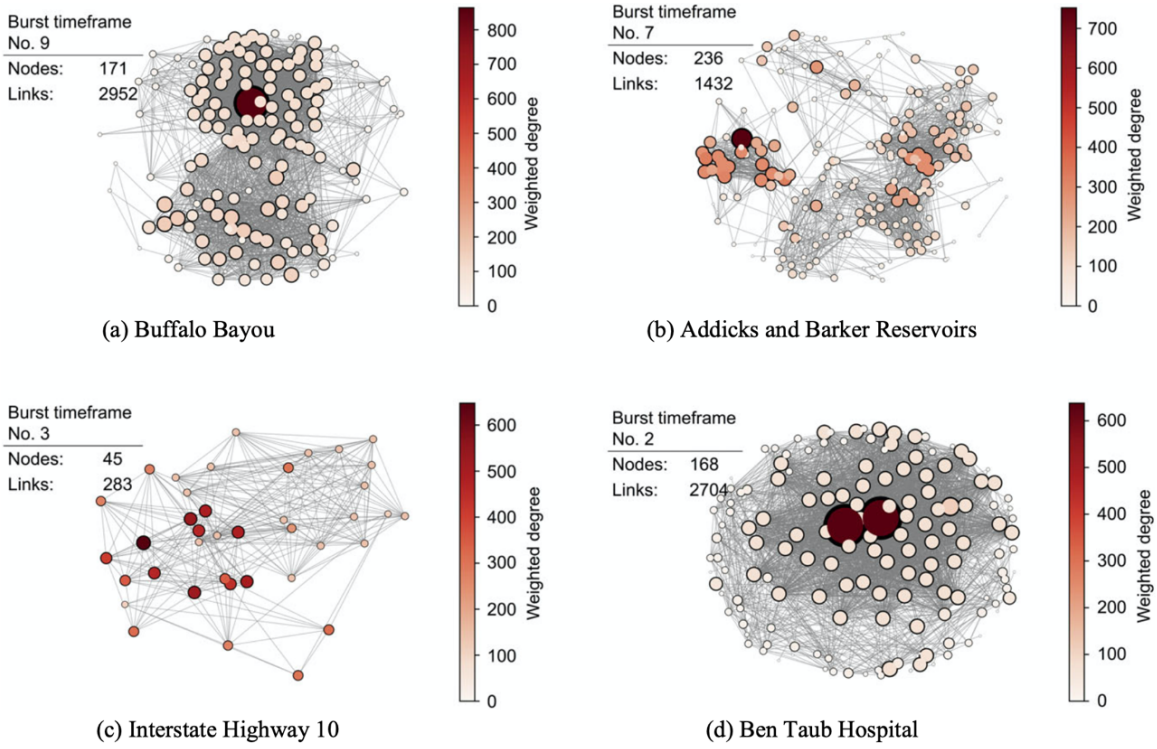

Figure 6 Semantic graphs for critical infrastructure in burst time frames.

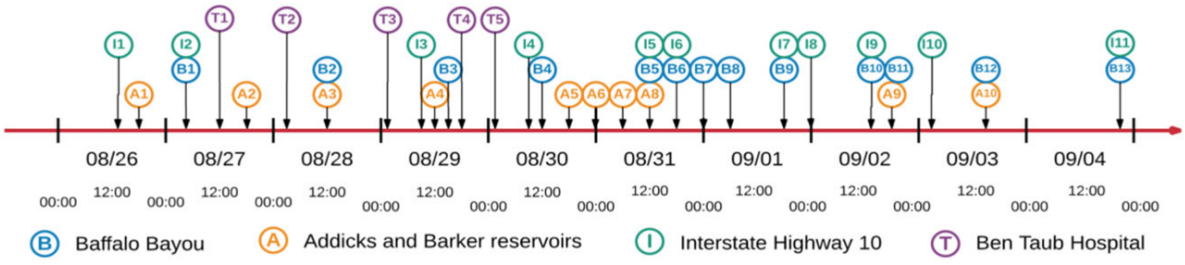

Figure 7 Unfolding of critical infrastructure disruptions detected from Twitter.

2.4.4 Validation

To examine the reliability of our graph-based method and validate the credibility of the identified situational information and detected disruptions, we plotted the weighted

degree distribution on log-log scales for semantic graphs shown in Figure 9 and referred to news articles to validate the content of critical tweets. One reason for plotting the degree distribution in log-log scales is to shrink the scales on axis, which is to respond to skewness towards large weighted degrees in our semantic graphs. As we mentioned earlier, the weighted degree of tweets varies from 0 to 800, and a few tweets are much larger than the bulk of the data. The log-log plot can reduce the skewness caused by this phenomenon. Meanwhile, the log-log plot is beneficial for showing the percent change or multiplicative factors. For example, in Figure 9(b), the number of tweets with the lowest weighted degree is about 10 times the number of tweets with the greatest weighted degree. Thus, the log-log plot can help us to better read the weighted degree distribution and identify the percent change in the number of tweets with different weighted degrees.

Figure 9 shows that the weighted degree distribution of the semantic graphs in burst time-frames is consistent with the intensity of colors and the size of nodes in semantic graphs in Figure 6. The first feature of the weighted degree distributions is that they do not follow any classic probability distribution models. The numbers of certain weighted degree varied dramatically. For example, in Figure 9(a), there are multiple crests appearing along with the increase of weighted degree. However, only one node in a semantic graph can reach the highest weighted degree. This feature exists in Figure 9(a)–(c), which validates the analysis in section 4.2 and the results in section 4.3. However, as shown in Figure 9(d), the count of nodes with the highest weighted degree is two. Our method gathered both tweets and found that these are retweets containing the same

credible and non-ambiguous information as the original tweets. Thus, both tweets and retweets reached the highest weighted degree in the semantic graph.

Furthermore, to demonstrate the credibility of the identified situational information, we examined the content in critical tweets by comparing to recorded information from news articles published in the aftermath of infrastructure disruptions. For example, "*It took Harris County officials until late Sunday, Aug. 27, to begin issuing similar warnings for communities upstream of both Barker and Addicks*." (Olsen, 2018) In addition, "*Reservoir gates were opened on August 28, releasing storm water into Buffalo Bayou*." (Flood Control District, 2017) "*the additional water will flow towards the Sam Houston Tollway, then south to the area around Interstate 10, known as the Katy Freeway and, eventually, Buffalo Bayou, which leads to downtown Houston*." (Fedschun, 2017) This information demonstrated the impacts of released water from reservoirs on highways and Buffalo Bayou, which was identified from our critical tweets. Another news article stated, "*Late Sunday night, local officials issued voluntary evacuation notices for residents around the reservoirs*" (Wax-Thibodeaus et al., 2017) This information can validate that the mandatory evacuation in neighborhoods near the reservoirs. "*HCFCD officials said the reservoir levels peaked on Aug. 30 at 109 feet at Addicks and 101.5 at Barker. With the releases, the reservoir levels are dropping*." (Tang and O'Neil, 2017) Also, "*Water levels in the two reservoirs had already reached record levels Monday evening, measuring 105 feet at Addicks and 99 feet at Barker*" (Wax-Thibodeaus et al., 2017). The information that reported in these articles can demonstrate the event of declining water level identified in the critical tweets.

Multiple news articles also provided information to validate the content of critical tweets associated with Ben Taub Hospital. For example, "*Ben Taub Hospital is surrounded by murky water. On Sunday, the hospital prepared to evacuate some of its 350 patients*." (Khazan, 2017) In addition, "*Ben Taub Hospital confirmed to NPR that they have reopened, that supply lines are steadily improving and that they have received a food delivery and are expecting another one today (August 30)*." (Hus and Sullivan, 2017) This information is the same as the content in the critical tweets on August 27 and August 30.

In summary, the situational information related to critical infrastructure disruptions and situational evolutions were validated by comparison between news articles and identified critical tweets. The proposed methodology is capable of eliminating the misinformation (false positive and false negative information) via the semantic comparison and weighted degrees. The information we detected is based on the most critical tweets, which have the closest semantic similarity to other relevant tweets. Meanwhile, by validating the detected information with actual events and news articles, there are no false positive/negative alarms exiting in the results. The findings show that all detected tweets are credible and non-ambiguous for the public and responders to understand the temporal and spatial patterns of the situation relative to critical infrastructure and help them better respond to these events. The method can be a complement to other less subjective mechanisms in social sensing. That is because social sensing can be negatively affected when it is precipitated by populated with rumors, misconceptions, deliberate or unintended information, particularly in the case of disasters that are prone to human panic and overreaction.

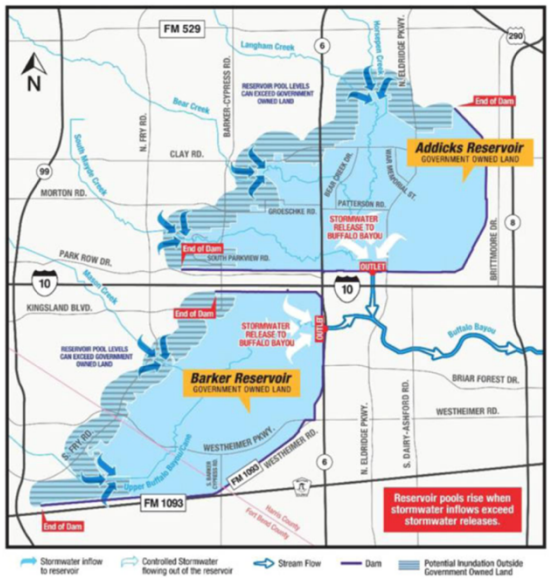

Figure 8 Reservoir map: main structures, locations, and water outflow. (Wax-Thibodeaus et al., 2017)

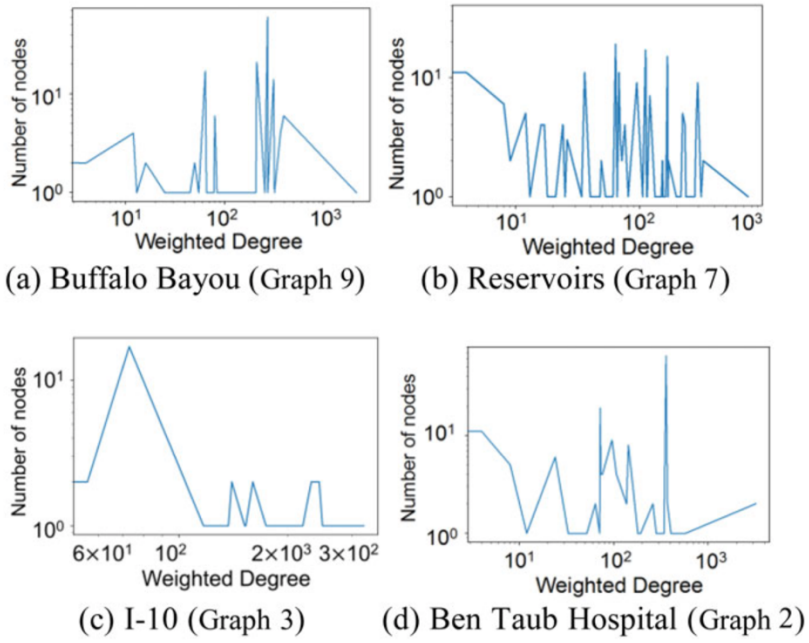

Figure 9 Weighted degree distribution on log–log scales in burst time frames.

2.5 Concluding Remarks

This paper proposed a graph-based method, which focuses on social sensing of infrastructure functionality, to detect credible situational information relative to critical infrastructure disruptions and situational evolution from social media data in disasters. The application of this proposed method was demonstrated in a case study of Hurricane Harvey in Houston. The results showed that the primary disruptive events related to the investigated critical infrastructure (i.e., Buffalo Bayou, Addicks and Barker reservoirs, Interstate Highway 10, and Ben Taub hospital) and their adverse impacts on communities could be detected from the critical tweets. The findings also showed that the situational information related to the critical infrastructure on social media provided insights into the spatial and temporal unfolding of infrastructure disruptions. For example, this study captured two important situational evolvement patterns of infrastructure: co-evolution of interdependent critical infrastructure (the situation of reservoirs, Buffalo Bayou, and I10); and short-term disruption events (the situation of Ben Taub Hospital). In terms of the characteristics of the evolvement patterns, the information obtained from the proposed methodology can help stakeholders better understand infrastructure disruptions and their impacts on residents. This information plays an important role in improving disaster response and recovery.

From the methodological perspective, the proposed graph-based method provided a new analytical and computational methodology for social sensing of infrastructure disruptions. All identified critical tweets contained detailed information about the situation

of critical infrastructure in disasters, as well as the societal impacts of infrastructure disruptions. Hence, the results are more insightful than groups of tokens based on the word frequencies in existing studies (e.g., topic modeling and clustering). In addition, this method distinguishes the credibility of online information on social media. For example, retweets are not sufficient in demonstrating the credibility of its original tweets. Rumors with sensitive words (e.g., "reservoirs will spill", which would affect large-scale residents) would also be retweeted many times. To overcome this issue (that is not being addressed in existing studies), the proposed graph-based method put more weight on the content similarity between the tweets posted by multiple users. Hence, this method can improve the credibility of the critical tweets as well as the reliability of infrastructure disruption findings.

From a practical perspective, the method proposed in the paper provides infrastructure agencies and disaster responders with a technical tool to determine the occurrence of the disruptions, the location of critical infrastructure, when disruptions happen, how severe the disruptions are, what communities are involved, and what actions have been taken for a response. The stakeholders can better capture the performance of critical infrastructure using such situational information, and make better decisions such as allocating shelters, distributing resources, and mobilizing relief crews. In addition, this method enables effective evaluation of critical infrastructure performance in the aftermath of disasters to inform future hazard mitigation planning and infrastructure prioritization.

Social sensing of infrastructure disruptions involves dealing with semantic uncertainty, which causes some limitations to the proposed computational methodology.

First, the ontology uncertainty would affect the process of filtering relevant tweets. Despite the careful selection of the keywords, some relevant tweets may still be missing. For example, some residential users may not mention the name of the infrastructure. Specifically, residential users might say that "water released; my house is flooded". This tweet is highly related to the case of water release from reservoirs in our study. However, due to the limitation of the keywords, this tweet is not included in our dataset. Second, semantic similarity uncertainty induced by the dimensionality of tweet vectors would affect the measurement of similarities among the tweets. For example, the size of the dataset for different infrastructure varies. The larger the dataset is, the more tokens would be included in the dataset, and subsequently, the higher the dimension of the tweet vectors is. In most cases, those uncertainties will not affect the outputs of our method, but these uncertainties should be considered to ensure the reliability of the results.

A general limitation of social sensing approaches still persists in the proposed method. Tweets deliver the information about the functionality loss and impacts of critical infrastructure disruptions (e.g., power outage, road closure, and water release) on the residents. Due to that, social sensing methods may need to wait for the cumulation of the tweets within one hour, which makes the methods no faster than conventional surveillance or sensor monitoring-based methods in fast-paced events. Instead, social sensing methods can capture detailed and localized situational information which is critical for residents to adjust themselves and respond to the disruptions. The criticality of the tweets would be correlated to the extent of the adverse impacts of the damages, and subsequently indicates the criticality of the infrastructure. Other critical infrastructure such as police station,

schools, and churches may not make direct impacts on residents' lives and is rarely reported on Twitter. Thus, it is difficult to detect their situation via social sensing.

This computational methodology can be further extended in the following areas: (1) enhancing the algorithm of vectoring in tweets to make it more feasible in disaster and critical infrastructure domain; (2) developing algorithms to identify the relevant entities in critical tweets and exploring their relationships for better disaster preparedness planning and response; and (3) testing the capabilities of the method in regular daily setting to demonstrate its broader applications; (4) implementing visibility graph to analyze time series of the situation of critical infrastructure disasters.

CHAPTER III

COLLECTIVE-SENSE MAKING IN ONLINE SOCIAL NETWORKS UNDER CRISIS STRESS[*]

Social cohesion is an important determinant of community well-being, especially in times of distress such as disasters. This study investigates the phenomena of emergent social cohesion, which is characterized by abrupt, temporary, and extensive social ties with the goal of sharing and receiving information regarding a particular event influencing a community. In the context of disasters, emergent social cohesion, enabled by social media usage, could play a significant role in improving the ability of communities to cope with disruptions in recent disasters. In this study, we employed a network reticulation framework to examine the underlying mechanisms influencing emergent social cohesion in online social media while communities cope with disaster-induced disruptions. We analyzed neighborhood-tagged social media data (social media data whose users are tagged by neighborhoods) in Houston during Hurricane Harvey to characterize four modalities of network reticulation (i.e., enactment, activation, reticulation, and performance) giving rise to emergent social cohesion. Our results show that, unlike regular social cohesion, communication history and physical proximity do not significantly affect emergent social cohesion. The results also indicate that weak social ties play an important

[*] This chapter is reprinted with permission from "Emergent social cohesion for coping with community disruptions in disasters" by Fan, C., Jiang, Y., and Mostafavi, A., 2020. *Journal of the Royal Society Interface*. Mar 25;17(164):20190778.

role in bridging different social network communities, and hence reinforce emergent social cohesion. The findings can inform public officials, emergency managers and decision-makers regarding the important role of neighborhood-tagged social media, as a new form of community infrastructure, for improving the ability of communities to cope with disaster disruptions through enhanced emergent social cohesion.

3.1 Introduction

The objective of this study is to characterize the dynamics of emergent social cohesion in neighborhood-tagged social networks in coping with disaster disruptions. Information seeking, and sharing is one of the main components of human protective actions in facing with disasters. With the increasing use of social media, online communication is increasingly prominent in information gathering and sharing among community members, especially during times of crises (Sutton et al., 2015; Zhang et al., 2019). This is because, when disasters cause inevitable disruptions in physical infrastructure and subsequent distress on humans, social networks enable information sharing and adjustment behaviors that play a key role in helping communities cope with disaster impacts (Akhtar et al., 2012; Balcik et al., 2010). Social cohesion has been shown to be an important element for human wellbeing (Misra et al., 2017; Roca and Helbing, 2011), especially in times of distress and crises (Lazega et al., 2006). Particularly, the increasing use of social media during disasters could give rise to emergent social cohesion, which is characterized by abrupt, temporary, and extensive social ties with the goal of sharing and receiving information regarding a particular event influencing a community

(Kim and Kang, 2010). Existing literature have already examined online social networks (OSNs) from multiple important aspects such as: fundamental structure of social networks (Prasad et al., 2018; Sekara et al., 2016); information diffusion (Altay and Pal, 2014; Morone and Makse, 2015; Qiu et al., 2017; Vosoughi et al., 2018b); and social segregation (C Fan et al., 2020; Wang et al., 2018). Some methodologies and techniques have been employed to examine user activities, network structures, and information propagation on social media for different purposes. For example, community network analysis has been used for examining roles of different actors/organizations, as well as information diffusion (Chao Fan et al., 2020d; Papadopoulos et al., 2017). Or, topic analysis has been used to evaluate important topics discussed by communities. While each of these studies (and the adopted analytics) provide insights about a particular modality in online social networks, they do not inform about the relationship among various modalities influencing important phenomena such as emergent social cohesion. To this end, this study aims to examine various modalities and mechanisms in OSNs influencing emergent social cohesion in disaster-impacted communities using an integrated approach. Understanding emergent social cohesion in OSNs and its underlying dynamics may hold the key to promote formal policies for social media selection and usage during disasters by city officials, emergency managers, and community leaders.

In this study, we specifically examine the dynamics of emergent social cohesion in neighborhood-tagged social media during disaster disruptions. Among different social media platforms, most of them, such as Twitter, tag their users with a city, a state, or a country in their profiles to enable a large-scale communication among massive users

regarding different topics and events (such as disaster-induced events) (Bagrow et al., 2019). Community disruptions, however, tend to be localized and vary from one neighborhood to the other. For example, one neighborhood may be affected by flooded roads while another neighborhood might be dealing with sewage backup. Without tags of neighborhood information, it is hard for social media users to share and receive information regarding the same disruption event with users from the nearby neighborhood and cope with disruptions. The examination of the effect of geographic proximity on emergent social cohesion is not feasible to do using Facebook and twitter data since the distance and neighborhoods locations are not known. Hence, analyzing neighborhood-tagged OSNs makes it possible to uncover the relationships among neighborhood-specific disruptive events, human activities, and cohesion in OSNs. Such characterization would be unattainable through the use of other communication technology tools such as Twitter (Chao Fan et al., 2020c; Y. Kryvasheyeu et al., 2016). In this study, we examine the underlying dynamics of emergent social cohesion in OSNs using a theoretical Network Reticulation framework and based on four modalities: enactment, activation, reticulation, and network performance in neighborhood-tagged OSNs. The study utilizes neighborhood-level social media data (from Nextdoor) related to the 2017 Hurricane Harvey in Houston in analyzing each modality of network reticulation and their relationship to the emergence and stability of social cohesion.

Hurricane Harvey was a category-four tropical storm which affected Houston, the fourth largest city in the United States, from August 26 to August 29 in 2017 (Sebastian et al., 2017). The extremely high intensity of the rainfall brought by Hurricane Harvey led

to the water levels of Addicks and Barker reservoirs in the west of Houston to their maximum (Fan and Mostafavi, 2019b; Tang and O'Neil, 2017). To prevent the reservoirs from abrupt disruptions, a large amount of water was released from the reservoirs and flooded the nearby 28 neighborhoods. We collaborated with the volunteers living in these neighborhoods and collected unique and publicly available data from their Nextdoor accounts in which user profile's location is verified by user's physical address and tagged by a neighborhood name. The dataset spans 19 days, from August 20 to September 7, including 7 days before Hurricane Harvey and 12 days during Hurricane Harvey and the subsequent flooding. Surveying the affected area, the identified 28 neighborhoods has various number of users (SI Appendix, Table S1.). In total, our dataset includes 2,690 active users who posted or commented at least one message, 1,939 posts, and 32,776 comments. Daily OSNs are mapped based on this dataset, in which active users are abstracted as nodes and the post-comment relationships are abstracted as edges (i.e., social ties) (SI Appendix, Fig. S1.).

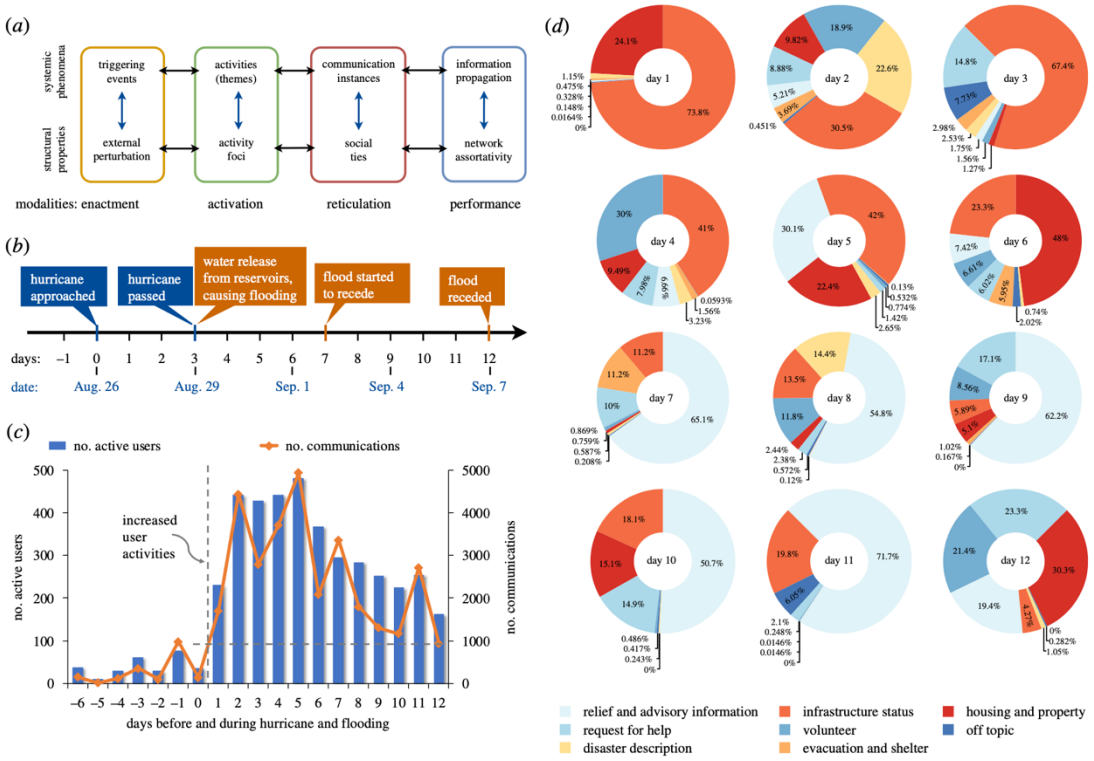

Figure 10 Modalities of the Network Reticulation Theoretical framework and empirical results for the case study. (a) Modalities of the NRT framework. Each modality (i.e. enactment, activation, reticulation and performance) is composed of two components: systemic phenomena and structural properties. (b) Disaster events happened in the neighbourhoods near reservoirs, including Hurricane Harvey and water release from reservoirs. The first day when the hurricane approached the neighbourhoods is tagged as 1. (c) Number of active users and communications on social media before and during the hurricane and flooding. (d) The proportion of eight themes in online communications among users from 28 neighbourhoods for 12 days, in which the proportions were weighted by the number of communications under the posts regarding a certain theme.

3.2 Network Reticulation Theory

Communication theories such as Corman's Network reticulation theory (NRT) (Corman and Scott, 1994), Giddens' structuration theory (Giddens, 1984), and Homans' theory of the human groups (Homans, 1950) have defined basic concepts and processes related to communication networks, such as the concept of triggering events, activity foci, and communication relationships. These theoretical elements can enrich the existing analytics used for evaluating distinct modalities in online social networks and provide an integrative framework for examining the relationships among various modalities influencing important phenomena in online social networks. Hence, built upon these theoretical concepts from the communication field, we proposed an extended network reticulation theory as an integrative framework for examining four modalities and their relationships that affect emergent social cohesion in online social networks in disasters (see Figure 10(a)). The NRT framework utilized in this study characterizes the dynamics of social networks based on four modalities: enactment, activation, reticulation, and performance. Each modality is a concept that relates the systematic phenomena to structural features in online social networks (Giddens, 1984). Enactment modality represents disruptive events (e.g., community disruptions and infrastructure failures) which trigger human activities in social networks. Events tend to evolve, trigger activities in individuals, and cause transformation in the structure of online social networks. For example, the information sharing behavior is more active when the environmental events occur and situation evolves, comparing to the behaviors before the events. Activation

modality specifies user activities—posting and commenting about disruption events. Specifically, activities such as reporting and discussing situations in neighborhoods (e.g., house damages, floodwater levels, and road closures) stimulate communication instances in online social networks. Due to the dynamic nature of the unfolding of disaster-induced events, the activity themes (See the definition in Materials and Methods) vary from one activity foci to the other and over time. Accordingly, activity foci are identified to represent cohesive cluster of online users corresponding to a particular activity theme in OSNs during a specific time period. Reticulation modality characterizes the structural properties of communication instances among clusters of online social networks corresponding to different activity foci. Specifically, reticulation modality signifies the creation and reinforcement of social ties among users regarding specific activity foci. Finally, network performance modality determines the influence of user activities on the structure of online social networks. In particular, we determine the measure of network assortativity at both network level and activity foci level and its changes over time to signify the structural anatomy and stability of emergent social cohesion in OSNs. We employed the NRT framework and its four modalities in examining emergent social cohesion in neighborhood-tagged OSNs during the 2017 Hurricane Harvey and the subsequent flooding event in Houston.

3.2.1 Enactment Modality

The enactment modality in the NRT framework focuses on examining the nature and timing of the triggering events (e.g., Hurricane Harvey and water release from reservoirs), in order to better understand their impacts on the affected neighborhoods. As

shown in Figure 10(b), Hurricane Harvey started having impacts on the neighborhoods in the West of Houston on Day 0 (August 26, 2017). It dropped torrential and unprecedented amounts of rainfall over the Houston metropolitan area on Day 1 and 2, and then weakened and moved towards Louisiana after Day 3 (August 29, 2017). Due to the heavy rainfall, the two major flood control infrastructure, Addicks and Barker reservoirs, reached their maximum capacity. To protect the reservoirs from breaching, the U.S. Army Corps of Engineers decided to release the water from these two reservoirs without issuing any statement, inundating thousands of houses in nearby neighborhoods (Allen, 2017). The entire duration of the flooding sustained for 10 days spanning from the end of the hurricane until flood water receded. The houses in West Houston had never flooded before; and 80 percent of the residents did not have any flood insurance (Shilcutt and Asgarian, 2017). Hurricane Harvey and the subsequent flooding event resulted in an extreme panic among the affected neighborhoods. People in those neighborhoods had to seek situational information, look for relief resources, and evacuate. As such, the communications of people on Nextdoor increased significantly during that period. As shown in Figure 10(c), more than 200 active users from these neighborhoods communicated on Nextdoor each day during Hurricane Harvey and flooding, generating more than 1,000 posts and comments (see details in Appendix A, Table 9). The posts and comments are analyzed in the same way, and both are considered as communications among online users. The peak of the communication and active users occurred at the end of Hurricane Harvey and the beginning of the flooding. When the flood started to recede, the activities of the users decreased as well.

3.2.2 Activation Modality

In our NRT framework, the triggering events cause user activities related to seeking and sharing information to cope with disruptions. User activities on the neighborhood-tagged social media include posting queries to seek help or ask questions, as well as commenting posts to respond or share information. The activation modality helps linking the enactment modality (triggering events) to the reticulation modality (communication instances). In the activation modality, online users organize and create the conditions that necessitate communication instances and social ties with each other. In this study, the activation modality identifies activity themes and foci, around which the reticulation of communications unfolds. Hence, collectively, four modalities enable the understanding of emergent social cohesion in online social networks during disasters.

From day 1 to day 2, when the hurricane landed, the most concerned activity theme was the status of infrastructure (accounting for 73.8% in all communications on day 1) including road, power, and water (Figure 10(d)). Beginning on day 3, water release from the flood control reservoirs started and the released water flooded the nearby neighborhoods. Hence, again, infrastructure-related communication was the main activity theme discussed by users (accounting for 67.4% in all communications on day 3). Meanwhile, more and more requests or coordination for help from the users in these affected neighborhoods were posted on the social media (7.98% of all communication on day 4). The damages to housing and properties became increasingly severe, whose theme increased from 9.49% of all communications on day 4, to 22.4% of all communications on day 5, and finally reached 48% of all communications on day 6. When the flood water

started to recede on day 7, residents focused more on relief and advisory information (65.1% in all communications on day 7). The relief theme included information related to insurance, recovery tips as well as federal aid (accounting for more than 50% of all communications between day 7 and 11). When the flood water receded on day 12, multiple activities including volunteering, requests for help, relief information seeking, and housing and properties had equal shares of communications. This indicates that, as the triggering events dissipated, the prominence of main activity themes dissipated as well. This analysis shows direct relationship of activity themes with the timing of triggering events.

The primary activities and themes are the results of activity foci, which can be examined as structural clusters in OSNs communicating activity themes (Corman and Scott, 1994). We employed the Louvain algorithm to detect the activity foci in the OSNs (see Materials and Methods: Activity foci and network modularity) (Waltman and Van Eck, 2013). In the activity foci, users collectively drew up on information in order to co-act with each other and cope with the disruptions. The more severe the triggering events in the physical environment, the more individuals tend to find and develop new activity foci (Lazega et al., 2006). Being consistent with the structural approach underlying the focus theory (Burt, 1984), the number of activity foci in the days at the beginning of flooding (especially from day 2 to day 6) is greater than other days. This is because, information seeking is an important component of human protective action and people had to look for a variety of information to cope with the adverse impacts flooding (Figure 10(d)).

Evaluation of the activity foci based on the structural network properties enables evaluating what users and activity themes give rise to emergent social cohesion. For example, Figure 11(a) depicts the activity foci and their focused themes in OSN on day 6. The activity themes can be identified from the content generated by the users among the activity foci. Each activity focus has its own focused themes such as volunteer and infrastructure status, which bring users together to share the information and resources. The presence of activity themes and foci further facilitates collective protective action, and hence enhances cohesiveness among users in activity foci. As shown in Figure 11(b), comparing to the density of the entire network, the densities of activity foci are significantly high. This implies, users in each activity foci are densely connected to the users within the same activity foci and have less edges connected to the users outside the activity foci. The results are consistent with the results of modularity, which measures internal (and not external) connectivity. The higher the modularity, the more connected the activity foci (i.e., nodes in the activity foci are closely connected, and are less connect to the nodes outside the activity foci) (Newman and Girvan, 2004). The information related to nodes and edges for each activity foci can be found in Appendix A, Table 7.

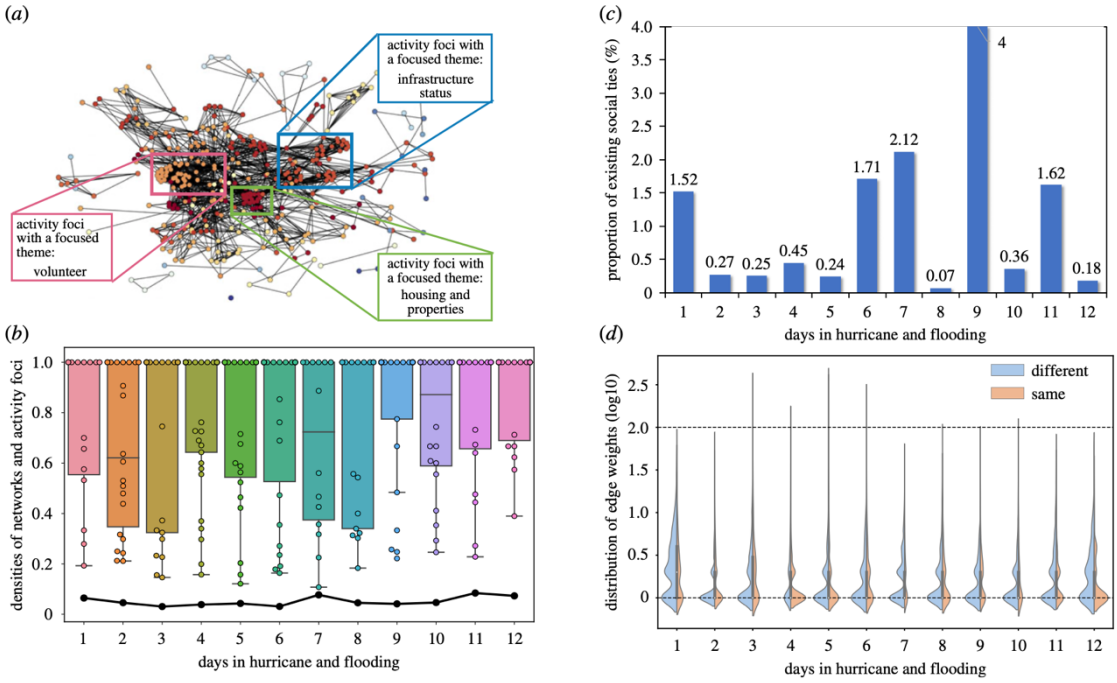

Figure 11 Network reticulation outcomes. (a) An illustration of the focused themes of activity foci in the OSN of day 6. (b) Densities of daily networks (black dots) and activity foci (boxes and colorful dots). (c) The proportion of existing social ties in OSNs during the disasters (see Material and methods). (d) The distribution and mean of weights of social ties in each OSN. There are two types of social ties with regard to the neighborhoods of the connected users: the social ties connect the users from the same neighborhood (orange), and the social ties connect the users from different neighborhoods (blue). The weights of social ties were the frequency of communications.

3.2.3 Reticulation Modality

Activities by users on social media lead to the formation of communication instances (a.k.a. social ties). To examine the extent to which the increase in communication instances and social ties was due to triggering events, we examined the effects of two latent factors: communication history and user locations proximity.

3.2.3.1 Effects of communication history and physical proximity

Communication history was analyzed to determine whether the emergent social cohesion was more influenced by triggering disruption events or by the past communication of users. We calculated the proportion of existing social ties, which were established during 7 days before the hurricane landed (Figure 11(c)). The results show that the proportions of prior social ties to post-event social ties are very low across the entire 12 days. All of the proportions do not exceed 4% and the proportions are even less than 0.5% in 7 days (i.e., day 2, 3, 4, 5, 8, and 11). These results demonstrate that, unlike the case of regular social cohesion, the communication history did not have a significant influence on the formation of social ties in emergent social cohesion.

Another latent factor is the physical proximity of users (Burt, 1987; Jackson et al., 2018). As every user is tagged by their neighborhoods, we defined the physical proximity between users based on the distance between their neighborhoods (SI Appendix, Fig. S3A). The measurement of the distances between neighborhoods is defined in the Materials and Methods section. Appendix A, Figure 29B displays the communication frequencies between neighborhoods across the entire period of analysis (see the heatmaps for daily communication frequency in Appendix A, Figure 28). However, the Pearson's

correlation coefficients indicate that physical proximity has weak correlation with the frequency of online communications between different neighborhoods. Thus, physical distance does not hinder the process of emergent social cohesion in the context of community disruptions, either. The findings imply that the main reticulation mechanisms (creation or reinforcement of social ties) were derived from activity themes triggered by disruptive events, and not the communication history and physical proximity.

3.2.3.2 Spatial and temporal changes in social ties

We mapped the weight distribution of social ties for each day in the OSNs (Figure 11(d)). The distribution of weights for social ties vary across different days. Generally, the weight for most edges is 1 regardless of whether the users connected by an edge are from the same neighborhood or not. This is also shown by the median weights of the weight distribution in each day (see Appendix A, Table 8). In addition, the number of edges connecting the users from different neighborhoods is greater than the edges connecting the users from the same neighborhood. This phenomenon is more significant in the days when a disruption event occurred (e.g., day 1 when hurricane started to land in the area, day 3 when water release from the reservoirs started, day 7 when flood started to recede, and day 12 when flood water finally receded). This indicates that user activities immediately after triggering events goes beyond the boundaries of their own neighborhoods. Because the users in disasters are not self-contained or self-sufficient for information processing (Prasad et al., 2018), they rely on information shared by others, as well as reactions and sentiments of others in processing information regarding disaster threats. Thus, when disaster situation evolves (i.e., triggering events occur), online users

would create more weak social ties to gather new situational information from different users and examine their sentiments and reactions. This finding indicates that weak social ties connecting a large number of users from different neighborhoods play a primary role in emergent social cohesion. Unlike regular social cohesion with strong social ties (Kawachi and Berkman, 2000), weak ties are building blocks of emergent social cohesion.

3.2.4 Performance Modality

As discussed earlier, activity themes enable emergent social cohesion in groups of users (a.k.a., communities or activity foci) and create weak social ties between the users discussing the same topics. In this section, we investigate the network structural properties as a result of emergent social cohesion to gain deep insights into the role of neighborhood-tagged social media in improving information propagation.

Mixing patterns in networks is an important approach to study the tendency for nodes in networks to be connected to other nodes that are similar (or dissimilar) to them in terms of selected node attributes such as node degree and user profile features (see Materials and Methods) (Newman, 2003). To dissect the structure of emergent social cohesion and understand how the cohesion structure contributes to the information propagation, we examined the mixing patterns based on degree (Figure 12(a)) and neighborhood (Figure 12(b)) attributes of the nodes and analyzed difference of the mixing patterns at two levels: network level and activity foci level.

3.2.4.1 Degree assortativity

Degree assortativity measures the extent to which nodes with similar degrees connected to each other (do gregarious people tend to associate with other gregarious

people) (Newman, 2003). Figure 12(a) shows that most of the activity foci in OSNs across the 12 days of hurricane and flooding are disassortative. That is, the activity foci most often paired unlike nodes in which their degrees are quite different. In addition, the degree assortative mixing patterns also vary during the evolvement of the disaster situation, especially when new triggering events happened. For example, the mean of degree assortativity for the activity foci reached to 0 (non-assortative) on day 3 when the Hurricane Harvey passed and the flooding from the reservoirs started, and on day 7 when the flooding started to recede. During these days when new events happened, activity foci lost the mixing tendencies. At the network level, however, the daily OSNs exhibits a tendency of assortative mixing (i.e., users with the similar degree connect to each other) (Figure 12(a)). In evaluating the degree assortativity for each daily network, the social ties among different activity foci in OSNs are considered. These ties crossed the boundaries of activity foci and bridge the gaps among the users in different activity foci and discussing different themes. In doing so, the degree assortativity of the networks increased about 0.4 from the means of degree assortativity of the activity foci in each daily network.

Building upon this result, we can examine the structures of the social network emerging on Nextdoor by assembling the cliques in accordance with the mixing patterns (Figure 12(c)). The posting and commenting functionality on Nextdoor enable users to form cliques in which users who commented in the same post are fully connected with each other. Thus, the social networks formed on Nextdoor are the result of assembling the cliques with certain mixing patterns. Initially, cliques emerged when disaster-related posts were generated by users and attracted attentions of other users to comment. Different users

joined different posts based on their theme of interests. Users with similar interests in the themes form cohesive activity foci built upon multiple cliques. The activity foci gravitate more users with varying levels of degrees. This assembling mode contributes to the formation of the hierarchy in social networks with various degrees of users.

3.2.4.2 Neighborhood assortativity

To assess assortative mixing pattern for neighborhoods (the extent to which activity foci in OSNs include users from the same neighborhood), we calculated the assortativity coefficient of activity foci and examined the distribution and means of the assortativity over time (Figure 12(b)). As the result shows, the means of neighborhood assortativity coefficients for activity foci during Hurricane Harvey and flooding are around 0. The maximum value for the mean of assortativity coefficients is only 0.18. The result indicates that the majority of the activity foci in the emergent OSNs are non-assortative regarding neighborhoods. That is, activity foci involved users from different neighborhoods to generate and share information in disasters. To further support this finding, we examined the proportion of neighborhoods in each activity foci in these 12 OSNs (Figure 12(d)). Each pie chart was embedded in a node representing an activity focus. As shown in Figure 12(d), the majority of activity foci in OSNs are composed of multiple different neighborhoods, regardless of different sizes of the activity foci. This result also provides evidence that, instead of the geographical boundaries, cohesive activity foci are more driven by the information needs of users related to triggering events and their impacts. Existing studies on Twitter show that social media has not affected geographical homophily (i.e., individuals from the same location tend to connect with each

other) and recent empirical research on online social networks found that people still tend to connect more often to geographically close people (Choudhury et al., 2011; Kulshrestha et al., 2012). These studies did not consider geographic homophily at the neighborhood scale. Our results indicate that neighborhood-tagged social media can enable users to break the physical boundaries of neighborhoods and achieve cross-neighborhood communication for information sharing and seeking to form cohesive activity foci.

Analyzing the neighborhood assortativity for the entire daily OSNs, we find that the majority of the daily OSNs have the neighborhood assortativity coefficients 0.2 to 0.6 higher than 0 and the mean values of neighborhood assortativity coefficients for their activity foci (Figure 12(b)). The average value for the neighborhood assortativity coefficients for these 12 days is 0.3, which signifies a weak assortativity for the neighborhoods. In addition, the changes in the neighborhood assortativity coefficients are consistent with the unfolding of disruption events. Specifically, day 3 (when Hurricane Harvey affected these neighborhoods) and day 7 (the last day with high water level in neighborhoods) both have low neighborhood assortativity coefficients, which implies that users tend to get information from different neighborhoods as part of their protective action information seeking.

Combining the findings at activity foci level and network level, we can identify an important mixing pattern. The neighborhood-tagged social media (Nextdoor) enabled users from different neighborhoods to form cohesive activity foci to share and seek information they needed. This also confirmed the role of activity foci in emergent social cohesion in OSNs, i.e., the primary reason for building social ties on social media is

communication activities which motivate users to seek/share information regarding a triggering event. However, the social ties that cross the boundaries of activity foci and enable the spread of information across different activity foci tend to be created by the users from the same neighborhood. These users play an important role as boundary spanners contributing to the emergent social cohesion within and across neighborhoods.

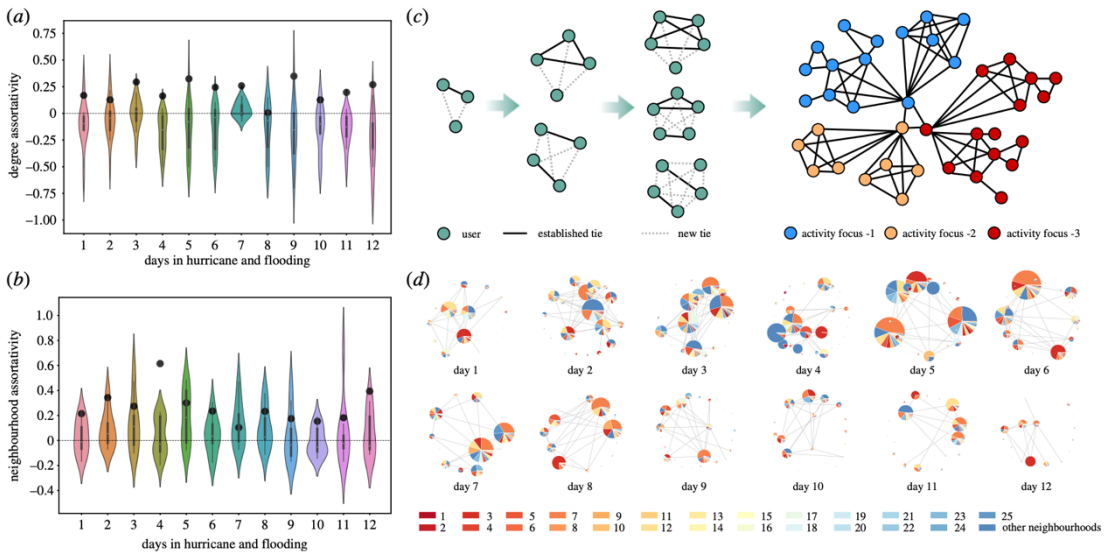

Figure 12 Network mixing patterns during hurricane and flooding. (a) Degree assortativity for daily OSNs (black dots); and the mean and distribution of the activity foci (colourful violin plot) in each day during the hurricane and flooding. (b) Neighbourhood assortativity for daily OSNs (black dots); and the mean and distribution of the activity foci (colourful violin plot) in each day during the hurricane and flooding. (c) Structural anatomy of daily OSNs for understanding emergent social cohesion and information propagation. (d) Activity focus-level OSNs with the proportions of various neighbourhoods by counting the number of users from the same neighbourhoods. Each pie chart represents an activity focus. The size

of a pie chart is consistent with the number of users in the activity foci. The connections between communities depend on the connections between the users in both communities. There are three neighborhoods without any active users on social media during disasters because there are only a few residents and corresponding registered users on Nextdoor. Meanwhile, a small group of people outside the investigated neighborhoods joined the communication, labeled as other neighborhoods.

3.3 Discussion

Our proposed theoretical network reticulation framework uncovers the underlying modalities and structural network properties affecting emergent social cohesion in the context of community disruptions in disasters. Specifically, the findings in this study show that community disruption triggers user activities on social media, and users form activity foci for communicating information related to different themes. Then, weak social ties bridge communication instances (i.e., activity foci) to enable the reticulation in networks, which subsequently shows a disassortative mixing of users to promote information propagation across physical and online community boundaries. Although the case study focused on how residents cope with a hurricane and flooding event, the theoretical framework and our findings could be generalized to other crises and geographic contexts.

One key finding was that disaster events trigger the emergence and evolvement of human protective activities in seeking information on social media. This information seeking and sharing behavior creates activity foci that gravitate additional users and leads

to creation of new links giving rise to emergent social cohesion. This finding implies the important role that neighborhood-tagged social media, such as Nextdoor, play in formation of activity foci related to different triggering events for which residents seek information, and hence improving the individual and collective protective action of the residents. This finding also has implication for online influential users or community leaders to initiate activity themes/foci and enhance cohesiveness of users (Patterson et al., 2010; Yang et al., 2019). These individuals with boundary-spanning weak ties between neighborhoods play an important role in scaling up the communication among neighborhoods. Future studies can examine the bridging and boundary spanning roles of these individuals to inform the efficient and effective information spread among online users from different neighborhoods.

Another key finding was that emergent social cohesion arises from cohesive activity foci which focus on specific disaster-related events and are constructed by weak social ties. In disaster contexts, activity foci become the gravitation centers that absorb users (create weak ties) across different neighborhoods with interest/need for information about the activity theme. Meanwhile, we observed that weak social ties were derived from activity themes, instead of communication history or physical proximity. This finding further confirms that people utilize social media during disasters for information seeking as part of their protective actions. In other words, the fundamental function of social media changes for people during disasters. Unlike regular social cohesion with strong social ties and physical homophily, the formation of inclusive activity foci and weak ties triggered by disaster events are the building blocks of emergent social cohesion. This result is also

consistent with the principles in Homophily/Heterophily theory that weak social ties are more heterophilous than strong ties (Brown and Reingen, 2002; Gross et al., 2006). Accordingly, creating weak social ties not only contributes to the inclusiveness of activity foci, but also makes an influence on emergent social cohesion and information spread. That is because, heterophilous communication facilitates the flow of information between diverse segments of a social network (Aral and Walker, 2014; Brown and Reingen, 2002).

The third key finding was that different assortative mixing patterns for OSNs and activity foci improve the information spread. This happens because the assemblage of multiple activity foci makes OSNs assortatively mixed by creating social ties between the users with similar degrees and from the same neighborhoods. At the same time, activity foci themselves are composed of the ties between the users with different degrees and from different neighborhoods. The findings illustrate the assemblage process of OSNs and the formation of the hierarchy in terms of the node degree and neighborhood attributes. This self-organized mixing pattern could give rise to emergent influential users who could be identified and used to seed urgent safety related information and speed up the diffusion of the information (Aral and Dhillon, 2018). Identifying the users who bridge the boundaries of activity foci using the degree and neighborhood features and seeding the information to these users can optimize the information propagation.

With the increased use of social media in disasters, emergency managers, public officials, and community leaders would need to optimize their strategies to improve information seeking protective action in communities. Understanding the structure and dynamics of social networks could inform about better intervention strategies to improve

the spread of situational information, the situation awareness of the affected population, and response and recovery of neighborhoods in disasters. Our theoretical network reticulation framework and the findings may provide important insights for public officials, emergency managers and community leaders regarding social media selection and usage policies for improving the capacity of communities in coping with disasters. Additionally, the proposed integrative framework can be further adopted in other studies and contexts to examine the dynamics of online social networks based on the characteristics and relationships among the four modalities. Therefore, the next critical question is how the identified emergent social cohesion vary from one disaster to another. Moreover, examining user behaviors on multiple social media tools could be examined in future studies to further inform about emergent social cohesion in disasters. A challenging problem, however, is to collecting quality data from different social media platforms for the same areas. Moreover, future studies can combine the data about phone calls with social media data to further examine social network interactions (specifically when there are disruptions in internet and telecommunication services). Nevertheless, emergent social cohesion would primarily arise due to formation of weak social ties on online social networks (phone calls are usually made with existing contacts which reinforce the existing social ties rather than creation of new communication instances).

3.4 Materials and Methods

The data were gathered by volunteers in different neighborhoods one week after Hurricane Harvey. The neighborhoods in this study is defined by Nextdoor. Since

Nextdoor allows the users to access all their historical data, the volunteers could gather communications for the period before the disaster as well. The volunteers used their personal Nextdoor accounts to gather communications among users in their own and nearby neighborhoods using the public posts. A public post is a message that the user consents to be publicly available for all users from nearby neighborhoods rather than only to his designated users. Communications among users through public posts were gathered anonymously. Nextdoor only allows the users to show their physical addresses, and no organizational or association identities are allowed to be disclosed. Social/institutional identity cannot be observed and collected from user profiles. Hence, there are no institutional mechanisms that affect the communication among the neighborhoods.

The neighborhoods were selected based on two criteria. First, these neighborhoods were flooded when the water was released from the reservoirs in West Houston during Hurricane Harvey. The water release was a major disruption and caused significant impacts, and thus provided an ideal setting for examining emergent social cohesion. Severe damages happened in the downstream area (see Appendix A, Figure 30). Since the impact of flooding was almost the same across different neighborhoods, we assumed that the use of online communication is not differentiated by the extent of impact experienced by these neighborhoods. Second, Nextdoor has some constraints related to the neighborhoods that a user can communicate with. The neighborhoods that we selected are within the geographical area affected by the reservoirs water release whose users could communicate with each other. The sizes of the neighborhoods are shown in Appendix A, Table 4.

3.4.1 Activity Foci and Network Modularity

Activity foci is a structural cluster in which the users connected to each other more closely than their connections to the users outside the activity foci. The idea of detecting activity foci was named as community detection in computer science. Modularity maximization (i.e., Louvain heuristic (Blondel et al., 2008)) is one of the widely used approaches for detecting communities, which measure the modularity of a network to examine how well a network is partitioned into communities. This approach compares the number of edges within a certain group to the expected number of edges in a null model. The modularity for a network is formulated as (Montes et al., 2017; Newman, 2003):

$$Q = \frac{1}{2m}\sum_{ij}\left[A_{ij} - \frac{d_i d_j}{2m}\right] \cdot \delta(d_i, d_j) \quad \textbf{(9)}$$

where m is the number of edges in the network, A_{ij} is the adjacency matrix of the network, d_i and d_j are the degrees of the nodes i and j. The higher the modularity (closer to 1), the more edges within the module that we expect by chance (Foster et al., 2010). Generally, the modularity higher than 0.3 means significant community structure. In this study, we adopted Louvain algorithm to detect communities by maximizing the modularity of the networks.

3.4.2 Communication History

Communication activities among the users on social media before the hurricane approached to the locations are considered as the communication history. In this study, the communication history is identified using the existing social ties established during

the 7 days before Hurricane Harvey. Then, we can measure the effect of communication history on the communication behaviors during hurricane and flooding by:

$$P = \frac{|E'|}{|E|} \quad \textbf{(10)}$$

where $|E'|$ is the number of social ties that have been created before Hurricane Harvey, and $|E|$ is the total number of social ties in the online social network. Low proportion of the social ties created before can indicate the low effect of communication history on emergent social cohesion during disasters.

3.4.3 Physical Proximity

To examine the effects of physical proximity on social cohesion in OSNs, physical proximity was defined to measure the distance between different neighborhoods (Gibbons et al., 2018). This study developed three levels of physical proximity: "within a neighborhood", i.e., both of the users live in the same neighborhood; "nearby neighborhoods", i.e., the users live in the neighborhoods bordering on each other; and "distant neighborhoods", i.e., the users live in the neighborhoods which do not border on each other.

3.4.4 Communication Frequency

Communication frequency within and between neighborhoods was a measurement to show the cohesiveness between two neighborhoods. The matrix of communication frequency between neighborhoods was used to calculate the correlation with physical proximity and illustrate the effects of physical proximity on emergent social cohesion. The communication frequency was computed by:

$$f = \frac{\sum_{u \in U, v \in V} Weight(u, v)}{|U| \cdot |V|} \quad \textbf{(11)}$$

in which U and V are collections of users in neighborhoods. U and V can be the same neighborhood (i.e., $|V| = |U| - 1$), in which the results show the communication frequency of users within the same neighborhood. The communication frequency of users in different neighborhoods can be obtained when U and V represents the users from different neighborhoods. Whether users come from the same neighborhood or not, as shown in Eq. **(11)**, we deem each communication is from two neighborhoods (they may be the same). This approach can overcome the discrepancy from the differences in number of users in different neighborhoods.

3.4.5 Content Coding

Two researchers manually coded each post for message content in our dataset by using a content-coding approach proposed in prior research (Sutton et al., 2014). Based upon the content themes presented by (Sutton et al., 2015), this study developed a new coding ontology, which is fit the content categories on our dataset, including 8 themes: housing and properties, i.e., information about damages of housing, loss of properties, and casualty; infrastructure status, i.e., information about infrastructure facilities; evacuation/shelter, i.e., information about pre-evacuations, mandatory evacuations, and sheltering information; disaster descriptions, i.e., descriptions of the disaster itself and its scales; relief/advisory information, i.e., relief information and response tips; request for help, i.e., actions about requesting for neighbors' on-site help; volunteer, i.e., information about volunteering or providing individual help to neighbors; and off topic, i.e., the posts

are not within the scope of disaster-related topics. The specific definition and examples of posts are available in Table 5. A set of posts were split-recorded by two coders and they exchanged and checked the codes for intercoder agreement. The coders agreed on theme codes in 96% of cases and the disagreements were resolved through discussion and consensus. The proportion of each theme in daily communications were calculated by taking into account the number of comments belonging to the posts coded as the theme. This computing approach is beneficial to exhibit the contribution of themes to the formation of social ties as well as emergent social cohesion.

3.4.6 Assortative Mixing in Networks

A good measure of the extent to which the nodes with similar degree or attribute connect to each other is assortativity. To quantify the level of assortative mixing of attributes in a community, this study employed the Eq. **(12)** to compute the assortativity coefficient (Newman, 2003):

$$r = \frac{Tr(M) - \|M^2\|}{1 - \|M^2\|} \qquad \textbf{(12)}$$

where M is the mixing matrix of the attribute, and $\|M^2\|$ is the sum of all elements of the matrix M^2. Here, for the purpose of our analysis, the examined attribute is users' neighborhoods. The assortativity coefficient ranges from -1 to 1. The larger the assortativity coefficient, the more perfect the assortative mixing. Specifically, $r = 1$ when there is perfect assortative mixing, $r = 0$ when there is no assortative mixing, and r is negative when there is disassortative mixing (Newman, 2003).

CHAPTER IV

UNDERSTANDING DYNAMICS OF PHYSICAL NETWORKS FROM HUMAN DIGITAL TRACES IN EMERGENCIES*

In this study, we propose a contagion model as a simple and powerful mathematical approach for predicting the spatial spread and temporal evolution of the onset and recession of floodwaters in urban road networks. A network of urban roads resilient to flooding events is essential for the provision of public services and for emergency response. The spread of floodwaters in urban networks is a complex spatial-temporal phenomenon. This study presents a mathematical contagion model to describe the spatial-temporal spread and recession process of floodwaters in urban road networks. The evolution of floods within networks can be captured based on three macroscopic characteristics—flood propagation rate (β), flood incubation rate (α), and recovery rate (μ)—in a system of ordinary differential equations analogous to the Susceptible-Exposed-Infected-Recovered (SEIR) model. We integrated the flood contagion model with the network percolation process in which the probability of flooding of a road segment depends on the degree to which the nearby road segments are flooded. The application of the proposed model is verified using high-resolution historical data of road flooding in Harris County during Hurricane Harvey in 2017. The results show that the model can

---

* This chapter is reprinted with permission from "A Network Percolation-based Contagion Model of Flood Propagation and Recession in Urban Road Networks." by Fan, C., Jiang, X., and Mostafavi, A., 2020. *Scientific Reports*, Aug, 10, 13481.

monitor and predict the fraction of flooded roads over time. Additionally, the proposed model can achieve 90% precision and recall for the spatial spread of the flooded roads at the majority of tested time intervals. The findings suggest that the proposed mathematical contagion model offers great potential to support emergency managers, public officials, citizens, first responders, and other decision-makers for flood forecast in road networks.

4.1 Introduction

Given the essential role transportation plays in emergency response, provision of essential services, and maintenance of economic well-being (Ganin et al., 2017), the resilience of urban road networks to natural hazards, especially flooding events, has received increasing attention (Ganin et al., 2017; Koks et al., 2019). Floodwaters in urban networks propagate over time and space, inducing a great deal of spatial-temporal uncertainty vis-a-vis protective actions, such as evacuation, and rapid emergency response (Wang et al., 2019). Developing effective prediction tools to forecast the characteristics of flooding events is critical to the enhancement of urban road network resilience (Chao Fan et al., 2020d).

Multiple studies have explored the spatial-temporal properties of floods in urban networks, including impact evaluation of environmental stress (Lhomme et al., 2013; Pulcinella et al., 2019; Serre et al., 2018) and cascading effects in road networks (Guan and Chen, 2018; Lu et al., 2018). In particular, empirical studies adopting remote sensors (Mousa et al., 2016), hydraulic data (Ramsey et al., 2011), or satellite images (Dixon et al., 2006) have attempted to capture the properties of urban flooding. Temporal evolution

of flood status is driven by the time-dependent profile of environmental stress, such as the duration of rainfall in hurricanes (Ramsey et al., 2011). This temporal information facilitates identification of the outbreak and inflection points for flooding in affected networks. Flooding also exhibits high spatial correlation (Youssef et al., 2015) in which the co-located road segments are more likely to be flooded in the immediately succeeding time increments, indexed to digital timestamps on the model (Douglas et al., 2000). Specifically, a hydrologic study has shown that proximity to flooded areas is a significant predictor of regional flood frequency based on regionalized flood quantiles for 575 Austrian catchments (Merz and Blöschl, 2005). While empirical studies illustrated the complex spatial-temporal dynamics of floods, their capabilities for flood prediction often rely on various types of hydro-geomorphological monitoring datasets and intensive computation (Nayak et al., 2005). Due to delay and computational cost issues, the existing physics-based hydrodynamic models may not be conducive to providing timely and reliable predictions for the spatial-temporal spread of floods and the failure of road segments within short time periods (Hossain et al., 2007).

To overcome the limitations in empirical models, machine learning techniques have been proposed and tested for predicting the spread of floodwaters in urban areas (C Fan et al., 2020; Mosavi et al., 2018). Compared to the hydrodynamic methods, machine learning models, such as multiple linear regressions (Tsakiri et al., 2018), deep neural networks (Sankaranarayanan et al., 2019), and Bayesian forecasting models (Dong et al., 2019b) require fewer input parameters, so that the models can be easily trained on historical flood event data. For example, Khosravi et al. tested four decision tree-based

machine learning models—logistic model trees, reduced error pruning trees, naïve Bayes trees, and alternating decision trees—for flood mapping (Khosravi et al., 2018). The results show that, with adequate training, these models can achieve greater than 80% accuracy for predicting the flooded locations. Youssef et al. integrated frequency ratio and logistic regression models to evaluate the correlation between flood occurrence and various potential factors and developed a model providing an acceptable prediction accuracy (Youssef et al., 2015). Although existing machine learning models can achieve good predictive performance to capture the flood propagation in urban networks, these models are limited due to their dependence on large sets of historical data for model training. In addition, existing machine learning models are designed to capture only the propagation of flood in urban areas. The flood recession process, which is also important for assessing the resilience of urban networks, is often ignored by the existing machine learning models.

Recognizing the limitations of existing models, there is a real need for mathematical models that can capture the spatial-temporal evolution of flooding without relying on a variety of input parameters and historical data such as the volume of waters and the width of the roads. Recent studies have demonstrated a surprisingly significant similarity among spreading processes in different systems, including the spread of traffic congestion in transportation, the contagion of infectious disease in populations, the diffusion of ideas in social networks (Chao Fan et al., 2020b), as well as the evolution of flooding in urban road networks (Barabási, 2013; Saberi et al., 2019). Motivated by these studies, our goal in this research was to describe the floodwater spreading process using

generalized mathematical contagion models, such as classical epidemic models (McCluskey, 2010). Existing epidemic models offer an analytical and numerical framework to quantify and forecast multiple spread phenomena in a variety of contexts. In particular, the popular susceptible-infectious-recovered (SIR) model created the basic building blocks of epidemic modeling using infectious and recovery rates. These mathematical models have two fundamental hypotheses: compartmentalization, in which each entity is associated with a state or compartment; and homogenous mixing, in which each entity has the same chance of contacting an inflected entity (Barabási, 2013). In the context of flooding, each road cell is associated with a state, functional-flow or flooded. Hence, the flooding propagation problem fits this compartmentalization hypothesis. While these hypotheses simplify the modeling of contagion by eliminating the need to know the structure of the networks, the mathematical models can still capture the temporal evolution of the fraction of infected entities in the networks very well.

Flood risk prediction is a task that should take into account both the temporal and spatial natures of the floodwater in road networks. Urban flood risk characterization requires not only knowledge of the fraction of flooded roads at each timestamp, but also needs to identify the geographic locations of flooded roads as flooding unfolds. Hence, pure mathematical models are not able to satisfy these requirements. To this end, the network percolation process has gained attention recently because it enables to capture of the propagation process through the topological connectivity in networks (Gao et al., 2012). As defined in percolation theory, the spread of infection relies on the probability of the infected neighbors, in which the heterogenous mixing assumption is held in local

components of the networks (Ball et al., 1997). Specifically, the infection spreads from an initial node along edges of the percolated network (Miller, 2009). Hence, the percolation process reflects the "amplification" effect of neighbors and weakens global network interactions. An infection is more likely to be transmitted to those the node comes encounters. This characteristic is essential for flood propagation prediction in urban networks since it considers the spatial co-location and constraints of urban networks. Without the temporal information about the fraction of flooded roads, however, the percolation process would fail to capture the temporal evolution of flooding in urban networks.

This study proposed and tested a network percolation-based contagion model that integrates the mathematical framework and network percolation process to predict the spatial propagation and temporal evolution of flooding in urban road networks. The mathematical framework fits the temporal dynamics of the flood situations, and the percolation process identifies locations of flooded road segments. To illustrate the performance of the model, we applied it to a case study of flood evolution in Harris County road networks during Hurricane Harvey. Potential control strategies are also identified based on the outcomes of the model in the case study.

4.2 The network percolation-based contagion model

The proposed model is composed of four components: road network modeling, flood spread characterization, flood percolation process, and model evaluation. This epidemic-like model of flood spread process in urban road networks considers both global

dynamics of flood scales and local probability of affecting other co-located roads within a set of neighbors.

4.2.1 Road Network Modeling

Road networks contain hundreds of thousands of road segments, most of which are quite short, about 100 meters to 800 meters each. The traffic status information collected at the road segment level provides sufficient spatial resolution to precisely estimate the scale of flooding in road networks.

Definition 1. A road segment is a basic unit with a starting point and an ending point, which can be assembled into a whole road in the order of the points.

Each point is associated with a longitude and a latitude so that it can be located on a geographical map. Then, a road segment can be represented as $(lat_s, lng_s, lat_e, lng_e)$, where lat_s and lng_s are the latitude and longitude of the starting point, while lat_e and lng_e are the latitude and longitude of the ending point.

Although road segments enable good resolution for understanding the situation in urban networks, flooded areas are usually not restricted in a banded road segment. Floodwaters tend to start from a point and spread in all directions. In addition, massive segments and their complex connections in the networks would also cause intensive computational cost. Hence, in modeling road networks, segment-to-segment modeling is limited to follow the nature of flood spread and achieve efficient computation. To this end, grid decomposition, a commonly used method (Zhou et al., 2016), is adopted in this study to generate equal-sized cells and divide the study area into small regions (see Figure 13).

Definition 2. A road cell is a square over a rectangular projection of the geographical map.

The spatial boundary of the cell can be represented as a set of geo-coordinates $(lat_{bl}, lng_{bl}, lat_{ur}, lng_{ur})$, where lat_{bl} and lng_{bl} are the latitude and longitude of the bottom left corner, while lat_{ur} and lng_{ur} are the latitude and longitude of the upper right corner. To covert the road segments to grid, we apply the following criteria to the road network:

$$s_i \in grid_j, \text{ if } lat_{bl} \leq \frac{lat_s + lat_e}{2} \leq lat_{ur} \text{ and } lng_{bl} \leq \frac{lng_s + lng_e}{2} \leq lng_{ur} \quad \textbf{(13)}$$

After grid decomposition, the road network assembled from road segments could be described as a series of cells. In practice, multiple factors would influence the outcome of grid decomposition. For example, a large cell would include many segments, which might lead to losing spatial resolution. Accordingly, the model would further lose the capability of capturing the spatial spread of flood. On the other hand, a small grid that cannot cover at least one road segment will partition the network into discontinuous components, and subsequently increase the computational cost. Hence, grid decomposition requires pre-testing to ensure that a cell in the grid is able to maintain spatial resolution without unduly burdening computation.

Once the road segments are assigned to cells, we remove cells lacking segments to reduce computational cost. The remaining cells form a network in which the cells are considered as nodes, and their shared borderlines are considered as links. By doing so, we can construct an undirected grid network $\mathcal{G}$ with average degree of $\langle k \rangle$ to represent the topology of the road networks. Average degree of a road cell is the average number of

adjacent cells per cell in the road network. To model the flood propagation and process, we then associate a dynamical binary state variable x to each of the N cells (also called nodes) of the grid network $\mathcal{G}$, such that $x_i(t) \in \{0,1\}$ represents the flood status of node i at time t. Using a standard notation, we divide the cells into two classes, functional flow (F) and flooded (C), corresponding respectively to the values 0 and 1 of the status variable x. Functional flow is a state in which traffic can utilize a road (regardless of traffic level). In the context of flooding spread process, the status C represents the cells which have been flooded. At each time t, the macroscopic flooding situation is given by the fraction of flooded cells $c(t) = \frac{1}{N}\sum_{i=1}^{N} x_i(t)$.

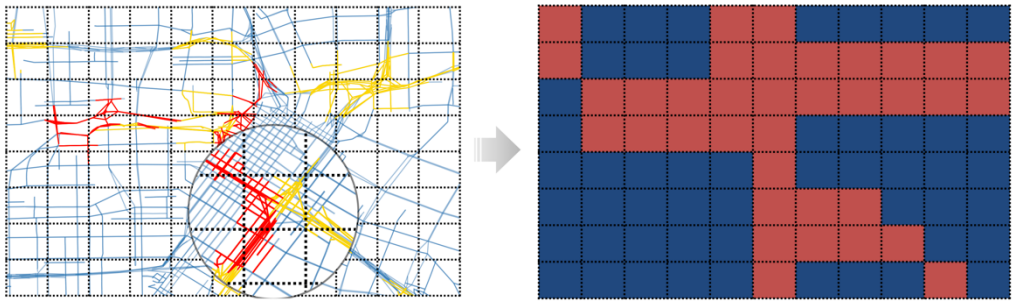

Figure 13 A schema of converting flooding status from a road network to grid.

4.2.2 Flood Spread Characterization

The flood propagation and recession process are temporally and spatially variant. To capture the temporal nature of flood evolution in urban road networks, the proposed model considers macroscopic characteristics to predict the temporal evolution of floodwater spread in urban networks.

In the first step, we define four flooding statuses for a cell: functional flow, exposed, flooded, and recovered, statuses by including the temporal attributes. $C(t)$ represents the number of flooded cells in the network at time t; $F(t)$ represents the number of functional flow cells at time t; $E(t)$ represents the number of cells that are in flood incubation stage (i.e., roads in the path of approaching floodwater but on which traffic still moves) at time t; and $R(t)$ represents the number of cells that have recovered from flooding at time t. Given a grid network $\mathcal{G}$ with an average degree of $\langle k \rangle$ and N nodes, each cell in the network has functional flow at time $t = 0$. That is, $F(t = 0) = N$ and $C(t = 0) = 0$. The flood initially occurs at a set of nodes and then propagates throughout the network. From a macroscopic perspective, a cell in the undirected network is on average connected to $\langle k \rangle$ other cells. The neighbors of a flooded cell are exposed to flood at a rate of β. In modeling the temporal evolution, the connections of the cells are assumed to be homogeneous, which forms the basis to formulate a general differential equation system. Then, the probability of a flooded cell being connected to a functional-flow link is $F(t)/N$ at time t. Therefore, a flooded cell comes into contact with $\langle k \rangle F(t)$. Since $C(t)$ flooded cells have water flowing, each at a rate β, and the exposed cells become flooded at a fixed rate α, the average number of new exposed cells $dE(t)$ during a unit timeframe dt is determined as follows:

$$\frac{dE(t)}{dt} = \beta\langle k \rangle \frac{C(t)\big(N - C(t) - E(t) - R(t)\big)}{N} - \alpha E(t) \qquad \textbf{(14)}$$

The exposed cells are not completely inundated, and traffic can still pass through, but they could be flooded within the next few timestamps. We call this stage, flood

incubation stage. The defined four statuses of the road cells are the only statuses that a road cell could have. Hence, the sum of the four status variables should be N. That is, $N = C(t) + E(t) + F(t) + R(t)$. To capture the fraction of the cells in each status, we use the following variables: $c(t)$ to represent the fraction of flooded cells in the grid network at time t; $f(t)$ to represent the fraction of functional-flow cells in which all road segments are accessible at time t; $r(t)$ to represent the fraction of recovered cells from flooding at time t; and $e(t)$ to represent the fraction of cells that are exposed to flooding but still in flood incubation at time t. Then, the differential equation for the change rate of exposed cells can be derived as follows:

$$\frac{de(t)}{dt} = \beta\langle k\rangle c(t)\big(1 - c(t) - e(t) - r(t)\big) - \alpha e(t) \quad \textbf{(15)}$$

where, the product of $\beta\langle k\rangle$ is called transmission rate or transmissibility. The transmissibility can be used to measure the capability of floodwater to spread in an urban network under the same propagation rate. This also allows us to understand the effects of the topological structure of an urban network on the transmission of floodwaters.

Since a fraction of the functional-flow cells become exposed at each timestamp, the decreasing rate of the fraction of functional-flow cells can be represented by:

$$\frac{df(t)}{dt} = -\beta\langle k\rangle c(t)\big(1 - c(t) - e(t) - r(t)\big) \quad \textbf{(16)}$$

Simultaneously, in a unit timeframe, a fraction of exposed nodes would be flooded at a rate α, and some of the flooded cells recover at a rate μ. Hence, the changing rate of the fraction of flooded cells and the fraction of recovered cells can be formulated as:

$$\frac{dc(t)}{dt} = -\mu c(t) + \alpha e(t) \quad \textbf{(17)}$$

$$\frac{dr(t)}{dt} = \mu c(t) \quad \textbf{(18)}$$

Evidently, in a large-scale network where N is large, the probability of a flooded cell being connected to a functional-flow cell could be close to zero. At the macroscopic scale, the assumption of homogeneous mixing makes the prediction more tractable and robust. It should also be noted that the model does not include mortality (i.e., significantly damaged roads that would not be functional after the floodwater recedes). Since it is not often the case that a flooded road cell is severely damaged, excluding the mortality is reasonable and realistic. Based on the former constructs, the model component derived for capturing the temporal dynamics of flooding scale using macroscopic characteristics is established (Figure 14A).

4.2.3 Network Percolation Process

The spatial nature of floodwater spread in urban networks is modeled using a network percolation process. The network percolation process describes the contagion effects of a flooded cell on its network neighbors (Teng et al., 2016). Specifically, the cells whose neighbors are flooded are more likely to be flooded than the cells whose neighbors are not flooded (Barabási and Pósfai, 2016). Similarly, floodwater is more likely to recede first from the cells whose neighbors are not flooded compared to the flooded cells whose neighbors are also flooded. To characterize this spatial aspect of flood spread, we define the probability of a node to be flooded or to be recovered in the next timestamp based on

the number of flooded neighbors. The propagation and recession processes are modeled as described below, respectively (see Figure 14B).

In the propagation process, the percolating cluster is a set of road cells which are flooded next to another bounded by functional-flow cells at a specific time interval. Since the extreme event, Hurricane Harvey in this study, affected a large area, multiple percolating clusters presented in the road network. They were spatially scattered across the network at the early stage of flooding. As the event progressed, some clusters broke through the bound and formed larger percolating clusters. We can obtain the number of flooded cells $N_c^{(t)}$ at a unit timestamp t by the predicted fraction of flooded nodes $c(t)$ and the total number of cells in the networks. The calculation can be formulated as:

$$N_c^{(t)} = N \cdot c(t) \tag{19}$$

The flooded cells at the unit timestamp t are composed of flooded cells $N_c^{(t-1)}$ at the last timestamp, plus the additional flooded cells $N_c^{(t)}$ at timestamp t, excluding the recovered cells. In reality, however, the fraction of recovered cells is negligible during the propagation period before reaching the flooding peak. Hence, in our model, the number of additional flooded cells, $N_p^{(t)}$, in the current timestamp t is obtained by:

$$N_p^{(t)} = N_c^{(t)} - N_c^{(t-1)} \tag{20}$$

As discussed earlier, the spatial pattern of the propagation process ($F \rightarrow E \rightarrow C$) is controlled by the fraction of flooded neighbors of a cell. Hence, we assign the probability of flooding (i.e., the fraction of flooded cells among all neighbors) to the unflooded cells. Each unflooded cell will be assigned a probability $p_i^{(t)} \in \left\{p_1^{(t)}, p_2^{(t)}, \cdots\cdots, p_k^{(t)}\right\}$, where

$k \leq N$. Then the cells are sorted based on their probabilities of flooding from high to low. The additional flooding cells at the timestamp t are identified from the cells with high probabilities of flooding, subject to the number of additional flooded cells, $N_p^{(t)}$. Hence, the percolation threshold is selected based on the number of additional flooded cells predicted by the proposed contagion model and the sorted probabilities of flooding to other cells.

Like the propagation process, flood recession ($C \rightarrow R$) can also be modeled in a way similar to the network percolation process. The percolating cluster is the set of road cells with functional flow next to another bounded by flooded cells. We first calculate the number of recovered cells $N_r^{(t)}$ at the timestamp t based on the value of $r(t)$ obtained from the flood dynamics model:

$$N_r^{(t)} = N \cdot r(t) \tag{21}$$

Floodwater starts receding after the peak of flooding; in actual experience, additional flooded cells usually do not occur. Hence, in the spatial prediction, the number of flooded cells $N_c^{(t)}$ at the current timestamp t is equal to the number of flooded cells $N_c^{(t-1)}$ at the last timestamp $t-1$, minus the number of recovered cells $N_r^{(t)}$ at the current timestamp t. The calculation can be formulated as:

$$N_c^{(t)} = N_c^{(t-1)} - N_r^{(t)} \tag{22}$$

In the next step, we assign the probabilities of flooding (i.e., the fraction of flooded cells among all neighbors) to the flooded cells. Each flooded cell is assigned a probability $p_i^{(t)} \in \left\{p_1^{(t)}, p_2^{(t)}, \cdots\cdots, p_k^{(t)}\right\}$. That is, the probability of floodwater receding is $1 - p_i^{(t)}$.

In a manner different from the propagation process (in which the cells are sorted based on their probabilities of flooding from high to low), we sort the cells based on their probabilities of flooding from low to high (i.e., probabilities of floodwater receding from high to low). The recovered cells at timestamp t are assigned a low probability of flooding.

Using the above calibration in the percolation process, we can mitigate the homogeneous mixing assumptions in the flood spread characterization model by adopting local heterogenous flood probabilities and achieve high accuracy in predicting the spatial distribution of flooded cells in urban networks.

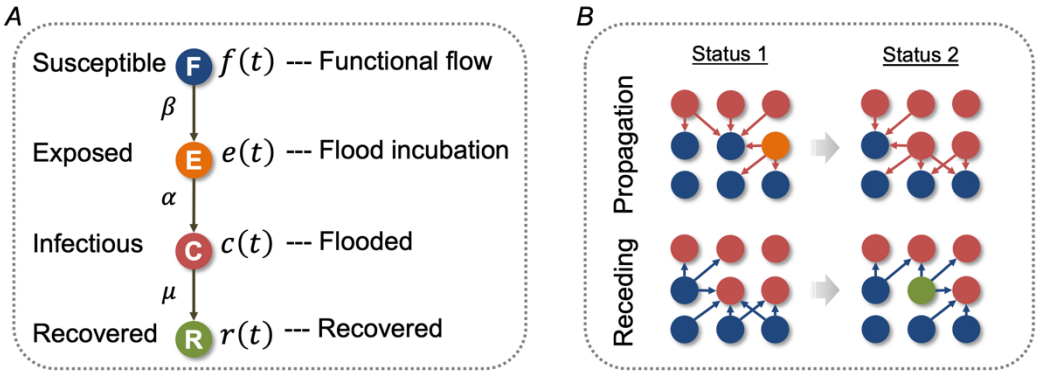

Figure 14 The network percolation-based contagion model of flood propagation and recession in urban road networks.

4.2.4 Model Evaluation

We employed two metrics to evaluate the performance of the model for predicting the temporal evolution and spatial propagation of flooding spread in urban networks. The first component of the model is a system of differential equations to capture the magnitude of flooded cells in networks. The objective of this component is analogous to addressing

a fitting curve. Hence, we use the root mean square error (RMSE) (Chai and Draxler, 2014) to measure the error of the model:

$$RMSE = \sqrt{\sum_{i=1}^{n} \frac{(\hat{y}_i - y_i)^2}{n}} \quad \textbf{(23)}$$

where, $\hat{y}_i$ is the predicted value, y_i is the observed value, and n is the number of observations. Ignoring the division by n under the square root, the formula can be considered as a formula for Euclidean distance between the vector of predicted values and observed values. Hence, the RMSE is a normalized distance between the predicted outcomes and the observations which can be used to evaluate the model accuracy. This can also serve as a heuristic for a training model, which will be used in a pattern search algorithm to obtain the numerical solution for the model。

The spatial nature of the flooding propagation and receding is captured by the outcomes of the flood spread characterization model and the network percolation process. The intersection between the set of predicted flooded road cells and the set of observed flooded road cells indicates the precision and recall of the model (Buckland and Gey, 1994). They are formulated as follows:

$$Precision = \frac{True\ positive}{True\ positive + False\ positive} \quad \textbf{(24)}$$

$$Recall = \frac{True\ positive}{True\ positive + False\ negative} \quad \textbf{(25)}$$

where true positive is an outcome where the model correctly predicts the flooded class, false positive is an outcome where the model incorrectly predicts the flooded class, and

false negative is an outcome where the model incorrectly predicts the unflooded class. The calculated precision and recall allow us to assess the performance of the model by identifying the specific correctly predicted road cells.

4.3 Results

4.3.1 Study Context and Data Collection

To illustrate the application and performance of the proposed network percolation-based contagion model of flood spread, we tested the model using high-resolution data related to flooded roads in Harris County during Hurricane Harvey in 2017. Hurricane Harvey was a Category 4 storm that made landfall in Houston (Harris County) on August 26, 2017, dissipated inland August 30, 2017 (Sebastian et al., 2017). The torrential rainfall brought by Harvey caused intensive flooding in Harris County, where the floodwaters damaged more than 290 roads and highways (Ibrahim, 2017). The flooding occurred August 27 through on September 4, 2017. We collected the traffic data for 19,712 roads in Harris County from INRIX, a private company providing location-based data and analytics. The INRIX traffic data covers all available road roads - from interstates to intersections, country roads to neighborhoods. The data includes the average speed for each road segment in 15-minute intervals. The timeframe of data is August 1 to September 30, covering the entire flooding period. In this case study, we used squares with a length of 400 meters for generating the grid network.

In the INRIX dataset, the flooded road segments can be identified by a designation of NULL for average speed, meaning there was no vehicle driving through the segment.

Comparing the data before and after Hurricane Harvey, we found that the NULL average speed appears only during the flooding period. By cross-checking the flooded roads on government reports, most of the roads with NULL speed were flooded at that time. Although the average speed data was collected in 15-minute intervals, the flood situation did not evolve significantly in such a short time period. To better capture the flood propagation and receding process, we aggregated the data at 4-, 8-, and 12-hour intervals to test the performance of the model. Each interval was assigned a binary value of flooding status to the road segments based on their average speed. As documented in the model section, the value would be 0 if there is no NULL speed record, and the value would be 1 if there is a NULL speed record in the dataset (indicating functional flow status for the roads).

4.3.2 Pattern Search for Parameter Estimation

It is often the case that the analytical solution to the differential equation system cannot be generated. That is because the functions are usually not continuous or differentiable (Davidon, 1991). To efficiently estimate the parameters in the proposed model, we applied a global pattern search algorithm (Raja, 2014) as a derivative-free numerical optimization method to fit the curves for each variable (i.e., $f(t)$, $e(t)$, $c(t)$, and $r(t)$) (Saberi et al., 2019). The objective function in this optimization process is the RMSE, which will be minimized by searching for the optimal propagation rate β, recovery rate μ, and exposed rate α. To start with this algorithm, we first specified initial values for the three parameters. The change of the parameters could be either increased or decreased in each step. The algorithm would compute the RMSE for each step until it finds an

optimal point at which the current RMSE is smaller than the previous one. If the algorithm cannot find the optimal point using the current step size, it will use half of the current step size and repeat the computing process. Then all three parameters will move to the optimal values. The algorithm runs iteratively until one of the stopping criteria is met: the maximum number of iterations is reached or the step size is smaller than a certain threshold. In this study, we set the maximum number of iterations to be 2,000, and the threshold for the step size is 0.0001. The initial values for models with time intervals are the same, $\beta = 1$, $\alpha = 1$, and $\mu = 0$. Through our tests, the selection of values around these initial values would yield similar results for the parameters.

Table 3 shows the estimated values for the parameters and the optimized RMSE for three models. The RMSE increases a little bit with the increase of the length of the time intervals. That is because the fraction of road cells that are flooded (i.e., $c(t)$) is greater in longer time intervals than in shorter time intervals. But, all three models fit the flood spread patterns in road cells well since the RMSE value accounts for only a very small proportion of the peak value of $c(t)$. In addition, the propagation rate β remains the same across three models. This result indicates that the length of the time interval does not affect the capability of the model to predict flooding propagation. The flood incubation rate α and recovery rate μ, however, decrease with the increase in the length of the time interval. That is because the number of flooded road cells increases with the increase in time intervals. Hence, a great number of road cells would be in the flood incubation state, which leads to a low rate of α (Figure 15D, E, and F). As such, the recovery rate must be small to represent a large number of flooded road cells. This result reveals that the length

of the time interval has an influence on parameter estimation, but it does not significantly affect the fitting performance.

Table 3 Estimated values for the parameters in the contagion model.

Length of time interval	RMSE	β	α	μ	β/μ
4 hours	0.020	0.9998	0.1267	0.8348	1.1977
8 hours	0.024	0.9998	0.0830	0.4073	2.4547
12 hours	0.027	0.9998	0.0780	0.2702	3.7002

4.3.3 Prediction results

Once the optimal values for the parameters are obtained, we can capture the temporal evolution of flood propagation and recession in urban network by showing the spread curves for each variable (i.e., $f(t)$, $e(t)$, $c(t)$, and $r(t)$) (Figure 15D, E, and F).

Basic reproduction number $R_0 = \beta/\mu$ is used as a measure of the number of secondary flooded cells generated by the first flooded cell over the course of the flooding unfolding (Weitz and Dushoff, 2015). Mathematically, when R_0 is smaller than 1, the propagation will not occur as the recovery rate is greater than the propagation rate (Chowell et al., 2004). In the Hurricane Harvey case study, the estimated R_0 is greater than 1 across all three models and increases with the length of time interval (see Table 3). This result explains how rapidly floodwaters spread. The closer the value of R_0 to 1, the more stable the flooding situation is. In this case, we can observe that the flood situation would change more slightly if the time interval is shorter than 4 hours, since R_0 would be close to 1. When the time interval increases from 4 hours to 8 hours, the value of R_0 jumps

from 1.20 to 2.45, meaning that in every 4- to 8-hour increment, the flood situation would change more drastically.

In addition, the changes in $c(t)$ allow us to predict the extent of flood in the networks and critical timestamps for breakout and peak (see Figure 15A, B, and C). The figures show the flood spread characterization in Eq. **(15)**-**(18)** are fit to the empirical flooding data very well. We can observe that at the beginning of the hurricane (the hourly timestamps in day 1 and day 2), the number of flooded cells grew exponentially between every 4-, 8-, or 12-hour increment, and reached the peak in the middle of day 3. After that timestamp on day 3, the flood receded gradually. Using the results, we can estimate the time that the urban road network needs to recover from flooding. In this case, evidently, the recovery rate was slow, which led to a long period for recovery at some severely flooded locations.

In the next step, we examined the predictive performance for both spatial spread and temporal evolution for the flooding, shown in Figure 16. All models perform very well in terms of predicting the specific locations of flooded segments based on the flooding data at the last timestamp. The best performance of these models appears during the peak and receding period, while the performance is not particularly good at the beginning of the flooding. That is because the locations of the initial flooded cells depend on the rainfall magnitude and spatial patterns of precipitation in different areas. The emergence of initial flooded cells is difficult to be identified by the model without additional information about the precipitation pattern. After a few hours, however, the flood propagation and recession closely follow the percolation process since the majority of the initial flooded cells were

identified correctly at that time. Hence, the model could predict the spatial spread of flooding after the locations of initial flooding are identified. In terms of the precision metric, the best model is the model based on a 4-hour time interval, and with the increase of the length of the time interval, the performance of the model decreases a little bit. In terms of the recall metric, these three models show similar performance and show promise for special and temporal floodwater characteristics, especially during the peak and recession period.

The three sets of figures in Figure 17 show the true positive and false positive results for the road segments in the network. Here we converted the cells back to their segments. All segments in the flooded cells are considered flooded segments. We plotted three figures for each model at different timestamps: beginning, peak, and recession periods. As we observed in the figure, the flooding initially occurred at different locations in the timestamp of the beginning period (Figure 17, left panel). With the continuous rainfall, the floodwater propagated from the initial flooded road segments to their neighbors (middle panel of Figure 17). After Hurricane Harvey dissipated on August 30, the flood started to recede from the road segments at the edge of the flooded area (Figure 17, right panel). The figures show that more than 90% of the flooded segments are captured by the proposed model, and the predictive performance decreases a bit with the increase of the length of the time interval. These findings support that the proposed model can accurately predict the spatial and temporal characteristics of flooding spread in urban networks.

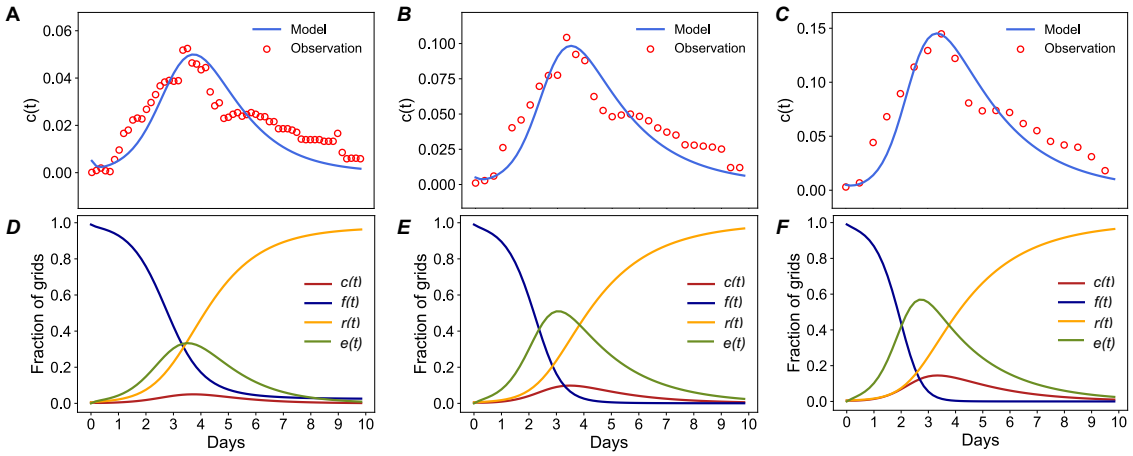

Figure 15 Four-state model of flood propagation and recession in the road network. Analogous to the susceptible-exposed-infected-recovered model subject to a time-varying disaster profile. Day 0 is August 26, 2017; and Day 9 is September 4, 2017. A and D are the results from the model for 4-hour time interval; B and E are the results from the model for 8-hour time interval; and C and F are the results from the model for 12-hour time interval.

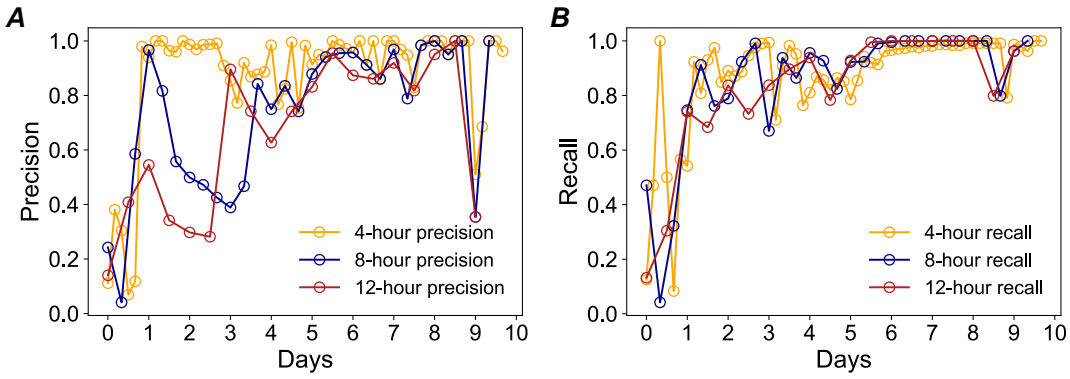

Figure 16 Prediction performance of the proposed model for flood propagation and receding. (A) Precision of the model for different time intervals; and (B) Recall of the

model for different time intervals. Day 0 is August 26, 2017; and Day 9 is September 4, 2017.

Figure 17 Examples of three prediction models for different phases of the flooding period (i.e., propagating, peak, and receding phases). (A) the model for predicting the situation in next 4 hours; (B) the model for predicting the situation in next 8 hours; and (C) the model for predicting the situation in next 12 hours. The true positive (yellow) and false positive (red) road segments are all actual flooded road segments from the empirical INRIX data in a specific time interval.

4.3.4 Adaptation of the model

The proposed network percolation-based contagion model could be used to model flood spread in other regions and flooding events. Different extreme events have different attributes such as varying durations, intensities and geographical scales, which result in varying numbers and durations of flooded roads. To demonstrate the adaptation of the model in other contexts, we conducted further controlled experiments to examine the adaptation of the model to different topological properties of urban networks (average degree), the propagation rate which reflects the stress of rainfall, and flood incubation rate and recovery rate. We change the value of one parameter that was learned from the INRIX data and control other parameters to be constant as shown in Table 3. The results show the extent to which different parameters could affect the predicted outcomes. This experiment also provides evidence for supporting the generalizability of the proposed contagion model for different cities and various intensities of flooding.

First, we tested the effect of average degree of an urban network on the flood dynamics by keeping the same values for other parameters. Figure 18A shows the changes in model results for predicting the flood status in 4-hour time intervals. With the increase of the average degree $\langle k \rangle$ of the networks, the growth rate of the flooded cells increases significantly during the propagation phase. That is because the network with a large $\langle k \rangle$ will allow the flooded road cells to infect more neighbors, which expedites the spread of flood even when the propagation rate remains the same. In addition, a large $\langle k \rangle$ would decrease the time to reach the peak of flooding since the flooded cell would have more

connected neighbors. In contrast, a small $\langle k \rangle$ would lead to a longer period of flooding, although the fraction of flooded cells will not reach to the same flooding scale as the urban networks with a large $\langle k \rangle$.

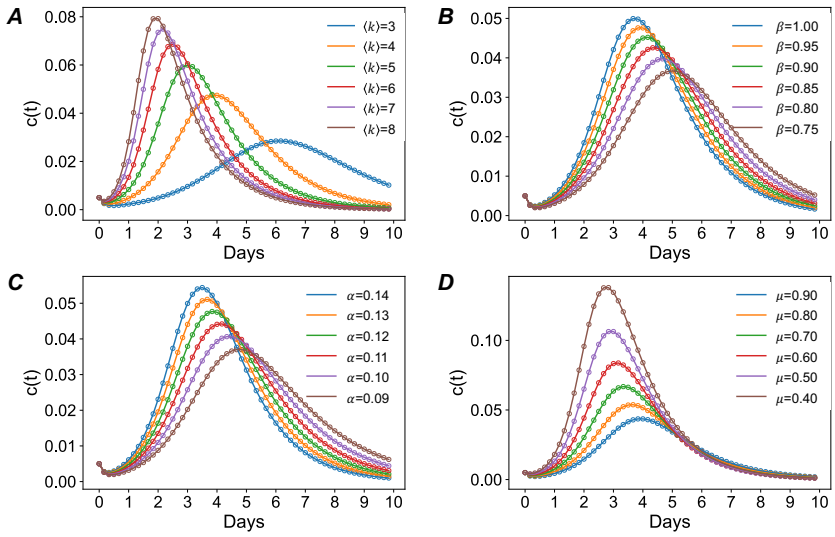

Figure 18 Test results for the adaptation of the model using different topological structures of urban road networks (A); different propagation rate (B); different incubation rate (C); and different recovery rate (D).

We further tested the effects of the three macroscopic parameters (i.e., β, α, and μ) on the predicted flood spread (see Figure 18B, C, and D). On the one hand, similar to the impact of the average degree, the increase in the propagation rate β and the flood incubation rate α would decrease the time to reach the peak of flooding and the number of flooded cells at the peak, but increase the time to recover to the normal situation. On the other hand, an increase in the recovery rate μ significantly decreases the number of flooded cells at the peak, but the time to reach the peak and the time to recover to a normal

situation are not changed significantly. The results of these experiments show that by adjusting parameters, the model can be adapted to different scenarios with various intensities of flood events and topological structures of urban networks.

4.4 Discussion and Concluding Remarks

We have presented a predictive model which integrates flood spread characterization and network percolation processes to forecast the propagation and recession of flood in urban road networks. The model is formulated as a system of ordinary differential equations relying on three characteristics: flood propagation rate β, flood incubation rate α, and recovery rate μ, analogous to the SEIR model. Using the output of the model, the network percolation process is obtained to model the spatial patterns of the flooded road cells over time. The study showed the application of the proposed model in an empirical case study of urban flooding in Harris County road networks during Hurricane Harvey in 2017. The application of the model using empirical data informs about some key findings and implications for urban flood risk prediction.

First, the extent to which flooding builds up in a network and how fast it recovers are shown to be dependent on the basic reproduction number $R_0 = \beta/\mu$, which can help us infer the effective time period in response to the flooding in road networks. In the case study, we found that the basic reproduction number changed significantly when the time interval increased from 4 hours to 8 hours. This result indicates that flood situation evolves slightly in time intervals shorter than 4 hours, but, the situation changes dramatically for time intervals that are longer than 4 hours. Hence, to better monitor the flood in road

networks, the status of roads should be observed in every 4 hours. While urban networks in different cities may have different topological properties and experience different rainfall magnitudes, the proposed model can be adapted by adjusting the parameters. Results can inform the decision-makers about the spatial propagation and temporal evolution of flooding.

Second, the spatial mechanisms of flood propagation and receding in urban networks is captured based on a network percolation process. This finding highlights the contagion effects of a flooded cell on its neighbors. Since the road cells are spatial networks, different from social contact networks, the spread of flood would be limited by geographical constraints. Hence, the local contagion from a cell to another cell through the link connecting them would be the main spreading pattern. Practically, this finding provides an important implication for flood control in urban systems. One effective control strategy would be to increase drainage capacity and to build retention ponds around the roads with a high likelihood of flooding. This strategy can reduce the proportion of flooded cells among the unflooded cell neighbors, which can contribute to reducing the probability of flooding in the next timestamp.

Third, the model and its application show good performance in predicting the scale and locations of flooded road cells in disasters. In addition to the response strategies, this model could also support proactive strategies for coping with future flood events. In particular, the proposed model can be incorporated in an early warning system. The system can help officials and the public be aware of the flood situations in the coming hours so that they can perceive flooding risks surrounding them and make proactive preparations.

For example, cars and buses drove through floodwater during Hurricane Harvey (Bajaj et al., 2017). With the predicted outcomes of this contagion model, people can be informed about roads at a high risk of flooding in the next few hours. This predictive information could significantly contribute to reducing the economic loss of transportation agencies, and possible loss of life of residents.

Finally, the model we introduced in this paper is simple and robust and can be adapted to various phenomena. Unlike hydrodynamic models and machine learning models that rely on significant data and computational resources, the proposed mathematical model provides a simple but powerful tool for predicting the spatial-temporal evolution of flooding in urban networks. Also, the proposed network percolation-based contagion model can be adapted for modeling other network spread phenomena. Future studies can further investigate the proposed model in other general predictive tasks, such as the spread of traffic congestions in road networks (Gehlot et al., 2020), infectious diseases in human contact networks (Valdez et al., 2020), and innovations in global communities (Chao Fan et al., 2020c). This model also has some limitations; for instance, for initial flooded segments that without flooded neighbors, it is usually difficult to predict these segments without other information. Future studies can focus on improving the model to precisely predict initial flooded road segments based on rainfall magnitude and capacity of urban drainage systems. In addition, the model considers the parameters such as propagation rate being constant throughout the process, in order to provide a simple but fairly accurate tool for flood prediction. Future studies

could extend our model by considering the dynamics of the beta to improve the performance of the model.

CHAPTER V

SIMULATING URBAN MOBILITY NETWORK DYNAMICS IN EMERGENCIES FOR IMPACT ANALYSIS

The objective of this study is to propose and test an adaptive reinforcement learning model that can learn the patterns of human mobility in a normal context and simulate the mobility during perturbations caused by crises, such as flooding, wildfire, and hurricanes. Understanding and predicting human mobility patterns, such as destination and trajectory selection, can inform emerging congestion and road closures raised by disruptions in emergencies. Data related to human movement trajectories are scarce, especially in the context of emergencies, which places a limitation on applications of existing urban mobility models learned from empirical data. Models with the capability of learning the mobility patterns from data generated in normal situations and which can adapt to emergency situations are needed to inform emergency response and urban resilience assessments. To address this gap, this study creates and tests an adaptive reinforcement learning model that can predict the destinations of movements, estimate the trajectory for each origin and destination pair, and examine the impact of perturbations on humans' decisions related to destinations and movement trajectories. The application of the proposed model is shown in the context of Houston and the flooding scenario caused by Hurricane Harvey in August 2017. The results show that the model can achieve more than 76% precision and recall. The results also show that the model could predict traffic patterns and congestion resulting from to urban flooding. The outcomes of the analysis

demonstrate the capabilities of the model for analyzing urban mobility during crises, which can inform the public and decision-makers about the response strategies and resilience planning to reduce the impacts of crises on urban mobility.

5.1 Introduction

The resilience of communities to crises such as flooding, wildfires, pandemics and other extreme events hinges on a deep understanding and effective simulation of the impacts of the crisis on human and physical environment (Zhu et al., 2019). Urban mobility plays a vital role in community resilience to crises by enabling populations to access critical facilities, such as healthcare, pharmacies, and grocery stores, for instance, (Liu et al., 2019); hence, the ability to simulate and examine the impacts of crises on urban mobility is essential to effectively improve the resilience of cities (Sadri et al., 2020). Studies, including Lei et al. (Lei et al., 2020), have examined the vulnerability and resilience of transportation systems during natural disasters and other crises. The majority of existing studies focus primarily on examining the vulnerability of physical road networks (Fan et al., 2020; Dong et al., 2020) and quantifying the effects of crises on traffic patterns (Oh et al., 2020; W. Wang et al., 2020). A critical missing component is the capability to simulate crisis perturbation scenarios for predictive evaluation of the impacts on movement trajectories and traffic patterns at urban scale to inform emergency-response and resilience-planning decisions. To address this gap, the goal of this study is to create and test a deep learning model that can capture individuals' movement patterns

during normal situations and impose crisis-induced perturbations to simulate impacts on movement trajectories and traffic patterns.

With the wide use of smartphones and apps with location services, a person's digital footprints can be generated based on daily trips, which allow researchers to gather fine-grained data related to individuals' movement trajectories during normal situations for model training and prediction (Olmos et al., 2018). Prior studies have attempted to address mobility simulation through statistical models and machine-learning techniques at different scales (Yan et al., 2017). One stream of the existing studies focuses on quantitative assessments of the dynamical and statistical properties of human travel (Kitamura et al., 2000). With more prevalence of location data related to mobile phone users, González et al. (2008) demonstrated that human movement trajectories have a high degree of temporal and spatial regularity, as they follow simple reproducible patterns. This finding has significant implications for the predictability of individual mobility patterns in normal conditions. Furthermore, measuring the entropy of an individual's trajectory, Song et al. (Song et al., 2010b) showed a 93% potential predictability of human mobility under normal situations. The statistical metrics provide essential knowledge about the travel distance, radius, and frequently visited locations of humans (Song et al., 2010a). Despite these advances in the statistical characterization of aggregated human mobility patterns, limited models exist that could capture the temporal sequence of activities and spatial distribution of activities of each individual. The majority of the standard mobility models have limited capability for predicting individual mobility at a local scale, such as a neighborhood, in a specific timestamp.

With advances in machine-learning techniques and enhanced computational power, it is now possible to learn and simulate finer-grained mobility patterns, such as the sequential patterns of individual location histories (Tang et al., 2019). In particular, deep neural networks (DNN) are prevalent in learning and simulating human dynamics and density from large data sets (Li et al., 2017). For example, Wang et al. (S. Wang et al., 2020) designed a DNN architecture with an alternative-specific utility using behavioral knowledge to analyze human choices of their travel mode in normal circumstances. Hosseini et al. (Khajeh Hosseini and Talebpour, 2019) introduced a deep learning-based methodology to predict traffic state using convolutional neural networks (CNN) by taking the individual vehicle-level data as inputs. The CNN model is further improved to capture citywide crowd activities with parameter efficiency and stability (Liang et al., 2020). These deep learning techniques offer significant improvements in predicting individual mobility patterns with high resolution in terms of locations and timestamps (Wang and Sun, 2020).

Human mobility, including origin-destination matrixes and the trajectories for each origin and destination pair, however, is strongly influenced by the condition of road networks, specific gathering events, friendship effects (Cho et al., 2011), and residents' travel habits and lifestyles (Zong et al., 2019). In particular, crises such as natural disasters cause perturbations in physical infrastructure and roads that influence human movement trajectories. For example, inundated road segments and buildings would necessitate evacuation of affected residents, thus reducing travel demand in certain areas (Chao Fan et al., 2020a). Human trajectory data in the context of crises for model training and

mobility simulation are scarce, as this data is rarely recorded in historical record (Deville et al., 2014), necessitating adaptive models for simulating human mobility under crisis scenarios (e.g., flooding, wildfires, and blizzards.) Information related to movement trajectories and traffic patterns in such extreme and complex situations is rarely recorded in historical data. The lack of data makes the simulation of human mobility during crisis conditions challenging (Lu et al., 2012)

To address this information gap, this study tested an adaptive reinforcement learning model that can (1) learn individual mobility patterns from data collected from regular daily activities; and (2) simulate mobility under extreme events. The model incorporates both time and location factors as the input features and allows users (e.g., practitioners and decision makers) to adjust the environmental parameters for various application objectives in depending upon scenarios. To illustrate the application as well as the performance of the model in both prediction and application, we trained the model using data related to human mobility activities in Houston during March and April 2017, and used the model to simulate movement trajectory densities and traffic patterns during the flooding caused by the Hurricane Harvey in August 2017. The potential of the model for applications in emergency response and pandemic prediction is also discussed.

5.2 Related Work

5.2.1 Resilience of Urban Mobility to Crises

The role of urban mobility in a crisis such as access by emergency responders has been emphasized in the existing literature (Wang, 2015). Assessing strategies to enhance

the resilience of urban mobility is essential to mitigate the negative effects of crises and to improve the effectiveness of response efforts. To this end, existing studies (Dong et al., 2019a; Wang and Taylor, 2016) have put forth methodologies to evaluate the vulnerability of physical road networks and have proposed appropriate strategies for enhancement of urban mobility resilience. In another stream of work, Fan et al. developed a mathematical contagion model to predict the spread of floodwaters over road networks that informs about the disruptions of the urban mobility networks in flooding events (Chao Fan et al., 2020a). Dong et al. proposed a machine-learning model that coupled road networks and water channels to examine the impacts of flooding on road networks through the lens of network dependencies (Dong et al., 2020). Despite the success of prior models, the majority of their efforts are focused on physical road networks, such as the accessibility to critical facilities. To expand the understanding of collective mobility patterns in crises, Wang et al. (2016) used empirical data to examine the impact of natural disasters on population travel distances and radius of gyrations. The result of their study indicates inherent resilience of urban mobility in crises. The majority of the existing studies (such as Lu et al., 2012) have used empirical approaches or analytical methods (such as network science-based models) to examine mobility patterns when a population is hit by a crisis. A critical missing piece, however, is predictive data-driven models that can realistically simulate the spatial-temporal patterns of urban mobility during a crisis. Such predictive models and their resulting information should inform about the spatial distribution of the vehicles on road networks and emerging traffic jams caused by crisis perturbations, such as road inundations. This information is crucial for emergency response and mobility

resilience enhancement; however, using empirical data from past crises, one could only evaluate one scenario of crisis impacts. The key to addressing this gap is a predictive data-driven model that can learn the patterns of movements by individual vehicles during normal situations and which is capable of imposing crisis-related perturbations to simulated changes in mobility patterns. Such models for urban mobility simulation in a crisis situation could offer a unique and effective approach that enables city planners, emergency managers, and decision makers to capture the spatial and temporal patterns of population movements during extreme events, and facilitate contingency and hazard mitigation planning.

5.2.2 Mobility Destination and Trajectory Prediction

Simulating urban mobility is an important problem with a wide range of applications, such as traffic control, accident warning, pandemic prediction, and urban planning (Chao et al., 2020). Therefore, there is a need for general and robust methods to predict the destinations and trajectories for drivers, especially in populated urban areas (Zhao et al., 2018a). A number of prior studies have explored multiple methods to quantify, model and simulate human mobility, ranging from destination (next place) prediction (Noulas et al., 2012) to route selection. This section discusses existing research work to show the achievements in addressing the challenge and to highlight the need for adaptive models to simulate urban mobility under crises situations.

First, a number of existing studies have proposed and tested methods for next-place prediction (Ma et al., 2013). Next-place prediction, also called destination prediction in local urban scale, predicts the movement patterns of individuals and accordingly

estimates the flow of population in both spatial and temporal manners. In next-place prediction, the majority of the methods deal with the pairs of origins and destinations based on individuals' historical trip data. As mentioned earlier, statistical evidence shows the presence of regularity in human daily mobility patterns (Song et al., 2010b). Hence, to detect and learn this regularity, one commonly adopted approach is to develop clustering algorithms such as k-means and DBSCAN (Density-based Spatial Clustering of Applications with Noise) algorithm based on historical travel data and to identify association rules between the origin and destination (Chu and Chapleau, 2010). Multiple studies (Du et al., 2019) indicated that the clustering-based approaches have achieved very high performance in next-place prediction under normal circumstances. Location embedding is another method to capture location semantics with comprehensive numerical representations (Cheng et al., 2013; Wang and Li, 2017). For example, Shimizu et al. proposed a place-embedding method that can learn fine-grained representation with spatial hierarchical information and which achieved higher accuracy in predicting the next place of human trips in urban areas (Shimizu et al., 2020).

Second, in addition to single destination prediction, existing studies have also explored models for sequential patterns of individual travel to places (Zhao et al., 2018b). In this task, Markov chain-based models, including Mobility Markov Chain (Gambs et al., 2012), Mixed Markov Chain (Asahara et al., 2011), and Hidden Markov Model (Mathew et al., 2012), are commonly used to predict the location sequence of a given person/vehicle. Associated with location sequences but more related to route selection, other research is concerned with predicting the trajectory selected by an individual from

an origin to a destination has garnered significant attention over the past few years (Qiao et al., 2015). The predicted trajectories allow researchers to not only estimate travel time (Tang et al., 2018), but also to analyze travel demand over urban road networks (Dabiri et al., 2020). Due to the complexity of trajectory prediction and required data scale, only a limited number of studies have examined this problem. The most commonly used approach is the shortest-path algorithm that constructs routable graphs from historical trajectory data and then computes the route based on travel frequencies (Wei et al., 2012). This approach relies on traffic flow on specific road segments, but does not consider origin and destination pairs, that significantly influence route selection (Yang et al., 2017). More recent studies direct attention to the behavioral mobility patterns of individuals by inferring home and workplace, duration of activities. and other relevant temporal and spatial features for route prediction (Alexander et al., 2015). For example, Jiang et al. proposed a mechanistic modeling framework, called TimeGeo, that can generate mobility behaviors with a resolution of 10 minutes and hundreds of meters (Jiang et al., 2016).

In summary, recent works have significantly advanced methods of simulating urban mobility and trajectory prediction under normal conditions based on the evidence of regularity in human movement and activity patterns. Still unsolved, however, is the challenge of adaptability of a model for simulating urban mobility when people are exposed to disruptive conditions, such as life-threatening situations during crises such as flooding, wildfires, and even pandemics. Modeling approaches with limited adaptability would not be useful in assessing movement trajectories and traffic under crisis situations. Advances in adaptive reinforcement learning models provide opportunities for simulating

mobility under crises situations. In the following section, we will elaborate the proposed adaptive reinforcement learning model and then show its application in the context of flood impact analysis in Houston during Hurricane Harvey in 2017.

5.3 Methodology

The proposed adaptive reinforcement learning model comprises three modules: destination prediction, trajectory prediction, and crisis scenario application (Figure 19). The proposed model uses the human movement trajectory data as input, learns mobility patterns in regular situations, then simulates the trajectories and traffic conditions in crisis situations through adjusting the reward table. The mathematics and steps are formulated and elaborated in the following sub-sections.

5.3.1 Preliminary Definitions

In this section, we first define the notations and terminologies that are used in this study.

Definition 1. A **trajectory** T_i, also named as **waypoints**, **route** or **path**, is a spatial trace of a vehicle (or an individual) generated by their mobile apps in geographical space. T_i contains a sequence of locations with specific latitudes and longitudes: $\left[\left(x_0^i, y_0^i, t_0^i\right), \dots, \left(x_{k^i}^i, y_{k^i}^i, t_{k^i}^i\right), \dots, \left(x_{n^i}^i, y_{n^i}^i, t_{n^i}^i\right)\right]$, where $x_{k^i}^i \in \mathbb{R}$ and $y_{k^i}^i \in \mathbb{R}$ are the latitude and longitude of a trace record i at the k^ith location at time $t_{k^i}^i \in \mathbb{R}$, and $k^i \in \left[0,1, \dots, n^i\right]$.

Definition 2. A **trip** t_i, also called **O-D pair**, is a pair of origin and destination for a given trace record i. Trips can be extracted from trajectory data.

Definition 3. A **provider** is a service provider which is allowed to anonymously collect locations from mobile devices. The providers are sorted into four categories: consumer vehicles, taxi/shuttle/town car services, field service/local delivery fleets, and for-hire/private trucking fleets. Each provider's services fall exclusively into one category.

Definition 4. A **grid world** is a grid based on a geographical map. The cells in the grid world are in the same shape and with equal area. Each cell represents a specific state (or location) showing is the location of a vehicle. This term is used to address the Markov decision process (MDP).

Definition 5. A **policy**, π, is a set of choices of actions for an agent (people or vehicle in this study) at each state.

Based on these definitions, the destination prediction problem can be described thus: given an origin with spatial coordinate $\left(x_0^i, y_0^i, t_0^i\right)$ and a specific scenario, predict the spatial coordinate of the destination $\left(x_{n^i}^i, y_{n^i}^i\right)$. The trajectory prediction problem can further be described as: given a pair of origin $\left(x_0^i, y_0^i, t_0^i\right)$ and destination $\left(x_{n^i}^i, y_{n^i}^i\right)$ with time information, predict a trajectory, $\left[\left(x_0^i, y_0^i, t_0^i\right), \ldots, \left(x_{k^i}^i, y_{k^i}^i\right), \ldots, \left(x_{n^i}^i, y_{n^i}^i\right)\right]$, that a vehicle (or an individual) will go through from the origin to the destination. The specific time in a location on the path to the destination is uncertain due to the dynamic traffic states and data collection frequency. Hence, in this study, the trajectory prediction task will predict only the route a vehicle (or an individual) will select from an origin to a destination, while the specific time for the location of the vehicle (or the individual) on the route will not be estimated.

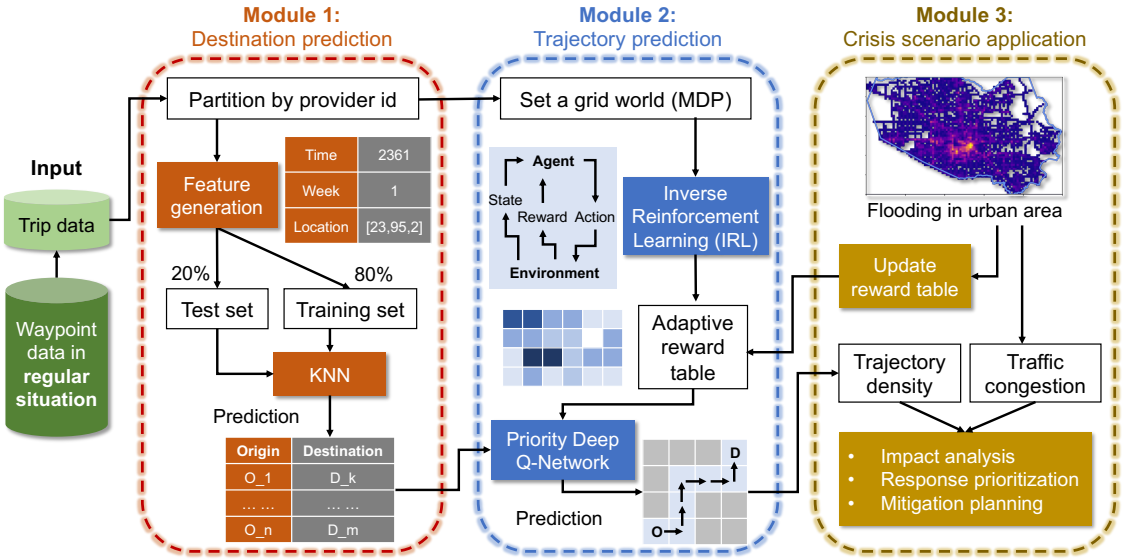

Figure 19 A schema of the proposed adaptive reinforcement learning model for simulating urban mobility.

5.3.2 Feature Generation

Estimated The first module of the model is a tool that can predict the destination of a vehicle, given an origin at a specific time. As suggested by existing studies, human movements are spatial- and time-dependent, meaning that each pair of origin and destination should include both temporal and spatial features to ensure the model is both accurate and general. To achieve this, this section discusses the process of generating relevant features.

For the temporal dimension, each trip sets the start time at the origin, showing the time of the day and day of the week. Empirical results show that urban mobility presents a significant weekly recurrent pattern (Cho et al., 2011). To incorporate this feature and to mitigate the effect of mobility variations across different days in a week, we converted

the time of the day and day of the week into an integrated feature, called t_n. Specifically, we considered that any time within a week can be represented by a real number from 0 to 1 (García, 2017). 0 represents the start of Monday (00:00 a.m., Monday), and 1 represents the end of Sunday (23:59 p.m., Sunday). Each day can be divided into 24 bins based on hours. Then, a specific time can be translated by:

$$t_n = \frac{\left(hours + \frac{mins}{60} + 24 \cdot weekday\right)}{7 \cdot 24} \quad \textbf{(26)}$$

where $hours$ represents the hours of the time in 24-hour system, $mins$ represents the minutes of the time, and $weekday$ represents the number of the days from Monday (for example, $weekday = 2$ for Wednesday). In this way, we can specify the time feature of a trip in a continuous manner across different times in a week.

Since people tend to have recurrent movement patterns during the weekday and special travels during the weekend (Saturday and Sunday), we also considered this difference in the model by using the category of weekday and weekend as a separate feature, w_n. The value of the trips in this feature can be represented using the following rule:

$$w_n = \begin{cases} 0 & weekday \\ 1 & weekend \end{cases} \quad \textbf{(27)}$$

The location of the origin and destination is usually recognized by the latitude and longitude coordinates. The resolution of the coordinates tends to be in meters. This raises a significant challenge for the predictive models to accurately learn the locations from the training data and predict location for a given origin. Also considering extremely

high-resolution coordinates will also increase computational cost for the model. To simplify this process and maintain fairly high resolution, we round the coordinates into numbers with three decimals places, (This threshold is flexible and can be selected based on the requirement of the resolution.) Similar to the idea of grid, the coordinates are associated to a cell and represented by a centroid of the corresponding cell. Furthermore, since the earth is an ellipsoid which should be described as a three-dimensional space, we projected the latitude and longitude to a Euclidean 3D space using the following formula (García, 2017):

$$\begin{aligned} x_{st} &= \cos\left(x_0^i\right) \cdot \cos\left(y_0^i\right) \\ y_{st} &= \cos\left(x_0^i\right) \cdot \sin\left(y_0^i\right) \\ z_{st} &= \sin\left(x_0^i\right) \end{aligned} \quad \textbf{(28)}$$

Through this approach, we can obtain three location features to represent a location of an origin (x_{st}, y_{st}, z_{st}). We also did the same transformation for the coordinates of the destination in the training data and obtain (x_{ed}, y_{ed}, z_{ed}).

5.3.3 K-nearest Neighbor Regression for Destination Prediction and Evaluation

Once the five features for an origin are prepared, we can train a supervised learning model to learn the movement patterns by extracting the association between origins and destinations from the historical data in regular conditions. Among the commonly used learning methods (Jia et al., 2017), k-nearest neighbor (k-NN) regression demonstrates high performance in predicting the location feature values of the destinations. The k-NN regression method assigns weights based on the contributions of the neighbors for the

predicted outcomes (location features in this study). The nearer the neighbors, the more contribution they can offer on the outcome values.

Specifically, the k-NN model will take the list of trips $t_i = (\boldsymbol{O}^i, \boldsymbol{D}^i)$ as the training set, including all time and location features of origin and destination. $\boldsymbol{O}^i = (t_n^i, w_n^i, x_{st}^i, y_{st}^i, z_{st}^i)$, and $\boldsymbol{D}^i = (x_{ed}^i, y_{ed}^i, z_{ed}^i)$. Then, we defined the number (k) of nearest neighbors that would contribute to predicting the destination. The value of k should be learned from the training data by minimizing the root mean square error (RMSE) which is defined below. The distance between every two neighbors (two origins: $\boldsymbol{O}^i$ and $\boldsymbol{O}^j$) is calculated using Euclidean norm (L^2 norm), $\|\cdot\|$, as shown below:

$$\|\boldsymbol{O}^i - \boldsymbol{O}^j\| = \sqrt{(t_n^i - t_n^j)^2 + (w_n^i - w_n^j)^2 + (x_{st}^i - x_{st}^j)^2 + (y_{st}^i - y_{st}^j)^2 + (z_{st}^i - z_{st}^j)^2} \quad \textbf{(29)}$$

The location feature values of the predicted destination are the average values of the location feature for the corresponding destinations of the k-nearest origins. This process generates three location feature values for the predicted destination. We then convert the location features back to the latitude and longitude with three decimal places of accuracy, analogous to the centroid of the destination cell. This coordinate is the predicted coordinates for the destination. By adjusting the value of k and calculating corresponding RMSE based on all pairs of predicted coordinates and actual coordinates, we can find an optimized value of k which can minimize the RMSE with high predictive performance.

This process is analogous to addressing a regression problem. Hence, we use the RMSE (Chai and Draxler, 2014) to measure the error between the actual and the predicted values:

$$RMSE = \sqrt{\frac{1}{N}\sum_{i}^{N}\frac{1}{2}\left[\left(x_{n^i}^{i} - x_{n^i}^{\prime i}\right)^2 + \left(y_{n^i}^{i} - y_{n^i}^{\prime i}\right)^2\right]} \quad \textbf{(30)}$$

where $x_{n^i}^{\prime i}$ and $y_{n^i}^{\prime i}$ are the latitude and longitude of the predicted destination for a trace record i, and N is the number of traces in the test data. Since we calculate the RMSE for each trace, the value of N, here, should be 1. The RMSE takes the Euclidean distances between the predicted outcomes and the observations which are then normalized across distances among all test data.

5.3.4 Markov Decision Process and Reinforcement Learning

Once the destinations are predicted for given origins, the next step is to estimate the trajectories between the origins and destinations. An effective and commonly used approach is to structure the space of learned policies, which more generally called Markov decision process. The Markov decision process is a stochastic control process with a tuple of (S, A, P, R), where S is a set of states $s_i \in S$, here meaning the cell in a representing vehicle location; A is a set of actions $a \in A$ which includes the four directions a vehicle can move from one cell to another in this context; $P(s_i'|s_i, a)$ is the transition probability that action a in state s_i for agent i leads to state s_i' in the next timestamp. Following a transition matrix $T(s_i, a, s_i')$; and $R(s_i, a, s_i')$ is the reward function that specifies the

reward a vehicle will immediately receive after transitioning from state s_i to state s_i' due to action a.

To simplify the state space and also to enable the matrix computation, we create a grid world that represents all possible states of an agent in the environment. With a start state (i.e., the origin of a vehicle) and the terminate state (i.e., the destination), the objective of this MDP is to learn an optimal policy $\pi: S \rightarrow A$, that can maximize the total rewards for an agent to move in the grid world (Ziebart et al., 2008). To learn a policy, we first need to specify the parameters in the model, the probability distribution over a trajectory $P(\zeta|T,\kappa)$ (ζ is a trajectory; and κ is the reward weights), transition matrix T, and the reward function R. The calculation starts with the transition matrix T. In this study, we assume that the agents have the same probability to go in each direction a among the four directions. Hence, the transition probability is set to be equal (the value is 1 if the action can be taken) among the four directions. Since the agent is usually not allowed to move out of the grid and the destination, we set the transition probabilities of some actions at the border and destination cell to be 0.

Then, the probability P_T that an agent will be in the state s_i' at next step given a state s_i, an action a, and a transition matrix T, can be computed as $P_T(s_i'|a,s_i)$. The probability distribution over a trajectory $P(\zeta|T,\kappa)$ would be proportional to the product of all probabilities over the path:

$$P(\zeta|T,\kappa) \propto \prod_{s_i,a,\, s_i' \in \zeta} P_T(s_i'|a,s_i) \tag{31}$$

To learn the reward function from historical trajectory data, we maximize the likelihood of the historical trajectory data under the maximum entropy distribution:

$$\kappa^* = \underset{\kappa}{\operatorname{argmax}} \sum_{data} \log P\left(\tilde{\zeta}|T, \kappa\right) \tag{32}$$

where $\tilde{\zeta}$ specifically refers to the historical trajectories. Solving this function by gradient-based optimization method, we can obtain the reward weights for the grid world. The reward value of a trajectory is simply the sum of the state rewards, which is calculated by the product of the path feature and the reward weights.

$$R\left(\mathbf{f}_{\tilde{\zeta}}\right) = \sum_{s_i \in \zeta} \kappa^T \mathbf{f}_{s_i} \tag{33}$$

where $\mathbf{f}_{\tilde{\zeta}}$ is the path feature, which is the sum of the grid feature of each state, $\mathbf{f}_{s_i}$. The formula is shown as follows:

$$\mathbf{f}_{\tilde{\zeta}} = \sum\nolimits_{s_i \in \tilde{\zeta}} \mathbf{f}_{s_i} \tag{34}$$

In implementing the model, the first challenge we encounter is the computational cost for training the agent on the grid world. That is because, in each step, when the agent wants to determine the action and next state, the model has to do matrix multiplications. Since we include the whole Houston metropolitan area to create the grid world, the matrix would be very large and, thus, calculating the reward would and informing the agent to make a decision would require an onerously long calculation time. This cost is usually not allowed for the model that wants to be applied to various contexts, especially in crisis settings. In fact, the cells distant from the origin and destination are not to make any impact

on the trajectory selection of an agent. To reduce the computational cost, hence, in the implementation process, we draw only a small bounding box that can incorporate both origin and destination. Then, all cells in the bounding box are considered to be in the reward matrix to do reward calculations.

The second challenge would be the effect of the historical trajectories on the immediate reward values. As discussed earlier, the reward values in the reward table are learned from the historical trajectories that pass through the cell. For an origin and destination pair, we aim to find a trajectory to connect these two cells. The historical trajectories that connect other O-D pairs would, however, give weights to other cells in the reward table. Sometimes, the weights from the trajectories for other O-D pairs are quite high, inducing the agent to go other directions, moving around some high reward cells, and even leaving the actual destinations. To mitigate the effect of noisy historical trajectories, we include only the historical trajectories that pass through the given origin and destination to learn the reward table. This solution would effectively overcome the noise in the reward tables, reduce the training time, and finally improve the efficiency and performance of the model in learning reward tables.

5.3.5 Transformation of the Reward Function

The reward table for each pair of origin and destination is the key to predicting the trajectory that an agent would select under a specific circumstance. Through examining the reward function learned from the Markov decision process, some common problems hinder an agent to find the optimal policy.

First, due to the sparsity of the data, it is often the case that the immediate rewards among all cells are quite close to each other, meaning that an agent would be not able to effectively distinguish the benefits of two states to make an accurate choice of the next state. As a result, the model is usually unstable, generating different trajectories in different rounds of implementation. In addition, the reward values learned by the reinforcement learning model are always positive for all cells in the grid world. The agent tends to get stuck in some cells with relatively high rewards since the next state does not offer substantial reward to enable a moving action. To address these pitfalls, we conducted a normalization to project the values of the immediate rewards to a negative space with a range of $[-1,0]$. The normalized reward matrix is denoted as R'. The process can be formulated using the following equation:

$$r'_{ij} = \frac{r_{ij} - r_{max}}{r_{max} - r_{min}} \quad \textbf{(35)}$$

where r_{ij} is the immediate reward in cell at ith row and jth column in the grid in according to reward function R; r_{max} and r_{min} are the maximum and minimum immediate reward respectively among all cells in the same grid. By doing so, the range of the reward values will be extended and distributed in a greater space. The negative values of the rewards can enable the agent to move out of some cells halfway on the trajectory and get a high reward only at the destination cell.

Second, in the reward table, the reward of an action given to the agent does not always compel the agent to move towards the destination due to a high density of the road networks and concentration of historical trajectories. That means an agent tends to move

around the cells with high reward values, sometimes even moving back to the origin. The agent, however, should intentionally move towards the destination. The closer the next state to the destination, the higher reward the agent can obtain. To this end, we created a new matrix, L, that can be added up to the reward table to compensate for the effect of proximity to the destination on trajectory selection. Empirically, the reward distribution accounts for the closeness to the destination centers at the destination cell. The reward has to be reduced if the agent does not get to the destination or if the agent moves further from it. The idea of the reward distribution is similar to the Gaussian distribution. Hence, we employed the Gaussian distribution to assign rewards to the cells in the grid world. The reward regarding the closeness to a destination is denoted as l_{ij} for the cell at ith row and jth column. The value of l_{ij} can be obtained using the following formula:

$$l_{ij} = f(i) + f(j) - \delta \tag{36}$$

$$f(i) = \frac{1}{\sigma\sqrt{2\pi}} e^{-\frac{1}{2}\left(\frac{i-\mu}{\sigma}\right)^2} \tag{37}$$

$$f(j) = \frac{1}{\sigma'\sqrt{2\pi}} e^{-\frac{1}{2}\left(\frac{j-\mu'}{\sigma'}\right)^2} \tag{38}$$

where $f(i)$ and $f(j)$ are the reward values calculated based on the row and column; μ and μ' are the row and columns of the destination, respectively; σ and σ' are calculated as the variance of rows and columns. δ is a parameter that controls the range of the reward values. Regarding the contribution of the closeness to the destination, the value of δ can be tuned to improve the prediction performance of the model.

Third, the model usually does not converge at the destination cell because the reward at the destination is not significantly higher than other states. The agent would go back and forth around the destination cell. To address this problem, we simply assigned a large reward to the destination cell so that and the process can be converged when the agent arrives at and stops at the destination. The matrix can be created based on the formula shown as follows:

$$d_{ij} = \begin{cases} 500 & if\ ij\ is\ the\ destination \\ 0 & otherwise \end{cases} \quad \textbf{(39)}$$

where d_{ij} is the extra reward given to the destination cell, while other cell would receive no reward.

After all transformation matrices are prepared, finally, the reward table for a pair of origin and destination can be obtained by combining all of these matrixes:

$$R_t = R' + L + D \quad \textbf{(40)}$$

Using this transformed reward table, we can train agents for each origin and destination pair to effectively learn the optimal policy.

5.3.6 Optimal Trajectory Prediction and Evaluation

Once the reward table for each pair of origin and destination is prepared, we define that the expected utility starting in s_i and acting optimally is $V^*(s_i)$. The expected utility starting out having taken the action a from state s_i and thereafter acting optimally is defined as $Q^*(s_i, a)$. Here $Q^*(s_i, a)$ is computed by:

$$Q^*(s_i, a) = \sum_{s_i'} T(s_i, a,\ s_i')[R_t(s_i, a,\ s_i') + \gamma V^*(s_i')] \tag{41}$$

where γ is a hyperparameter that can be adjusted to balance the contributions of the reward function and the expected utility. Based on the historical data, we can maximize the value of a state by:

$$V^*(s_i) = \max_a Q^*(s_i, a) \tag{42}$$

Finally, we can learn the optimal policy:

$$V^*(s_i) = \max_a \sum_{s_i'} T(s_i, a,\ s_i')[R_t(s_i, a,\ s_i') + \gamma V^*(s_i')] \tag{43}$$

$$\pi^*(s_i) = \operatorname*{argmax}_a \sum_{s_i'} T(s_i, a,\ s_i')[R_t(s_i, a,\ s_i') + \gamma V^*(s_i')] \tag{44}$$

A deep Q-network (DQN) with prioritized experience replay is adopted to solve the behavioral policy and predict the optimal trajectory that the agent would select for a given O-D pair. Consider a historical trajectory where the model has learned and estimated the Q^* value for an action. The empirical trajectories should be encouraged to be sampled in the prediction. To prioritize the empirical trajectories, we first measure the difference between the predicted Q^* value and the experienced Q^* value in the same state for the same action, which is represented by δ_i:

$$\delta_i = R_t(s_i, a,\ s_i') + \gamma V_{\theta}^{*}\text{-}(s_i') - Q_{\theta}^{*}(s_i, a) \tag{45}$$

where θ^{-} represents the target deep neural network, and θ represents the current deep neural network. The equation can further be reformulated as:

$$\delta_i = R_t(s_i, a,\ s_i') + \gamma Q_{\theta}^{*}\text{-}\left(s_i', \underset{a}{\operatorname{argmax}}\, Q_{\theta}^{*}(s_i', a)\right) - Q_{\theta}^{*}(s_i, a) \tag{46}$$

The left-hand side of the equation, $R_t(s_i, a,\ s_i') + \gamma Q_{\theta}^{*}\text{-}\left(s_i', \underset{a}{\operatorname{argmax}}\, Q^{*}(s_i', a)\right)$, is the target value, and the right-hand side of the equation, $Q_{\theta}^{*}(s_i, a)$, is the predicted value. This equation provides a quantitative measure of how much the deep neural network can learn from the given experience sample i. This is notated as the Double-Q temporal difference (TD) error. To find an appropriate θ and an optimal trajectory, the TD error is minimized by using expectation of the samples from the replay buffer D:

$$\min_{\theta} \mathbb{E}_{(s_i, a, R,\, s_i')} \sim D\left[\left(R_t(s_i, a,\ s_i') + \gamma Q_{\theta}^{*}\text{-}\left(s_i', \underset{a}{\operatorname{argmax}}\, Q_{\theta}^{*}(s_i', a)\right) - Q_{\theta}^{*}(s_i, a)\right)^{2}\right] \tag{47}$$

By doing so, we can predict the optimal trajectory for each pair of origin and destination.

The performance of trajectory prediction is measured based on the overlaps between the actual and the predicted trajectory. Since we created the grid world for the Markov decision process and optimal policy learning, the trajectories are characterized by the cells. The intersection between the set of cells in the predicted trajectory and the set of cells in the actual trajectory indicates the precision and recall of the model for O-D pairs

(Buckland and Gey, 1994). Hence, we adopted the following formulas for measuring the precision and recall for each O-D pair to assess the performance of the model:

$$Precision = \frac{True\ positive}{True\ positive + False\ positive} \quad \textbf{(48)}$$

$$Recall = \frac{True\ positive}{True\ positive + False\ negative} \quad \textbf{(49)}$$

where $True\ positive$ is the number passing cells that the model correctly predicts and that presents in the actual trajectory; $False\ positive$ is the number of passing cells that the model incorrectly predicts and that are not in the actual trajectory; $False\ negative$ is the number of cells that are incorrectly predicted to be out of the trajectory. The calculation of the precision and recall allows us to quantitatively assess the performance of the model for each O-D pair and to identify the specific correctly predicted cells.

5.3.7 Crisis Scenario Application with Contextual Factors

The adaptability of the model is an important feature that enables the model to be widely used in various contexts, especially in crises situations, such as flooding, hurricanes, wildfires, and pandemics. The major change in the model due to the variation of the contexts is the destination and immediate reward when agents make their decisions on the actions. Therefore, in this section, we discuss the steps and strategies to update the destination selection and the reward table. The detailed steps are shown below:

- *Step 1*: sampling the origins based on the historical data (or the density of population);

- *Step 2*: predicting the destinations corresponding to each sampled origin using the well-trained first module of the model. In particular contexts, such as crises, some destinations might have been damaged or closed. Based on the observed situations, these destinations must be removed from results and only reachable destinations retained.

- *Step 3*: generating the situation matrix F to represent the situation between the origin and destination and updating the transformed reward table with the situation matrix F. Take the flooding event as an example. The value of each cell f_{ij} in the situation matrix F can represent the extent of flooding in that cell, such as the number of flooded road segments or the area of the flooded cell. Then, multiplied by a parameter $1/\beta$ to normalize the values, we can add the matrix to the transformed matrix or subtract the transformed matrix with the situation matrix, following the formula shown below:

$$R_t = R' + L + D - F/\beta \quad \textbf{(50)}$$

where, the value of β can be selected based on the contribution of the situation to the trajectory selection of the agents.

- *Step 4*: predicting the trajectory of the given origin and destination using the updated reward table and the priority deep Q-network.

- *Step 5*: augmenting the prediction results. It is important to note that the model can simulate only the trajectory for each origin and destination pair, instead of directly

predicting the number of vehicles on the road. The model, however, has the capability to simulate traffic conditions on the road based on the simulated trajectories. In this step, the algorithm can first simulate the trajectory for an origin and destination pair 50 times. Then the algorithm selects the cells with high pass-through probability. We use the number of times, n_{ij}, that the cell is included in the predicted trajectory as the weight of the cell, v_{ij}, and other cells are considered as zero, as the equation shown below:

$$v_{ij}^{(k)} = \begin{cases} n_{ij}^{(k)} & grids\ are\ selected \\ 0 & otherwise \end{cases} \quad \textbf{(51)}$$

Each pair of origin and destination would have one vehicle matrix, $V^{(k)}$, that encompasses the entire grid world. Since a cell would likely to be on multiple trajectories for different pairs of origins and destinations, for all pairs of origins and destinations, we use $c_{ij} = \sum_{k=1}^{N} v_{ij}^{(k)}$ to represent the number of vehicles passing through this cell, where N is the number of simulated pairs of origins and destinations.

Through the implementation of all these steps, we can arrive at a final traffic matrix C to represent the number of vehicles simulated in the cells on the grid world. This matrix would not only show the common trajectories that people would choose to reach their destinations, but also can inform the emergency response and resource allocation based on perturbations in mobility and traffic patterns in the context of crises. The capabilities

of the model in simulation of urban mobility during crises is illustrated in following sections.

5.4 Results

To demonstrate the performance and capabilities of the proposed model, we first introduced the data sets and then elaborated a specific use case of the model with an application in flooding impact analysis in the Houston metropolitan area in the context of Hurricane Harvey in 2017.

5.4.1 Data Collection and Preprocessing

The data set, which is used to train, tune, and evaluate the adaptive reinforcement learning model, comes from INRIX, a private location intelligence company providing location-based data and analytics. The reason why we employ these data are twofold. First, the INRIX data provides very detailed coordinates along with the trajectory of the vehicles. That is, INRIX collected the coordinates of the vehicles every few seconds. Hence, the temporal and spatial resolution of the data is high. Second, the INRIX data are collected over the entire Houston metropolitan area over a time period of two months (March through April 2017) at all times of the day. This yielded a dataset of more than 26 million trip records collected in a continuous timeframe. Third, the INRIX data contains the trips for hundreds of providers with four vehicle types. The vast volume of the trips and the diversity of vehicle types allow us to capture the various activity patterns and to enhance the robustness of the proposed approach in learning and simulating large-scale urban mobility.

To prepare this data for training, we selected providers with large record sizes and discarded roughly 20% of the trips that were too short (distance between origin and destination less than 5 miles) that might induce noise into the training process. Then, we randomly selected 80% of the trips as the training set and 20% of the remaining data as the testing set.

5.4.2 Destination Prediction

The first task is to predict the destinations, given the origins. We mainly train the model to automatically find an optimal value for the number of neighbors, k, which indicates the number of neighbors that should be included for estimating the coordinates of the destinations. Since we have a large number of providers with different types, we trained the model on the dataset from each provider separately.

Figure 20 shows the prediction performance of the models in four example providers. As shown in the figure, the RMSE goes from a very small value, about 0.005, and then grows gradually to 0.1 when 80% of the O-D pairs are predicted. Only 20% of the O-D pairs have an RMSE greater than 0.1. The result indicates that the model can accurately predict the destinations for given origins based on the parameters learned from training data. Since we filtered out short-distance trips, the lengths of the remaining trips in the training and testing data are relatively long. By measuring the distances between the actual destinations and the predicted destinations, we find that a few predicted destinations are less than 0.3-mile from the actual destination, about 10% of the predicted destinations are less than 0.6-mile from the actual destination, and more than 50% of the predicted destinations are within the 3-mile distance from the actual destination. Considering the

length of the trips themselves, the differences between the actual and predicted destinations are much shorter. Hence, the accuracy of the results is acceptable. Figure 21 further shows the spatial accuracy of some example O-D pairs. Figure 21 also shows the high performance of the model. Comparing the results among all providers, we also find that the model is quite stable with respect to the prediction performance and is not affected by the types of providers. This result demonstrates that the model is robust and generalizable to be applied to different data providers for destination prediction.

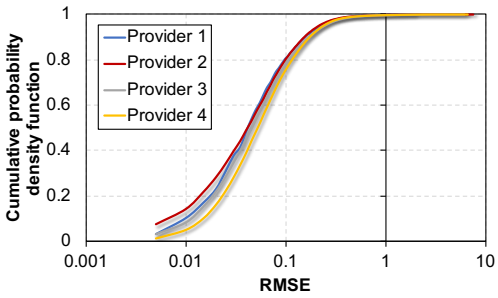

Figure 20 The performance of the model for destination prediction in four example providers. The average RMSEs for providers 1 through 4 are 0.0288, 0.0701, 0.0780, and 0.0824, respectively.

5.4.3 Trajectory Prediction

Once we acquire the destinations for given origins, we further use them to predict the optimal trajectories between the origins and destinations. The first step is to compute the reward table for each O-D pair. As discussed in the methodology section, we include only the cells within the bounding box. Figure 22 shows examples of reward tables for some of O-D pairs. The bounding box is a bit larger than the actual box tightly covering

the origin and destination. In the majority of the example tables, such as R1, R2, and R5, we can find that the some significantly highlighted cells have high reward values, and the agent can effectively determine the optimal trajectories from the origin to the destination. Although historical data do not have a significant footprint for some O-D pairs, such as R3 and R4, the model can still impulse the agent to find an optimal trajectory.

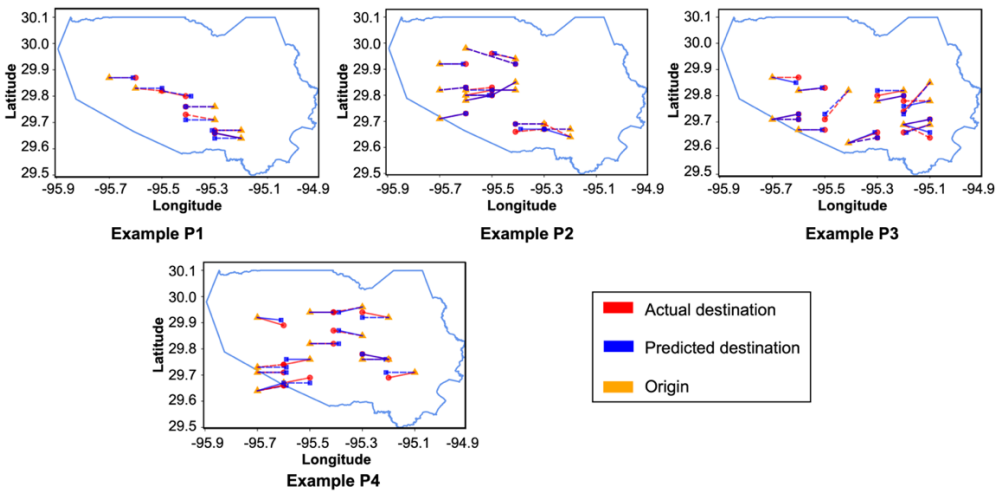

Figure 21 Example origin-destination pairs showing the performance of the model. (The blue polygon is the borderline of Harris County, Texas, USA.)

A quantitative assessment of the model performance is shown in Figure 23. We tested the model for multiple providers and O-D pairs. As the results suggest, the majority of the predicted trajectories are similar to the actual trajectories selected by the vehicles. Both average precision and recall are fairly high (although they are negatively affected by some extreme values). Figure 24 shows some examples of actual trajectories, predicted trajectories, and their overlaps. Despite the complexity of the historical trajectories transited by the vehicles, the model can still identify optimal trajectories for each pair of

origin and destination. The performance of the model is also stable when it is trained and tested on different types of providers and datasets. These results and findings indicate that the proposed model is robust and could be used for trajectory-finding tasks.

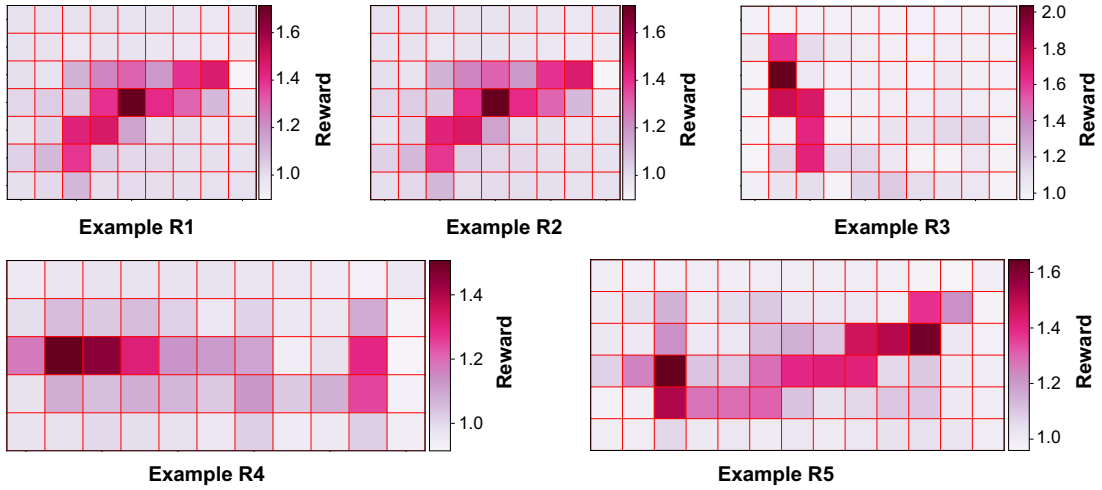

Figure 22 Example reward tables for origin and destination pairs, learned from training data using reinforcement learning.

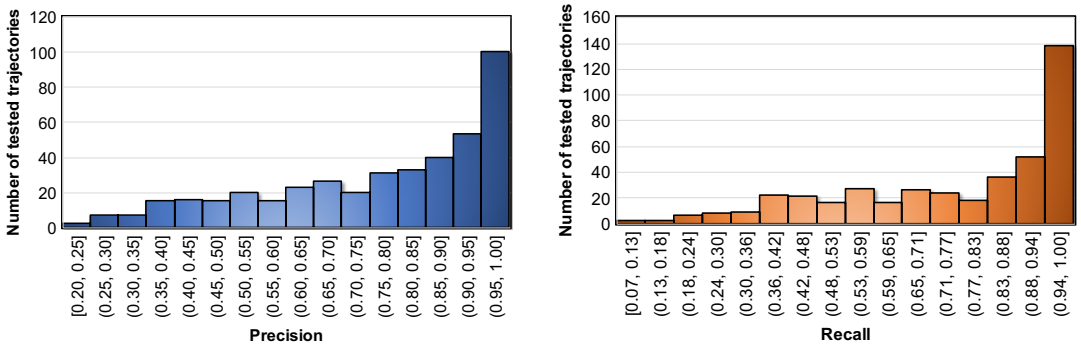

Figure 23 Performance of the trajectory prediction using module 2 of the proposed model. Average precision: 0.765; and average recall: 0.766.

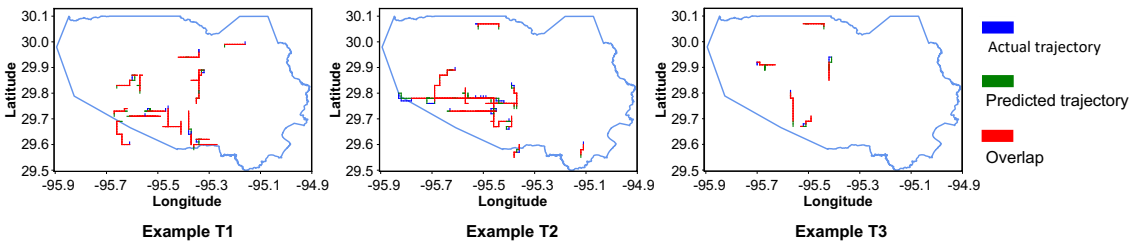

Figure 24 Example trajectories showing the performance of the model. The blue polygon is the borderline of Harris County.

5.4.4 Simulation for Flooding Impact Analysis

To illustrate the application and capabilities of the proposed adaptive reinforcement model, we implemented the model for the situation during Hurricane Harvey in late August 2017 in the Houston metropolitan area. Hurricane Harvey, a Category 4 tropical storm, landed in Houston on August 26, 2017, and dissipated inland August 30, 2017. August 27 is the date with extreme and sustained rainfall that subsequently caused large-scale flooding over the urban areas, especially on urban road networks. As reported in news articles and government reports, more than 115,000 buildings were damaged, and 290 roads and highways were flooded (Ibrahim, 2017; Sebastian et al., 2017). To illustrate the performance of the model, we selected a specific short time interval, 10:00 a.m. through 12:00 p.m., August 29, 2017. We simulated vehicles that would move during this time interval and estimated their trajectory to understand the traffic conditions under the perturbation of urban flooding. Here we measured the traffic conditions in different locations by using the number of vehicles that move across a cell.

To be consistent, the data set used to validate the capability of the proposed model for scenario application was also obtained from INRIX. For each road segment, the dataset includes the average speed in 5-minute intervals and the speed in free-flow conditions (estimated as the speed limit for the roads). The flood situation on the road segments can also be reflected by the INRIX data. In the INRIX average speed dataset, the flooded road segments are identified by a designation of NULL for the traffic speed since no traffic records and no vehicles are driving through flooded road segments. To test the accuracy and validity of the data for identifying flooded roads, we also did a comparison of the NULL records between the datasets collected before and during the Hurricane Harvey, and also checked the records with flooded roads from government reports (Dong et al., 2020). We found that the NULL records presented only during the flooding period and were consistent with the flooded locations.

Using this dataset, we identified the flooded road segments and quantified the extent of flooding in a cell. In the grid map for Houston, Harris County, each cell contains multiple road segments. To measure the extent of flooding in a specific cell, we considered the number of flooded road segments within a cell as a metric. As shown in Figure 25(a), the flooded cells are concentrated on the central area of Houston and along the major roads such as highways.

The traffic conditions in a cell can be captured by the actual traffic speed on the road segment. Since our model is mainly learned from the vehicles driving on major roads, here, we take into account only the road segments on which the speed limit is equal or greater than 50 km/hour so that all simulated results can be on the same road basis. This

step also contributes to eliminating the effect of speed limits (types) of roads on the results. Hence, we computed the average of the actual speed on these selected road segments as the metric for traffic conditions for each cell. Figure 25(b) shows areas where traffic was quite heavy due to flooding.

To understand the impact of flooding on the population movement patterns, especially in the trajectory selection, we implemented the proposed adaptive reinforcement learning model by adopting the flood conditions to adjust the parameters in the model. The cells with more flooded road segments would have higher negative values added to the reward table. Accordingly, the agent would be less likely to transit the severely flooded cell to reach their destination. The simulated results are shown in Figure 25(c) and (d). From these results, we found that the majority of the road segments hit hardest by the flood had fewer vehicles compared to the road segments where flooding was less severe (i.e., passable roads). This result indicates that, the model effectively simulated the trajectories selected by people who deliberately avoided flooded road segments. Hence, the road segments that were less flooded tend to have a great number of vehicles with low speed, or fewer vehicles with high speed. The results are quite realistic, which reveals the redistribution of vehicles and the utility of roads in urban road networks when flooding disrupted this area.

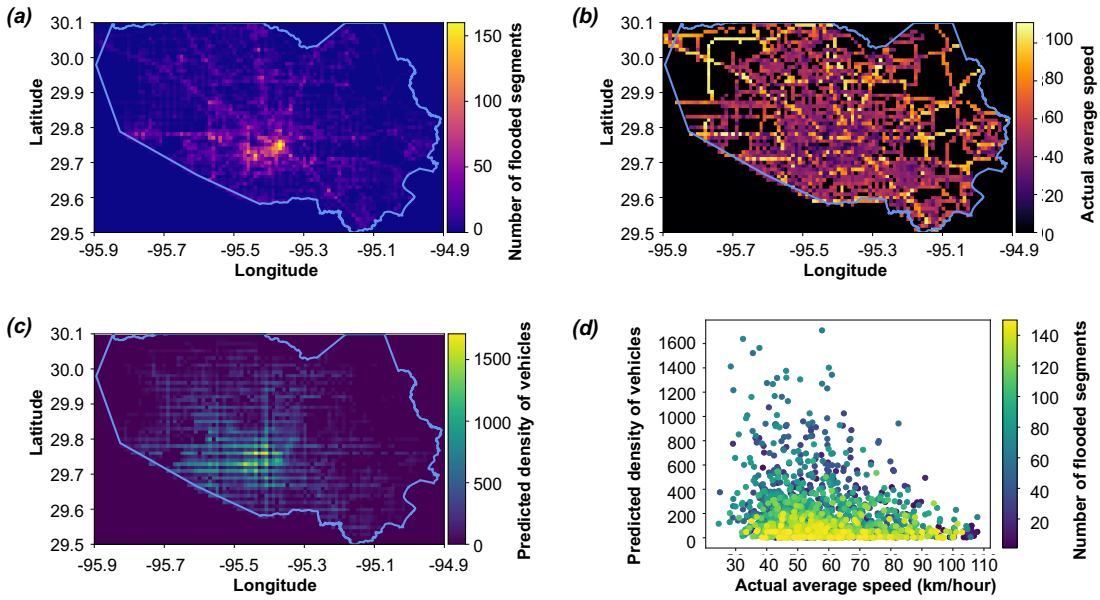

Figure 25 The simulation results in flooding scenario. (a) Number of flooded segments in Houston, Harris County (the blue borderline); (b) Actual average speed for major road segments during the investigated time period; (c) Predicted density of vehicles during the investigated time period; and (d) Relationships among three variables for simulation validation.

5.5 Discussion and Concluding Remarks

In this paper, we presented an adaptive reinforcement learning model that can simulate human mobility under crisis conditions based on the mobility patterns learned from historical data collected under normal circumstances. The proposed model can overcome the scarcity of mobility pattern data in crisis contexts, and also has the capability to simulate different crisis situations for impact analysis. The study showed the application of the proposed model using the digital trace data collected in Houston during regular

situations and demonstrated the adaptability of the model in the case of urban flooding during Hurricane Harvey in 2017. In the task of learning the devices' collective utility function for movement trajectories in our road networks, the time complexity of the KNN model for training is $\mathcal{O}(N \times D)$, where N is the sample size and D is the dimension of the sample. The reinforcement learning algorithm attains near-optimal average reward in polynomial time.

Although the proposed model is general and can be adaptive to various phenomena and applications, future research could address some limitations. First, although this study achieves good performance for predicting the destinations and trajectories at a relatively fine-grained scale, the prediction of local movements, such as visits to nearby neighborhoods and points of interest, still needs to be improved. Local movements provide essential information about the lifestyle of residents. This study predicts the pure coordinates of destination and trajectories regardless of the specific locations visited and the roads traversed. Inclusion of this information in creating the movement profile of populations and predicting local movements would be of interest and importance in applications related to city and emergency planning. Second, the model has a great potential to be used as an application for rapid prediction. Training the proposed algorithm and attaining the reward table, however, are still time-consuming, which would take a great amount of computational cost. In addition, the flooding situation is dynamic and evolves rapidly. Hence, there is a need of improving the efficiency of the algorithm so that it can be used for learning rewards efficiently across more cities and crises contexts.

CHAPTER VI

SUMMARY, CONTRIBUTIONS AND FUTURE WORK

The research presented in this dissertation makes significant theoretical and practical contributions to the areas of urban resilience in flooding emergencies. Through characterization and analyses of information, human, road and mobility network dynamics in flooding events, this research offers important insights about the extent to which technologies could obtain real-time and predictive capacities and aid emergency response as well as the extent to which human behaviors could be improved in coping with service disruptions in flooding emergencies. Overall, this body of work provides a deeper understanding of how human digital trace data and various types of network dynamics can enhance urban resilience, and subsequently reduce the loss of properties and lives in flooding emergencies. The specific theoretical and academic contributions and practical contributions of each study are presented in the sections below with highlighted corresponding chapters. Future work along the path of these studies is proposed finally.

6.1 Theoretical and Academic Contributions

First, the presented research in this study makes critical contributions surrounding the use of human digital trace data and computational methods in understanding the real-time and future situations in flooding emergencies. The results from the experiments in this dissertation provide empirical evidence about the performance of infrastructure and the reactions of populations in flooding emergencies. These empirical findings offer a

direct behavioral indication of the vulnerability of infrastructure systems and population groups, to the extent that specific infrastructure, locations and people are more sensitive to environmental perturbations, while others are more resilient. This evidence base addresses an important challenge in resilience research: unequal resilience capacities of urban systems in the face of the same emergencies. Hence, this research contributes to the theory of urban resilience by generating new knowledge about the characteristics of real-time situations, which is often overlooked in existing resilience studies. In addition, the evidence base could also support policies guiding the delivery by emergency management organizations of important lifesaving information and reactions to the public in risks.

Second, the proposed online network reticulation framework enables understanding the relationships among disaster-induced disruptive events, user activities, network reticulation, and network performance in dynamic online space during flooding emergencies. To my knowledge, this research provides the first systemic study of addressing the relationships between the situation in urban space and human reactions in online space. The results of the experiments empirically verified that weak social ties play an important role in breaking the physical boundaries of people in emergencies and amplify information spread across different communities. The findings uncovered by the proposed theory deepen our understanding of online social network dynamics with consideration of triggering events in urban space. The knowledge could also inform the design of mechanisms to improve user activities, and thus achieve better network performance for risk communication among affected populations. Apart from disaster studies, adoption of the online network reticulation theory can also enrich studies of social

behavioral dynamics in other contexts such as politics and marketing to better understand the interplay among user activities, the influence of social, political and technological events, and the performance of online social networks. Such understanding could inform the planning of marketing and political campaigning strategies.

6.2 Practical Contributions

6.2.1 Real-time situational awareness

This developed methods and tools in this dissertation have significant practical contributions and implications for real-time situational awareness in management processes. First, the methods and models enable the automatic mapping of credible situational information for critical infrastructure in disasters. This output can support multiple decision-making processes. For example, first responders can rapidly obtain information about disruptive events, and monitor the situation at different locations. In addition, by tracking the conditions of places with a variety of critical infrastructure, volunteers and relief organizations can be aware of the allocation of relief efforts so that they can deploy their resources to the locations where people's needs are not satisfied. Second, the evolution of the events for an infrastructure system identified by the proposed methods from social media can be used for forensic disaster analysis. For example, the situational information on social media might indicate the interactions among multiple infrastructure entities. This information contributes to probing more deeply into the complex interdependencies of infrastructure entities, and the underlying causes of cascading impacts. Hence, the automatic mapping enabled by the proposed methods can

enable a timely forensic investigation to inform disaster recovery and future risk mitigation. Finally, the methods can be further scaled to address automated mapping for several disasters occurring at the same time, when it is put into production. The relevant tweets for each disaster can be filtered using keywords and geographical bounding boxes that are specified by disaster responders with domain knowledge. Then, multiple methods can work parallelly with specified inputs for different disasters to automated map the situations.

6.2.2 Predictive situational awareness

The predictive models proposed in this dissertation contribute to predictive situational awareness in flooding emergencies. First, the proposed models and its adaptability to different crisis contexts can contribute to hazard mitigation and resilience improvement of urban areas. Predictive emergency warning and situational awareness are key components of hazard mitigation, which would benefit from an effective simulation of crises. Simulating flood propagation and human mobility during flooding emergencies is an essential step to capture the crisis and further inform early warning and mitigation planning. For example, using the proposed models, city planners, emergency managers, and decision-makers can simulate scenarios of flooding (such as 100-year and 500-year flood scenarios) and road inundations to enable examination of the effects of movement trajectories and traffic congestions in urban road networks. This output information could inform about areas that would experience significant flooding damages or traffic congestions induced by flooding. With sufficient examination of such contingencies, first

responders and decision-makers can effectively assess the extent to which reducing the flood vulnerability of a major road or highway would mitigate the flooding spread and traffic congestions to improve the resilience of cities in flooding emergencies. Also, the proposed models could be used to simulate road inundation and mobility disruptions between critical origins (such as areas where vulnerable populations, such as the elderly and low-income households, are located) and critical destinations (such as healthcare facilities). In addition, the outcomes of the proposed model can help with a prediction of road inundation and traffic congestions in the next couple of hours based on the real-time information, such as the flooded areas, to improve the accessibility of critical facilities and efficiency of responder dispatch.

Second, the presented studies also offer a new perspective on using mathematical models and deep learning techniques for flood prediction and mobility analysis. Although extremely big data related to human digital traces have been generated by the daily mobility activity of individuals, existing deep learning techniques are limited to the prediction of regular mobility patterns. The proposed models enable consideration of contextual factors, such as road conditions, road network connectivity and population distribution, in the simulation process, which would significantly extend the capabilities of existing deep learning models leaned from normal situations and applied to unfamiliar conditions, such as emergencies and traffic anomalies, to support decision-making and response strategies. For example, one can learn the mobility demand of the road networks from daily mobility data and predict the utility of each road segment by changing the

layout of the networks. This can help design efficient transportation networks and traffic control systems to improve the performance of urban road networks.

6.3 Proposed Avenues of Future Research

In this dissertation, I focus on real-time and predictive situational awareness using human digital trace data and computing techniques. The developed models and proposed theories provide insights into how we can design a powerful tool to enhance situational awareness in flooding emergencies. Beyond that, emergency management involves plenty of other components such as a diversity of relief organizations and their complex interactions in providing humanitarian relief actions. The need for improving the effectiveness and efficiency of organization coordination in emergency management has been widely recognized. To address this challenge, researchers from different disciplines such as information science, computer science, and social science have denoted efforts to employing information and communication technologies and developing advanced machine learning and mathematical approaches to capture the behaviors of organizations in the face of disasters and crises. Given the growing literature in the interdisciplinary field of emergency management, there is a dire need for interdisciplinary convergence towards a unified vision.

Hence, I outline three proposed avenues of future research that could build on the models and theories established in this dissertation:

- *Data integration and knowledge distillation:* The studies presented in this dissertation use textual content of social media posts and geographical

information from mobile phone data. Other types of data such as human speech, video streams, images and signal data could also provide important information regarding the situation in emergencies to complement the textual and geographical data. Yet, the utility of these data for emergency management and urban resilience remains unexploited. Future research work could extend our models and methods to other sources of data, develop an approach to integrate the information provided by these data, and create a knowledge graph to connect all entities, attributes, and their statuses together. The outcome of this work could not only contribute to precise and efficient situational awareness, but also significantly strengthen the predictive capability of existing methods and tools to project things unseen and future scenarios.

- *Multi-actor game-theoretic decision making:* This dissertation developed tools to extract information for real-time situations in emergencies. Thus, we can now capture the needs of the residents at different locations. Built upon the outputs of our tools, future work could conduct experiments and develop simulations to understand how relief organizations are coordinating with each other to distribute their resources to the people in need. Serious Gaming Learning and Coordination Environment (SGLCE) could be a useful tool to solve decision-aware serious gaming, coordination, and visualization of emergency response actions. What makes SGLCE helpful is its ability to simulate the coordination, information flow, and dynamic interactions among

relief organizations and identify an optimal policy to maximize the benefit of collaborative operation with an acceptable cost.

- *Dynamic network analysis for performance assessment:* I presented a study in examining the response of online social networks for risk communication and collective-sense making in this dissertation. However, emergency management for urban resilience involves a great number of entities such as human entities (e.g., residents and government officials), resource entities (e.g., food and driving water), and operation entities (e.g., a series of tasks directing the activities of stakeholders). Future work could create an integrative framework for performance analysis of the complex interactions among different types of entities. Using a dynamic network analysis approach, we could quantify the operational efficiency and coordination efficiency in the emergency management system, enabling increased visibility of the capacity and drawback in the synergy of heterogeneous entities.

Overall, the studies in this dissertation and future research could be integrated into a unified paradigm, Disaster City Digital Twin (see Figure 26). The digital twin paradigm would offer important capabilities of cities with an integration of different streams of research and create AI-based converging solutions for emergency management and urban resilience.

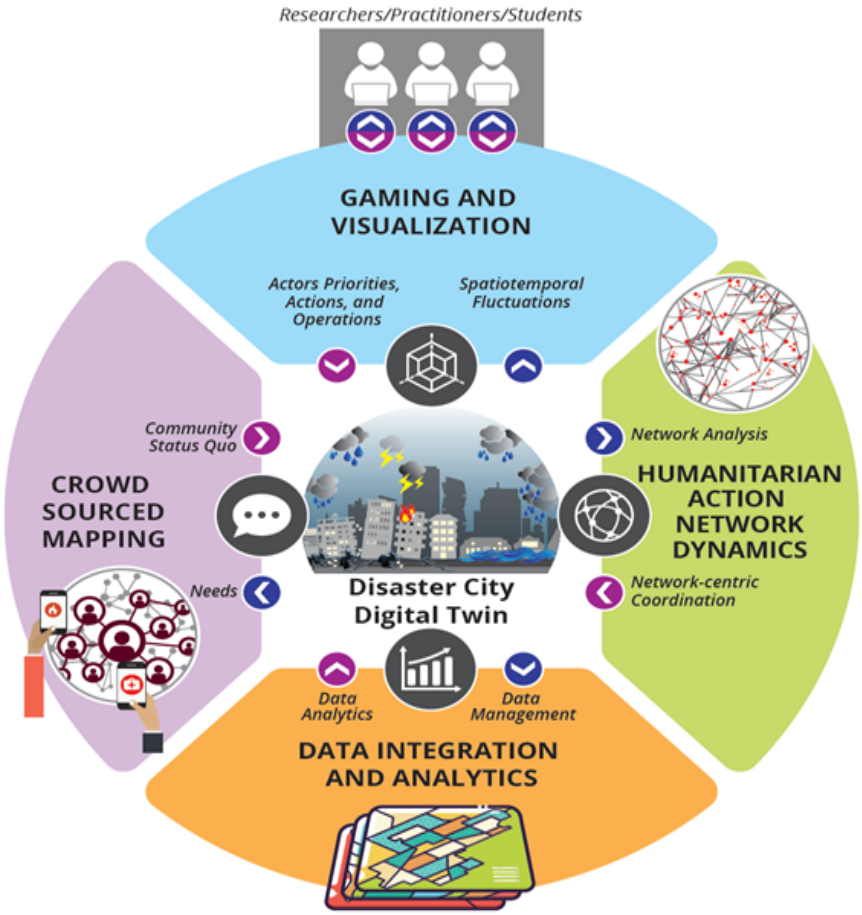

Figure 26 The Disaster City Digital Twin paradigm.

REFERENCES

Ahmadlou, M., Adeli, H., Adeli, A., 2010. New diagnostic EEG markers of the Alzheimer's disease using visibility graph. J. Neural Transm. 117, 1099–1109. https://doi.org/10.1007/s00702-010-0450-3

Akhtar, P., Marr, N.E., Garnevska, E. V., 2012. Coordination in humanitarian relief chains: chain coordinators. J. Humanit. Logist. Supply Chain Manag. 2, 85–103. https://doi.org/10.1108/20426741211226019

Alexander, L., Jiang, S., Murga, M., González, M.C., 2015. Origin–destination trips by purpose and time of day inferred from mobile phone data. Transp. Res. Part C Emerg. Technol. 58, 240–250. https://doi.org/https://doi.org/10.1016/j.trc.2015.02.018

Allen, K., 2017. Army Corps releases water from 2 Houston dams; thousands of homes to be affected - ABC News [WWW Document]. abs News. URL https://abcnews.go.com/US/army-corps-releases-water-houston-dams-levels-increased/story?id=49462262 (accessed 2.18.19).

Altay, N., Pal, R., 2014. Information Diffusion among Agents: Implications for Humanitarian Operations. Prod. Oper. Manag. 23, 1015–1027. https://doi.org/10.1111/poms.12102

Alvarez-Melis, D., Saveski, M., 2016. Topic Modeling in Twitter: Aggregating Tweets by Conversations. ICWSM,16 519–522.

Aral, S., Dhillon, P.S., 2018. Social influence maximization under empirical influence models. Nat. Hum. Behav. 2, 375–382. https://doi.org/10.1038/s41562-018-0346-z

Aral, S., Muchnik, L., Sundararajan, A., 2009. Distinguishing influence-based contagion from homophily-driven diffusion in dynamic networks. Proc. Natl. Acad. Sci. 106, 21544–21549. https://doi.org/10.1073/pnas.0908800106

Aral, S., Walker, D., 2014. Tie strength, embeddedness, and social influence: A large-scale networked experiment. Manage. Sci. 60, 1352–1370.

Arthur, R., Boulton, C.A., Shotton, H., Williams, H.T.P., 2018. Social sensing of floods in the UK. PLoS One 13, 1–18. https://doi.org/10.1371/journal.pone.0189327

Asahara, A., Maruyama, K., Sato, A., Seto, K., 2011. Pedestrian-Movement Prediction Based on Mixed Markov-Chain Model, in: Proceedings of the 19th ACM SIGSPATIAL International Conference on Advances in Geographic Information Systems, GIS '11. Association for Computing Machinery, New York, NY, USA, pp.

25–33. https://doi.org/10.1145/2093973.2093979

Atefeh, F., Khreich, W., 2013. a Survey of Techniques for Event Detection in Twitter. Comput. Intell. 0, n/a-n/a. https://doi.org/10.1111/coin.12017

Bagrow, J.P., Liu, X., Mitchell, L., 2019. Information flow reveals prediction limits in online social activity. Nat. Hum. Behav. 3, 122–128. https://doi.org/10.1038/s41562-018-0510-5

Bagrow, J.P., Wang, D., Barabási, A.L., 2011. Collective response of human populations to large-scale emergencies. PLoS One. https://doi.org/10.1371/journal.pone.0017680

Bajaj, V., Ma, J., Thompson, S., 2017. How Houston's Growth Created the Perfect Flood Conditions. New York Times. URL https://www.nytimes.com/interactive/2017/09/05/opinion/hurricane-harvey-flood-houston-development.html (accessed 10.18.19)

Balcik, B., Beamon, B.M., Krejci, C.C., Muramatsu, K.M., Ramirez, M., 2010. Coordination in humanitarian relief chains: Practices, challenges and opportunities. Int. J. Prod. Econ. 126, 22–34. https://doi.org/10.1016/j.ijpe.2009.09.008

Ball, F., Mollison, D., Scalia-Tomba, G., 1997. Epidemics with two levels of mixing. Ann. Appl. Probab. 7, 46–89. https://doi.org/10.1214/aoap/1034625252

Barabási, A.-L., 2013. Network science. Philos. Trans. A. Math. Phys. Eng. Sci. https://doi.org/10.1098/rsta.2012.0375

Barabási, A.-L., Pósfai, M., 2016. Network science. Cambridge University Press, Cambridge.

Becker, H., Iter, D., Naaman, M., Gravano, L., 2012. Identifying content for planned events across social media sites, in: Proceedings of the Fifth ACM International Conference on Web Search and Data Mining - WSDM '12. https://doi.org/10.1145/2124295.2124360

Benson, E., Haghighi, A., Barzilay, R., 2011. Event Discovery in Social Media Feeds. Proc. 49th Annu. Meet. Assoc. Comput. Linguist. https://doi.org/10.1007/978-0-387-69080-3_17

Blondel, V.D., Guillaume, J.L., Lambiotte, R., Lefebvre, E., 2008. Fast unfolding of communities in large networks. J. Stat. Mech. Theory Exp. 2008. https://doi.org/10.1088/1742-5468/2008/10/P10008

Brown, J.J., Reingen, P.H., 2002. Social Ties and Word-of-Mouth Referral Behavior. J. Consum. Res. https://doi.org/10.1086/209118

Buckland, M., Gey, F., 1994. The relationship between Recall and Precision. J. Am. Soc. Inf. Sci. 45, 12–19. https://doi.org/10.1002/(SICI)10974571(199401)45:1<12::AID-ASI2>3.0.CO;2-L

Buntain, C., Lin, J., Golbeck, J., 2015. Learning to Discover Key Moments in Social Media Streams. arXiv preprint arXiv:1508.00488

Burt, R.S., 1987. Social Contagion and Innovation: Cohesion versus Structural Equivalence. Am. J. Sociol. 92, 1287–1335.

Burt, R.S., 1984. Network items and the general social survey. Soc. Networks. https://doi.org/10.1016/0378-8733(84)90007-8

Castillo, C., Mendoza, M., Poblete, B., 2013. Predicting information credibility in time-sensitive social media. Internet Res. 23, 560–588. https://doi.org/10.1108/IntR-05-2012-0095

Castillo, C., Mendoza, M., Poblete, B., 2011. Information credibility on twitter. Proc. 20th Int. Conf. World wide web - WWW '11 675. https://doi.org/10.1145/1963405.1963500

Chai, T., Draxler, R.R., 2014. Root mean square error (RMSE) or mean absolute error (MAE)? – Arguments against avoiding RMSE in the literature. Geosci. Model Dev. 7, 1247–1250. https://doi.org/10.5194/gmd-7-1247-2014

Chao, F., Yucheng, J., Ali, M., 2020. Social Sensing in Disaster City Digital Twin: Integrated Textual–Visual–Geo Framework for Situational Awareness during Built Environment Disruptions. J. Manag. Eng. 36, 4020002. https://doi.org/10.1061/(ASCE)ME.1943-5479.0000745

Chen, J., Touati, C., Zhu, Q., 2017. A Dynamic Game Analysis and Design of Infrastructure Network Protection and Recovery. https://doi.org/10.1145/3152042.3152079

Cheng, C., Yang, H., Lyu, M.R., King, I., 2013. Where You Like to Go Next: Successive Point-of-Interest Recommendation. Int. Jt. Conf. Artif. Intell. Twenty-Third Int. Jt. Conf. Artif. Intell.

Cho, E., Myers, S.A., Leskovec, J., 2011. Friendship and mobility: user movement in location-based social network. KDD1082. https://doi.org/10.1145/2020408.2020579

Choudhury, M., Counts, S., Czerwinski, M., 2011. Identifying Relevant Social Media Content: Leveraging Information Diversity and User Cognition. Proc. 22nd ACM Conf. Hypertext hypermedia - HT '11. https://doi.org/10.1145/1995966.1995990

Chowell, G., Hengartner, N.W., Castillo-Chavez, C., Fenimore, P.W., Hyman, J.M., 2004. The basic reproductive number of Ebola and the effects of public health measures: the cases of Congo and Uganda. J. Theor. Biol. 229, 119–126. https://doi.org/https://doi.org/10.1016/j.jtbi.2004.03.006

Chu, K.K.A., Chapleau, R., 2010. Augmenting Transit Trip Characterization and Travel Behavior Comprehension: Multiday Location-Stamped Smart Card Transactions. Transp. Res. Rec. 2183, 29–40. https://doi.org/10.3141/2183-04

Cordeiro, M., 2012. Twitter event detection : combining wavelet analysis and topic inference summarization. In Doctoral symposium on informatics engineering. 11-16.

Corman, S.R., Scott, C.R., 1994. Perceived Networks, Activity Foci, and Observable Communication in Social Collectives. Commun. Theory 7, 171–190.

Dabiri, S., Lu, C., Heaslip, K., Reddy, C.K., 2020. Semi-Supervised Deep Learning Approach for Transportation Mode Identification Using GPS Trajectory Data. IEEE Trans. Knowl. Data Eng. 32, 1010–1023. https://doi.org/10.1109/TKDE.2019.2896985

Davidon, W.C., 1991. Variable Metric Method for Minimization. SIAM J. Optim. 1, 1–17. https://doi.org/10.1137/0801001

Department of Homeland Security, 2008. National Incident Management System. Natl. Incid. Manag. Syst. 1, 170. https://doi.org/10.1017/CBO9781107415324.004

Deville, P., Linard, C., Martin, S., Gilbert, M., Stevens, F.R., Gaughan, A.E., Blondel, V.D., Tatem, A.J., 2014. Dynamic population mapping using mobile phone data. Proc. Natl. Acad. Sci. 111, 15888 LP – 15893. https://doi.org/10.1073/pnas.1408439111

Dixon, T.H., Amelung, F., Ferretti, A., Novali, F., Rocca, F., Dokka, R., Sella, G., Kim, S.-W., Wdowinski, S., Whitman, D., 2006. Subsidence and flooding in New Orleans. Nature 441, 587–588. https://doi.org/10.1038/441587a

Dong, S., Wang, H., Mostafavi, A., Gao, J., 2019a. Robust component: a robustness measure that incorporates access to critical facilities under disruptions. J. R. Soc. Interface 16, 20190149. https://doi.org/10.1098/rsif.2019.0149

Dong, S., Yu, T., Farahmand, H., Mostafavi, A., 2020. Probabilistic Modeling of Cascading Failure Risk in Interdependent Channel and Road Networks in Urban Flooding. Sustain. Cities Soc. 62, 102398.

Dong, S., Yu, T., Farahmand, H., Mostafavi, A., 2019b. Bayesian modeling of flood control networks for failure cascade characterization and vulnerability assessment.

Comput. Civ. Infrastruct. Eng. https://doi.org/10.1111/mice.12527

Douglas, E.M., Vogel, R.M., Kroll, C.N., 2000. Trends in floods and low flows in the United States: impact of spatial correlation. J. Hydrol. 240, 90–105. https://doi.org/https://doi.org/10.1016/S0022-1694(00)00336-X

Du, R., Santi, P., Xiao, M., Vasilakos, A. V, Fischione, C., 2019. The Sensable City: A Survey on the Deployment and Management for Smart City Monitoring. IEEE Commun. Surv. Tutorials 21, 1533–1560. https://doi.org/10.1109/COMST.2018.2881008

Ebina, R., Nakamura, K., Oyanagi, S., 2011. A real-time burst detection method. Proc. - Int. Conf. Tools with Artif. Intell. ICTAI 1040–1046. https://doi.org/10.1109/ICTAI.2011.177

ENR Editors, 2017. How Badly Has Hurricane Harvey Damaged Texas Infrastructure? | 2017-08-28 | ENR [WWW Document]. Eng. News-Record. URL https://www.enr.com/articles/42639-how-badly-has-hurricane-harvey-damaged-texas-infrastructure (accessed 2.12.18).

Fan, Chao, Jiang, X., Mostafavi, A., 2020a. A Network Percolation-based Contagion Model of Flood Propagation and Recession in Urban Road Networks. Sci. Rep. 10, 1–12. https://doi.org/10.1038/s41598-020-70524-x

Fan, Chao, Jiang, Y., Mostafavi, A., 2020b. Emergent social cohesion for coping with community disruptions in disasters. J. R. Soc. Interface 17, 20190778. https://doi.org/10.1098/rsif.2019.0778

Fan, Chao, Jiang, Y., Yang, Y., Zhang, C., Mostafavi, A., 2020c. Crowd or Hubs: information diffusion patterns in online social networks in disasters. Int. J. Disaster Risk Reduct. 46, 101498. https://doi.org/https://doi.org/10.1016/j.ijdrr.2020.101498

Fan, C., Mostafavi, A., 2019a. A graph-based method for social sensing of infrastructure disruptions in disasters. Comput. Civ. Infrastruct. Eng. 34, 1055–1070. https://doi.org/10.1111/mice.12457

Fan, C., Mostafavi, A., 2019b. A graph-based method for social sensing of infrastructure disruptions in disasters. Comput. Civ. Infrastruct. Eng. mice.12457. https://doi.org/10.1111/mice.12457

Fan, C., Mostafavi, A., 2018. Establishing a Framework for Disaster Management System-of-Systems, in: 2018 Annual IEEE International Systems Conference (SysCon). IEEE, Vancouver, BC, Canada. https://doi.org/https://doi.org/10.1109/SYSCON.2018.8369545

Fan, C., Mostafavi, A., Gupta, A., Zhang, C., 2018. A System Analytics Framework for Detecting Infrastructure-Related Topics in Disasters Using Social Sensing, in: Smith, I.F.C., Domer, B. (Eds.), Advanced Computing Strategies for Engineering. Springer International Publishing, Cham, 74–91.

Fan, C, Wu, F., Mostafavi, A., 2020. A Hybrid Machine Learning Pipeline for Automated Mapping of Events and Locations From Social Media in Disasters. IEEE Access 8, 10478–10490. https://doi.org/10.1109/ACCESS.2020.2965550

Fan, Chao, Zhang, C., Yahja, A., Mostafavi, A., 2020d. Disaster City Digital Twin: A Vision for Integrating Artificial and Human Intelligence for Disaster Management. Int. J. Inf. Manage. 1–12.

Fedschun, T., 2017. Harvey floodwaters overflow Houston reservoir, separate levee breach reported. Fox News. URL http://www.foxnews.com/us/2017/08/29/harvey-floodwaters-put-houston-reservoirs-in-uncharted-territory.html (accessed 7.3.18).

Fischer-Preßler, D., Schwemmer, C., Fischbach, K., 2019. Collective sense-making in times of crisis: Connecting terror management theory with Twitter user reactions to the Berlin terrorist attack. Comput. Human Behav. https://doi.org/10.1016/j.chb.2019.05.012

Flood Control District, 2017. HCFCD - Flooding impacts in connection with the Reservoirs [WWW Document]. Harris Cty. Flood Control Dist. URL https://www.hcfcd.org/hurricane-harvey/flooding-impacts-in-connection-with-the-reservoirs/ (accessed 7.3.18).

Fohringer, J., Dransch, D., Kreibich, H., Schröter, K., 2015. Social media as an information source for rapid flood inundation mapping. Nat. Hazards Earth Syst. Sci. 15, 2725–2738. https://doi.org/10.5194/nhess-15-2725-2015

Foster, J.G., Foster, D. V., Grassberger, P., Paczuski, M., 2010. Edge direction and the structure of networks. Proc. Natl. Acad. Sci. 107, 10815–10820. https://doi.org/10.1073/pnas.0912671107

Gambs, S., Killijian, M.-O., del Prado Cortez, M.N., 2012. Next Place Prediction Using Mobility Markov Chains, in: Proceedings of the First Workshop on Measurement, Privacy, and Mobility, MPM '12. Association for Computing Machinery, New York, NY, USA. https://doi.org/10.1145/2181196.2181199

Ganin, A.A., Kitsak, M., Marchese, D., Keisler, J.M., Seager, T., Linkov, I., 2017. Resilience and efficiency in transportation networks. Sci. Adv. 3, e1701079. https://doi.org/10.1126/sciadv.1701079

Gao, J., Buldyrev, S. V., Stanley, H.E., Havlin, S., 2012. Networks formed from

interdependent networks. Nat. Phys. 8, 40–48. https://doi.org/10.1038/nphys2180

García, C., 2017. carlosbkm/car-destination-prediction [WWW Document]. Github. URL https://github.com/carlosbkm/car-destination-prediction (accessed 6.30.20).

Gehlot, H., Honnappa, H., Ukkusuri, S. V, 2020. An optimal control approach to day-to-day congestion pricing for stochastic transportation networks. Comput. Oper. Res. 119, 104929. https://doi.org/https://doi.org/10.1016/j.cor.2020.104929

Gibbons, J., Nara, A., Appleyard, B., 2018. Exploring the imprint of social media networks on neighborhood community through the lens of gentrification. Environ. Plan. B Urban Anal. City Sci. 45, 470–488. https://doi.org/10.1177/2399808317728289

Giddens, A., 1984. The constitution of society: Outline of the theory of structuration. Cognit. Ther. Res. 12, 448. https://doi.org/10.1007/BF01173303

González, M.C., Hidalgo, C.A., Barabási, A.-L., 2008. Understanding individual human mobility patterns. Nature 453, 779–782. https://doi.org/10.1038/nature06958

Gross, R., Acquisti, A., Heinz, H.J., 2006. Information revelation and privacy in online social networks. https://doi.org/10.1145/1102199.1102214

Guan, X., Chen, C., 2018. General methodology for inferring failure-spreading dynamics in networks. Proc. Natl. Acad. Sci. 201722313. https://doi.org/10.1073/pnas.1722313115

Gupta, A., Kumaraguru, P., 2012. Credibility ranking of tweets during high impact events. Proc. 1st Work. Priv. Secur. Online Soc. Media - PSOSM '12 2–8. https://doi.org/10.1145/2185354.2185356

Hackl, J., Lam, J.C., Heitzler, M., Adey, B.T., Hurni, L., 2018. Estimating network related risks: A methodology and an application in the transport sector. Nat. Hazards Earth Syst. Sci. 18, 2273–2293.

Homans, G., 1950. The Human Group. New Brunswick.

Hossain, F., Katiyar, N., Hong, Y., Wolf, A., 2007. The emerging role of satellite rainfall data in improving the hydro-political situation of flood monitoring in the under-developed regions of the world. Nat. Hazards 43, 199–210. https://doi.org/10.1007/s11069-006-9094-x

Huang, Q., Cervone, G., Zhang, G., 2017. A cloud-enabled automatic disaster analysis system of multi-sourced data streams: An example synthesizing social media, remote sensing and Wikipedia data. Comput. Environ. Urban Syst. 66, 23–37.

https://doi.org/10.1016/j.compenvurbsys.2017.06.004

Hus, A., Sullivan, B., 2017. After Harvey, Most Houston Hospitals Up And Running : Shots - Health News : NPR [WWW Document]. Natl. Public Ratio. URL https://www.npr.org/sections/health-shots/2017/08/30/547327581/in-houston-most-hospitals-up-and-fully-functional (accessed 7.3.18).

Ibrahim, A., 2017. Texas officials see long road from Harvey for state transportation network | The Texas Tribune [WWW Document]. Texas Trib. URL https://www.texastribune.org/2017/09/04/texas-officials-harvey-transportation/ (accessed 3.28.20).

Imran, M., Castillo, C., 2015. Towards a Data-driven Approach to Identify Crisis-Related Topics in Social Media Streams. Proc. 24th Int. Conf. World Wide Web - WWW '15 Companion 1205–1210. https://doi.org/10.1145/2740908.2741729

Imran, M., Elbassuoni, S., Castillo, C., Diaz, F., Meier, P., 2013. Extracting information nuggets from disaster- Related messages in social media. ISCRAM. 791–800.

Ipsen, I.C.F., Wills, R.S., 2006. Mathematical properties and analysis of Google's PageRank. Bol. la Soc. Esp. Mat. Apl. 34, 191–196.

Jackson, J.C., Jong, J., Bilkey, D., Whitehouse, H., Zollmann, S., McNaughton, C., Halberstadt, J., 2018. Synchrony and Physiological Arousal Increase Cohesion and Cooperation in Large Naturalistic Groups. Sci. Rep. 8, 1–8. https://doi.org/10.1038/s41598-017-18023-4

Jia, C., Li, Y., Carson, M.B., Wang, X., Yu, J., 2017. Node Attribute-enhanced Community Detection in Complex Networks. Sci. Rep. 7, 1–15. https://doi.org/10.1038/s41598-017-02751-8

Jiang, S., Yang, Y., Gupta, S., Veneziano, D., Athavale, S., González, M.C., 2016. The TimeGeo modeling framework for urban mobility without travel surveys. Proc. Natl. Acad. Sci. 113, E5370 LP-E5378. https://doi.org/10.1073/pnas.1524261113

Jongman, B., Wagemaker, J., Romero, B., de Perez, E., 2015. Early Flood Detection for Rapid Humanitarian Response: Harnessing Near Real-Time Satellite and Twitter Signals. ISPRS Int. J. Geo-Information 4, 2246–2266. https://doi.org/10.3390/ijgi4042246

Juffinger, A., Granitzer, M., Lex, E., 2009. Blog credibility ranking by exploiting verified content. Proc. 3rd Work. Inf. Credibil. web - WICOW '09 51. https://doi.org/10.1145/1526993.1527005

Kadri, F., Birregah, B., Châtelet, E., 2014. The impact of natural disasters on critical

infrastructures: A domino effect-based study. J. Homel. Secur. Emerg. Manag. 11, 217–241. https://doi.org/10.1515/jhsem-2012-0077

Kawachi, I., Berkman, L., 2000. Social cohesion, social capital, and health. Soc. Epidemiol.

Khajeh Hosseini, M., Talebpour, A., 2019. Traffic Prediction using Time-Space Diagram: A Convolutional Neural Network Approach. Transp. Res. Rec. 2673, 425–435. https://doi.org/10.1177/0361198119841291

Khazan, O., 2017. Hurricane Affecting Ben Taub Hospital in Houston, Texas - The Atlantic [WWW Document]. Atl. URL https://www.theatlantic.com/health/archive/2017/08/the-houston-hospital-running-out-of-food/538266/ (accessed 7.3.18).

Khosravi, K., Pham, B.T., Chapi, K., Shirzadi, A., Shahabi, H., Revhaug, I., Prakash, I., Tien Bui, D., 2018. A comparative assessment of decision trees algorithms for flash flood susceptibility modeling at Haraz watershed, northern Iran. Sci. Total Environ. 627, 744–755. https://doi.org/https://doi.org/10.1016/j.scitotenv.2018.01.266

Kim, J., Bae, J., Hastak, M., 2018. Emergency information diffusion on online social media during storm Cindy in U.S. Int. J. Inf. Manage. 40, 153–165. https://doi.org/10.1016/j.ijinfomgt.2018.02.003

Kim, Y.C., Kang, J., 2010. Communication, neighbourhood belonging and household hurricane preparedness. Disasters 34, 470–488. https://doi.org/10.1111/j.1467-7717.2009.01138.x

Kitamura, R., Chen, C., Pendyala, R.M., Narayanan, R., 2000. Micro-simulation of daily activity-travel patterns for travel demand forecasting. Transportation (Amst). 27, 25–51. https://doi.org/10.1023/A:1005259324588

Koks, E.E., Rozenberg, J., Zorn, C., Tariverdi, M., Vousdoukas, M., Fraser, S.A., Hall, J.W., Hallegatte, S., 2019. A global multi-hazard risk analysis of road and railway infrastructure assets. Nat. Commun. 10, 2677. https://doi.org/10.1038/s41467-019-10442-3

Kryvasheyeu, Yury, Chen, H., Obradovich, N., Moro, E., Hentenryck, P. Van, Fowler, J., Cebrian, M., 2016. Rapid assessment of disaster damage using social media activity. Sci. Adv. 1–12. https://doi.org/10.1126/sciadv.1500779

Kryvasheyeu, Y., Chen, H., Obradovich, N., Moro, E., Van Hentenryck, P., Fowler, J., Cebrian, M., 2016. Rapid assessment of disaster damage using social media activity. Sci. Adv. 2. https://doi.org/10.1126/sciadv.1500779

Kulshrestha, J., Kooti, F., Nikravesh, A., Gummadi, K., 2012. Geographic Dissection of the Twitter Network, in: Proceedings of the 6th International AAAI Conference on Weblogs and Social Media.

Kumar, S., Hu, X., Liu, H., 2014. A behavior analytics approach to identifying tweets from crisis regions. Proc. 25th ACM Conf. Hypertext Soc. media - HT '14 255–260. https://doi.org/10.1145/2631775.2631814

Lauw, H.W., Lim, E.-P., Pang, H., Tan, T.-T., 2005. Social Network Discovery by Mining Spatio-Temporal Events. Comput. Math. Organ. Theory 11, 97–118. https://doi.org/10.1007/s10588-005-3939-9

Lazega, E., Wasserman, S., Faust, K., 2006. Social Network Analysis: Methods and Applications. Rev. Française Sociol. https://doi.org/10.2307/3322457

Lee, G., Oh, N., Moon, I., 2012. Modeling and simulating network-centric operations of organizations for crisis management. Proceeding EAIA '12 Proc. 2012 Symp. Emerg. Appl. M&S Ind. Acad. Symp.

Lei, Z., Qian, X., Ukkusuri, S. V, 2020. Efficient proactive vehicle relocation for on-demand mobility service with recurrent neural networks. Transp. Res. Part C Emerg. Technol. 117, 102678. https://doi.org/https://doi.org/10.1016/j.trc.2020.102678

Lhomme, S., Serre, D., Diab, Y., Laganier, R., 2013. Analyzing resilience of urban networks: a preliminary step towards more flood resilient cities. Nat. Hazards Earth Syst. Sci. 13, 221–230. https://doi.org/10.5194/nhess-13-221-2013

Li, J., Mei, X., Prokhorov, D., Tao, D., 2017. Deep Neural Network for Structural Prediction and Lane Detection in Traffic Scene. IEEE Trans. Neural Networks Learn. Syst. 28, 690–703. https://doi.org/10.1109/TNNLS.2016.2522428

Li, X., Zhang, G., 2018. Perceived Credibility of Chinese Social Media: Toward an Integrated Approach. Int. J. Public Opin. Res. 30, 79–101. https://doi.org/10.1093/ijpor/edw035

Liang, Y., Ouyang, K., Wang, Y., Liu, Y., Zhang, J., Zheng, Y., Rosenblum, D.S., 2020. Revisiting Convolutional Neural Networks for Citywide Crowd Flow Analytics.

Liu, L., Qiu, Z., Li, G., Wang, Q., Ouyang, W., Lin, L., 2019. Contextualized Spatial–Temporal Network for Taxi Origin-Destination Demand Prediction. IEEE Trans. Intell. Transp. Syst. 20, 3875–3887. https://doi.org/10.1109/TITS.2019.2915525

Liu, W., Luo, X., Gong, Z., Xuan, J., Kou, N.M., Xu, Z., 2016. Discovering the core semantics of event from social media. Futur. Gener. Comput. Syst. 64, 175–185. https://doi.org/10.1016/j.future.2015.11.023

Long, R., Wang, H., Chen, Y., Jin, O., Yu, Y., 2011. Towards effective event detection, tracking and summarization on microblog data, in: Lecture Notes in Computer Science (Including Subseries Lecture Notes in Artificial Intelligence and Lecture Notes in Bioinformatics). https://doi.org/10.1007/978-3-642-23535-1_55

Lu, L., Wang, X., Ouyang, Y., Roningen, J., Myers, N., Calfas, G., 2018. Vulnerability of Interdependent Urban Infrastructure Networks: Equilibrium after Failure Propagation and Cascading Impacts. Comput. Civ. Infrastruct. Eng. 33, 300–315. https://doi.org/10.1111/mice.12347

Lu, X., Bengtsson, L., Holme, P., 2012. Predictability of population displacement after the 2010 Haiti earthquake. Proc. Natl. Acad. Sci. 109, 11576–11581. https://doi.org/10.1073/pnas.1203882109

Lu, X., Brelsford, C., 2014. Network structure and community evolution on Twitter: Human behavior change in response to the 2011 Japanese earthquake and tsunami. Sci. Rep. 4, 1–11. https://doi.org/10.1038/srep06773

Ma, X., Wu, Y.-J., Wang, Y., Chen, F., Liu, J., 2013. Mining smart card data for transit riders' travel patterns. Transp. Res. Part C Emerg. Technol. 36, 1–12. https://doi.org/https://doi.org/10.1016/j.trc.2013.07.010

Mathew, W., Raposo, R., Martins, B., 2012. Predicting Future Locations with Hidden Markov Models, in: Proceedings of the 2012 ACM Conference on Ubiquitous Computing, UbiComp '12. Association for Computing Machinery, New York, NY, USA, pp. 911–918. https://doi.org/10.1145/2370216.2370421

McCluskey, C.C., 2010. Complete global stability for an SIR epidemic model with delay — Distributed or discrete. Nonlinear Anal. Real World Appl. 11, 55–59. https://doi.org/https://doi.org/10.1016/j.nonrwa.2008.10.014

McMinn, A.J., Moshfeghi, Y., Jose, J.M., 2013. Building a large-scale corpus for evaluating event detection on twitter. Proc. 22nd ACM Int. Conf. Conf. Inf. Knowl. Manag. - CIKM '13 409–418. https://doi.org/10.1145/2505515.2505695

Merz, R., Blöschl, G., 2005. Flood frequency regionalisation—spatial proximity vs. catchment attributes. J. Hydrol. 302, 283–306. https://doi.org/https://doi.org/10.1016/j.jhydrol.2004.07.018

Miller, J.C., 2009. Percolation and epidemics in random clustered networks. Phys. Rev. E 80, 20901. https://doi.org/10.1103/PhysRevE.80.020901

Misra, S., Goswami, R., Mondal, T., Jana, R., 2017. Social networks in the context of community response to disaster: Study of a cyclone-affected community in Coastal West Bengal, India. Int. J. Disaster Risk Reduct. 22, 281–296.

https://doi.org/10.1016/j.ijdrr.2017.02.017

Montes, F., Jimenez, R.C., Onnela, J.-P., 2017. Connected but segregated: social networks in rural villages. J. Complex Networks 1–13. https://doi.org/10.1093/comnet/cnx060

Morone, F., Makse, H.A., 2015. Influence maximization in complex networks through optimal percolation. Nature 524, 65–68. https://doi.org/10.1038/nature14604

Mosavi, A., Ozturk, P., Chau, K., 2018. Flood Prediction Using Machine Learning Models: Literature Review. Water . https://doi.org/10.3390/w10111536

Mousa, M., Zhang, X., Claudel, C., 2016. Flash Flood Detection in Urban Cities Using Ultrasonic and Infrared Sensors. IEEE Sens. J. 16, 7204–7216. https://doi.org/10.1109/JSEN.2016.2592359

National Academy of Engineering, 2004. The Engineer of 2020: Visions of Engineering in the New Century. The National Academies Press, Washington, DC. https://doi.org/10.17226/10999

Nayak, P.C., Sudheer, K.P., Rangan, D.M., Ramasastri, K.S., 2005. Short-term flood forecasting with a neurofuzzy model. Water Resour. Res. 41. https://doi.org/10.1029/2004WR003562

Newman, M.E.J., 2003. Mixing patterns in networks. Phys. Rev. E - Stat. Physics, Plasmas, Fluids, Relat. Interdiscip. Top. 67, 13. https://doi.org/10.1103/PhysRevE.67.026126

Newman, M.E.J., Girvan, M., 2004. Finding and evaluating community structure in networks. Phys. Rev. E - Stat. Nonlinear, Soft Matter Phys. 69. https://doi.org/10.1103/PhysRevE.69.026113

Nguyen, D.T., Jung, J.E., 2017. Real-time event detection for online behavioral analysis of big social data. Futur. Gener. Comput. Syst. 66, 137–145. https://doi.org/10.1016/j.future.2016.04.012

Nik-Bakht, M., El-diraby, T.E., 2016. Communities of Interest-Interest of Communities: Social and Semantic Analysis of Communities in Infrastructure Discussion Networks. Comput. Civ. Infrastruct. Eng. 31, 34–49. https://doi.org/10.1111/mice.12152

Noulas, A., Scellato, S., Lambiotte, R., Pontil, M., Mascolo, C., 2012. A tale of many cities: Universal patterns in human urban mobility. PLoS One 7. https://doi.org/10.1371/journal.pone.0037027

Oh, S., Seshadri, R., Azevedo, C.L., Kumar, N., Basak, K., Ben-Akiva, M., 2020.

Assessing the impacts of automated mobility-on-demand through agent-based simulation: A study of Singapore. Transp. Res. Part A Policy Pract. 138, 367–388. https://doi.org/https://doi.org/10.1016/j.tra.2020.06.004

Olmos, L.E., Çolak, S., Shafiei, S., Saberi, M., González, M.C., 2018. Macroscopic dynamics and the collapse of urban traffic. Proc. Natl. Acad. Sci. 115, 12654 LP – 12661. https://doi.org/10.1073/pnas.1800474115

Olsen, L., 2018. Record reservoir flooding was predicted even before Harvey hit Houston - Houston Chronicle [WWW Document]. Chron. URL https://www.houstonchronicle.com/news/houston-texas/houston/article/barker-addicks-dams-flooding-predicted-army-corps-12632041.php (accessed 6.5.18).

Palen, L., Vieweg, S., Liu, S.B., Hughes, A.L., 2009. Crisis in a Networked World: Features of Computer-Mediated Communication in the April 16, 2007, Virginia Tech Event. Soc. Sci. Comput. Rev. 27, 467–480. https://doi.org/10.1177/0894439309332302

Papadopoulos, T., Gunasekaran, A., Dubey, R., Altay, N., Childe, S.J., Fosso-Wamba, S., 2017. The role of Big Data in explaining disaster resilience in supply chains for sustainability. J. Clean. Prod. 142, 1108–1118. https://doi.org/10.1016/j.jclepro.2016.03.059

Paprotny, D., Sebastian, A., Morales-Nápoles, O., Jonkman, S.N., 2018. Trends in flood losses in Europe over the past 150 years. Nat. Commun. 9. https://doi.org/10.1038/s41467-018-04253-1

Patterson, O., Weil, F., Patel, K., 2010. The role of community in disaster response: Conceptual models. Popul. Res. Policy Rev. https://doi.org/10.1007/s11113-009-9133-x

Pohl, D., Bouchachia, A., Hellwagner, H., 2012. Automatic identification of crisis-related sub-events using clustering. Proc. - 2012 11th Int. Conf. Mach. Learn. Appl. ICMLA 2012 2, 333–338. https://doi.org/10.1109/ICMLA.2012.170

Prasad, S., Zakaria, R., Altay, N., 2018. Big data in humanitarian supply chain networks: a resource dependence perspective. Ann. Oper. Res. 270, 383–413. https://doi.org/10.1007/s10479-016-2280-7

Pulcinella, J.A., Winguth, A.M.E., Allen, D.J., Dasa Gangadhar, N., 2019. Analysis of Flood Vulnerability and Transit Availability with a Changing Climate in Harris County, Texas. Transp. Res. Rec. https://doi.org/10.1177/0361198119839346

Qiao, S., Han, N., Zhu, W., Gutierrez, L.A., 2015. TraPlan: An Effective Three-in-One Trajectory-Prediction Model in Transportation Networks. IEEE Trans. Intell. Transp.

Syst. 16, 1188–1198. https://doi.org/10.1109/TITS.2014.2353302

Qiu, X., Oliveira, D.F.M., Sahami Shirazi, A., Flammini, A., Menczer, F., 2017. Limited individual attention and online virality of low-quality information. Nat. Hum. Behav. 1, 1–7. https://doi.org/10.1038/s41562-017-0132

Raja, M.A.Z., 2014. Numerical treatment for boundary value problems of Pantograph functional differential equation using computational intelligence algorithms. Appl. Soft Comput. 24, 806–821. https://doi.org/https://doi.org/10.1016/j.asoc.2014.08.055

Ramsey, E., Lu, Z., Suzuoki, Y., Rangoonwala, A., Werle, D., 2011. Monitoring Duration and Extent of Storm-Surge and Flooding in Western Coastal Louisiana Marshes With Envisat ASAR Data. IEEE J. Sel. Top. Appl. Earth Obs. Remote Sens. 4, 387–399. https://doi.org/10.1109/JSTARS.2010.2096201

Ritter, A., Mausam, Etzioni, O., Clark, S., 2012. Open domain event extraction from twitter. Proc. 18th ACM SIGKDD Int. Conf. Knowl. Discov. data Min. - KDD '12 1104. https://doi.org/10.1145/2339530.2339704

Roca, C.P., Helbing, D., 2011. Emergence of social cohesion in a model society of greedy, mobile individuals. Proc. Natl. Acad. Sci. 108, 11370–11374. https://doi.org/10.1073/pnas.1101044108

Rosser, J.F., Leibovici, D.G., Jackson, M.J., 2017. Rapid flood inundation mapping using social media, remote sensing and topographic data. Nat. Hazards 87, 103–120. https://doi.org/10.1007/s11069-017-2755-0

Saberi, M., Ashfaq, M., Hamedmoghadam, H., Hosseini, S.A., Gu, Z., Shafiei, S., Nair, D.J., Dixit, V., Gardner, L., Waller, S.T., González, M.C., 2019. A simple contagion process describes spreading of traffic jams in urban networks. arXiv Prepr. arXiv1906.00585 1–10.

Sadri, A.M., Hasan, S., Ukkusuri, S. V, Cebrian, M., 2020. Exploring network properties of social media interactions and activities during Hurricane Sandy. Transp. Res. Interdiscip. Perspect. 6, 100143. https://doi.org/https://doi.org/10.1016/j.trip.2020.100143

Sankaranarayanan, S., Prabhakar, M., Satish, S., Jain, P., Ramprasad, A., Krishnan, A., 2019. Flood prediction based on weather parameters using deep learning. J. Water Clim. Chang. https://doi.org/10.2166/wcc.2019.321

Scollon, C.K., 2013. Social Sensing for Urban Crisis Management : The Case of Singapore Haze, in: Social Informatics: 5th International Conference, SocInfo 2013. Springer International Publishing, Kyoto, Japan, pp. 478–491.

Sebastian, T., Lendering, K., Kothuis, B., Brand, N., Jonkman, B., van Gelder, P., Godfroij, M., Kolen, B., Comes, T., Lhermitte, S., 2017. Hurricane Harvey Report: A fact-finding effort in the direct aftermath of Hurricane Harvey in the Greater Houston Region.

Sekara, V., Stopczynski, A., Lehmann, S., 2016. Fundamental structures of dynamic social networks. Proc. Natl. Acad. Sci. 113, 9977–9982. https://doi.org/10.1073/pnas.1602803113

Serre, D., Barroca, B., Balsells, M., Becue, V., 2018. Contributing to urban resilience to floods with neighbourhood design: the case of Am Sandtorkai/Dalmannkai in Hamburg. J. Flood Risk Manag. 11, S69–S83. https://doi.org/10.1111/jfr3.12253

Shilcutt, K., Asgarian, R., 2017. The Deliberate Flooding of West Houston [WWW Document]. Houstonia. URL https://www.houstoniamag.com/articles/2017/10/16/barker-addicks-reservoirs-release-west-houston-memorial-energy-corridor-hurricane-harvey (accessed 7.6.19).

Shimizu, T., Yabe, T., Tsubouchi, K., 2020. Learning Fine Grained Place Embeddings with Spatial Hierarchy from Human Mobility Trajectories.

Song, C., Koren, T., Wang, P., Barabási, A.-L., 2010a. Modelling the scaling properties of human mobility. Nat. Phys. 6, 818–823. https://doi.org/10.1038/nphys1760

Song, C., Qu, Z., Blumm, N., Barabási, A.-L., 2010b. Limits of Predictability in Human Mobility. Science (80-.). 327, 1018 LP – 1021. https://doi.org/10.1126/science.1177170

Sutton, J., Gibson, C. Ben, Phillips, N.E., Spiro, E.S., League, C., Johnson, B., Fitzhugh, S.M., Butts, C.T., 2015. A cross-hazard analysis of terse message retransmission on Twitter. Proc. Natl. Acad. Sci. 112, 14793–14798. https://doi.org/10.1073/pnas.1508916112

Sutton, J., Spiro, E.S.., Fitzhugh, S.., Johnson, B.., Gibson, B.., Butts, C.T.., 2014. Terse message amplification in the Boston bombing response. ISCRAM 2014 Conf. Proc. - 11th Int. Conf. Inf. Syst. Cris. Response Manag. 612–621.

Tang, F., O'Neil, E., 2017. How the Barker and Addicks dams work, Houston Chronicle [WWW Document]. Houst. Chron. URL https://www.houstonchronicle.com/local/gray-matters/article/How-the-Barker-and-Addicks-dams-work-12171719.php (accessed 6.5.18).

Tang, K., Chen, S., Liu, Z., 2018. Citywide Spatial-Temporal Travel Time Estimation Using Big and Sparse Trajectories. IEEE Trans. Intell. Transp. Syst. 19, 4023–4034. https://doi.org/10.1109/TITS.2018.2803085

Tang, Y., Cheng, N., Wu, W., Wang, M., Dai, Y., Shen, X., 2019. Delay-Minimization Routing for Heterogeneous VANETs With Machine Learning Based Mobility Prediction. IEEE Trans. Veh. Technol. 68, 3967–3979. https://doi.org/10.1109/TVT.2019.2899627

Teng, X., Pei, S., Morone, F., Makse, H.A., 2016. Collective Influence of Multiple Spreaders Evaluated by Tracing Real Information Flow in Large-Scale Social Networks. Sci. Rep. 6, 1–11. https://doi.org/10.1038/srep36043

Troy, D.A., Carson, A., Vanderbeek, J., Hutton, A., 2008. Enhancing community-based disaster preparedness with information technology. Disasters. https://doi.org/10.1111/j.1467-7717.2007.01032.x

Tsakiri, K., Marsellos, A., Kapetanakis, S., 2018. Artificial Neural Network and Multiple Linear Regression for Flood Prediction in Mohawk River, New York. Water . https://doi.org/10.3390/w10091158

UNISDR, 2015. Sendai Framework for Disaster Risk Reduction 2015 - 2030. Third World Conf. Disaster Risk Reduction, Sendai, Japan, 14-18 March 2015. 1–25. https://doi.org/A/CONF.224/CRP.1

Valdez, L.D., Braunstein, L.A., Havlin, S., 2020. Epidemic spreading on modular networks: The fear to declare a pandemic. Phys. Rev. E 101, 32309. https://doi.org/10.1103/PhysRevE.101.032309

Vosoughi, S., Roy, D., Aral, S., 2018a. The spread of true and false news online. Science (80-.). 359, 1146–1151. https://doi.org/10.1126/science.aap9559

Vosoughi, S., Roy, D., Aral, S., 2018b. The spread of true and false news online. Science (80-.). 359, 1146–1151. https://doi.org/10.1126/science.aap9559

Waltman, L., Van Eck, N.J., 2013. A smart local moving algorithm for large-scale modularity-based community detection. Eur. Phys. J. B. https://doi.org/10.1140/epjb/e2013-40829-0

Wang, H., Li, Z., 2017. Region Representation Learning via Mobility Flow, in: Proceedings of the 2017 ACM on Conference on Information and Knowledge Management, CIKM '17. Association for Computing Machinery, New York, NY, USA, pp. 237–246. https://doi.org/10.1145/3132847.3133006

Wang, J., Sun, L., 2020. Dynamic holding control to avoid bus bunching: A multi-agent deep reinforcement learning framework. Transp. Res. Part C Emerg. Technol. 116, 102661. https://doi.org/https://doi.org/10.1016/j.trc.2020.102661

Wang, Q., 2015. Human Mobility Perturbation and Resilience in Natural Disasters.

Wang, Q., Phillips, N.E., Small, M.L., Sampson, R.J., 2018. Urban mobility and neighborhood isolation in America's 50 largest cities. Proc. Natl. Acad. Sci. U. S. A. 0, 201802537. https://doi.org/10.1073/pnas.1802537115

Wang, Q., Taylor, J.E., 2016. Patterns and Limitations of Urban Human Mobility Resilience under the Influence of Multiple Types of Natural Disaster. PLoS One 11, e0147299.

Wang, S., Mo, B., Zhao, J., 2020. Deep neural networks for choice analysis: Architecture design with alternative-specific utility functions. Transp. Res. Part C Emerg. Technol. 112, 234–251. https://doi.org/https://doi.org/10.1016/j.trc.2020.01.012

Wang, W., Yang, S., Gao, J., Hu, F., Zhao, W., Stanley, H.E., 2020. An Integrated Approach for Assessing the Impact of Large-Scale Future Floods on a Highway Transport System. Risk Anal. n/a. https://doi.org/10.1111/risa.13507

Wang, W., Yang, S., Stanley, H.E., Gao, J., 2019. Local floods induce large-scale abrupt failures of road networks. Nat. Commun. 10. https://doi.org/10.1038/s41467-019-10063-w

Wang, Y., Taylor, J.E., 2018. Urban Crisis Detection Technique: A Spatial and Data Driven Approach Based on Latent Dirichlet Allocation (LDA) Topic Modeling, in: Proceedings of the 2018 Construction Research Congress 2018. American Society of Civil Engineers (ASCE), New Orleans, Louisiana, USA., pp. 428–438.

Wang, Z., Ye, X., 2018. Social media analytics for natural disaster management. Int. J. Geogr. Inf. Sci. 32, 49–72. https://doi.org/10.1080/13658816.2017.1367003

Wax-Thibodeaus, E., Horton, A., Wang, A.B., 2017. Houston dam spills over for the first time in history, overwhelmed by Harvey rainfall - The Washington Post [WWW Document]. Washington Post. URL https://www.washingtonpost.com/news/post-nation/wp/2017/08/28/houston-releases-water-from-two-dams-in-attempt-to-prevent-uncontrolled-overflow/?noredirect=on&utm_term=.935bc622e4c0 (accessed 6.5.18).

Wei, L.-Y., Zheng, Y., Peng, W.-C., 2012. Constructing Popular Routes from Uncertain Trajectories, in: Proceedings of the 18th ACM SIGKDD International Conference on Knowledge Discovery and Data Mining, KDD '12. Association for Computing Machinery, New York, NY, USA, pp. 195–203. https://doi.org/10.1145/2339530.2339562

Weiler, A., Grossniklaus, M., Scholl, M.H., 2016. An evaluation of the run-time and task-based performance of event detection techniques for Twitter. Inf. Syst. 62, 207–219. https://doi.org/10.1016/j.is.2016.01.003

Weitz, J.S., Dushoff, J., 2015. Modeling Post-death Transmission of Ebola: Challenges for Inference and Opportunities for Control. Sci. Rep. 5, 8751. https://doi.org/10.1038/srep08751

Weng, J., Lee, B.-S., 2011. Event Detection in Twitter. Development 401–408. https://doi.org/10.1109/ICTAI.2007.23

Yan, X.Y., Wang, W.X., Gao, Z.Y., Lai, Y.C., 2017. Universal model of individual and population mobility on diverse spatial scales. Nat. Commun. 8, 1–9. https://doi.org/10.1038/s41467-017-01892-8

Yang, L., Kwan, M.-P., Pan, X., Wan, B., Zhou, S., 2017. Scalable space-time trajectory cube for path-finding: A study using big taxi trajectory data. Transp. Res. Part B Methodol. 101, 1–27. https://doi.org/https://doi.org/10.1016/j.trb.2017.03.010

Yang, Y., Zhang, C., Fan, C., Yao, W., Huang, R., Mostafavi, A., 2019. Exploring the emergence of influential users on social media during natural disasters. Int. J. Disaster Risk Reduct. 38, 101204. https://doi.org/10.1016/J.IJDRR.2019.101204

Youssef, A.M., Pradhan, B., Sefry, S.A., 2015. Flash flood susceptibility assessment in Jeddah city (Kingdom of Saudi Arabia) using bivariate and multivariate statistical models. Environ. Earth Sci. 75, 12. https://doi.org/10.1007/s12665-015-4830-8

Zhang, C., Fan, C., Yao, W., Hu, X., Mostafavi, A., 2019. Social media for intelligent public information and warning in disasters: An interdisciplinary review. Int. J. Inf. Manage. https://doi.org/10.1016/j.ijinfomgt.2019.04.004

Zhang, X., Chen, X., Chen, Y., Wang, S., Li, Z., Xia, J., 2015. Event detection and popularity prediction in microblogging. Neurocomputing 149, 1469–1480. https://doi.org/10.1016/j.neucom.2014.08.045

Zhang, Z., He, Q., Gao, J., Ni, M., 2018. A deep learning approach for detecting traffic accidents from social media data. Transp. Res. Part C Emerg. Technol. 86, 580–596. https://doi.org/10.1016/j.trc.2017.11.027

Zhao, Q., Mitra, P., 2007. Event Detection and Visualization for Social Text Streams. Event London 26–28.

Zhao, Z., Koutsopoulos, H.N., Zhao, J., 2018a. Detecting pattern changes in individual travel behavior: A Bayesian approach. Transp. Res. Part B Methodol. 112, 73–88. https://doi.org/https://doi.org/10.1016/j.trb.2018.03.017

Zhao, Z., Koutsopoulos, H.N., Zhao, J., 2018b. Individual mobility prediction using transit smart card data. Transp. Res. Part C Emerg. Technol. 89, 19–34. https://doi.org/https://doi.org/10.1016/j.trc.2018.01.022

Zhou, X., Chen, L., 2014. Event detection over twitter social media streams. VLDB J. 23, 381–400. https://doi.org/10.1007/s00778-013-0320-3

Zhou, Z., Dou, W., Jia, G., Hu, C., Xu, X., Wu, X., Pan, J., 2016. A method for real-time trajectory monitoring to improve taxi service using GPS big data. Inf. Manag. 53, 964–977. https://doi.org/https://doi.org/10.1016/j.im.2016.04.004

Zhu, L., Yu, F.R., Wang, Y., Ning, B., Tang, T., 2019. Big Data Analytics in Intelligent Transportation Systems: A Survey. IEEE Trans. Intell. Transp. Syst. 20, 383–398. https://doi.org/10.1109/TITS.2018.2815678

Ziebart, B.D., Maas, A., Bagnell, J.A., Dey, A.K., 2008. Maximum Entropy Inverse Reinforcement Learning, in: Proc. AAAI. pp. 1433–1438.

Zong, F., Tian, Y., He, Y., Tang, J., Lv, J., 2019. Trip destination prediction based on multi-day GPS data. Phys. A Stat. Mech. its Appl. 515, 258–269. https://doi.org/https://doi.org/10.1016/j.physa.2018.09.090

APPENDIX A

SUPPLEMENTARY INFORMATION FOR THE STUDY IN CHAPTER 3

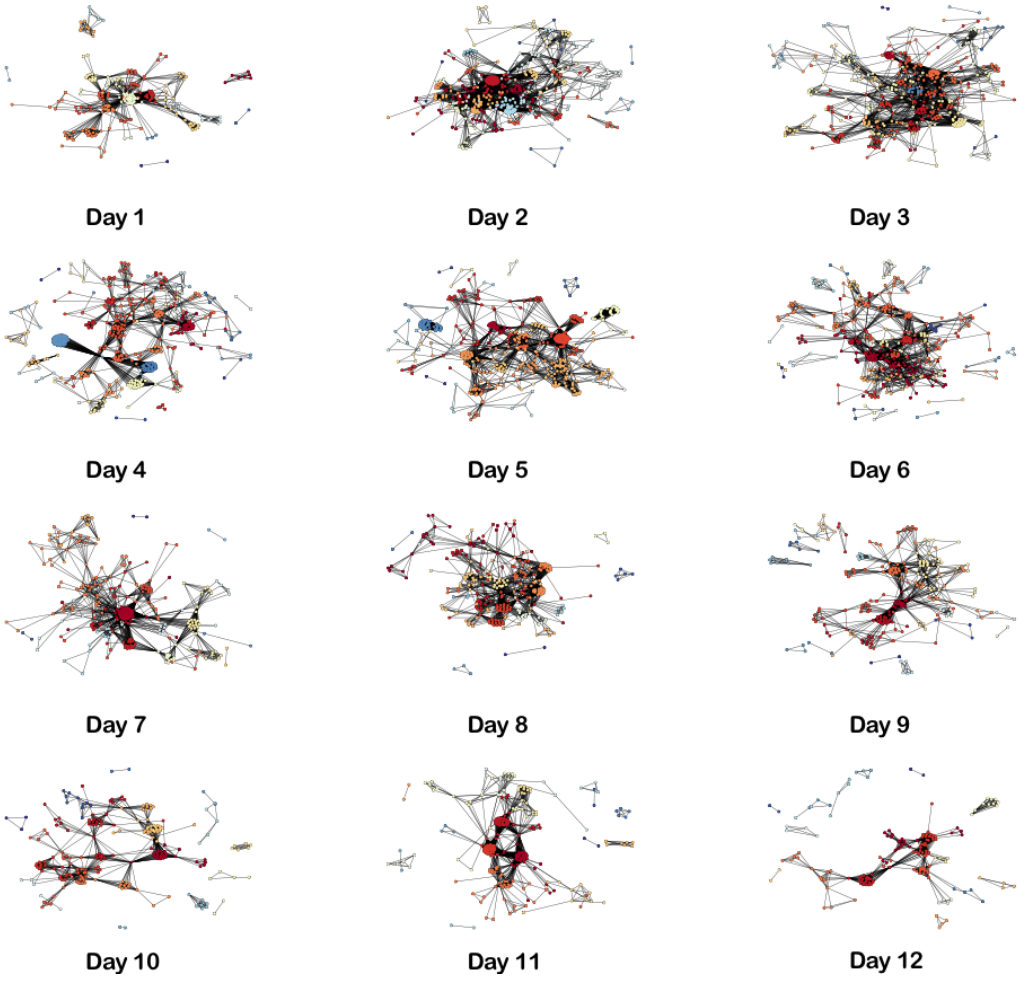

Figure 27 Daily online social networks during hurricane and flooding (different colors represent different activity foci).

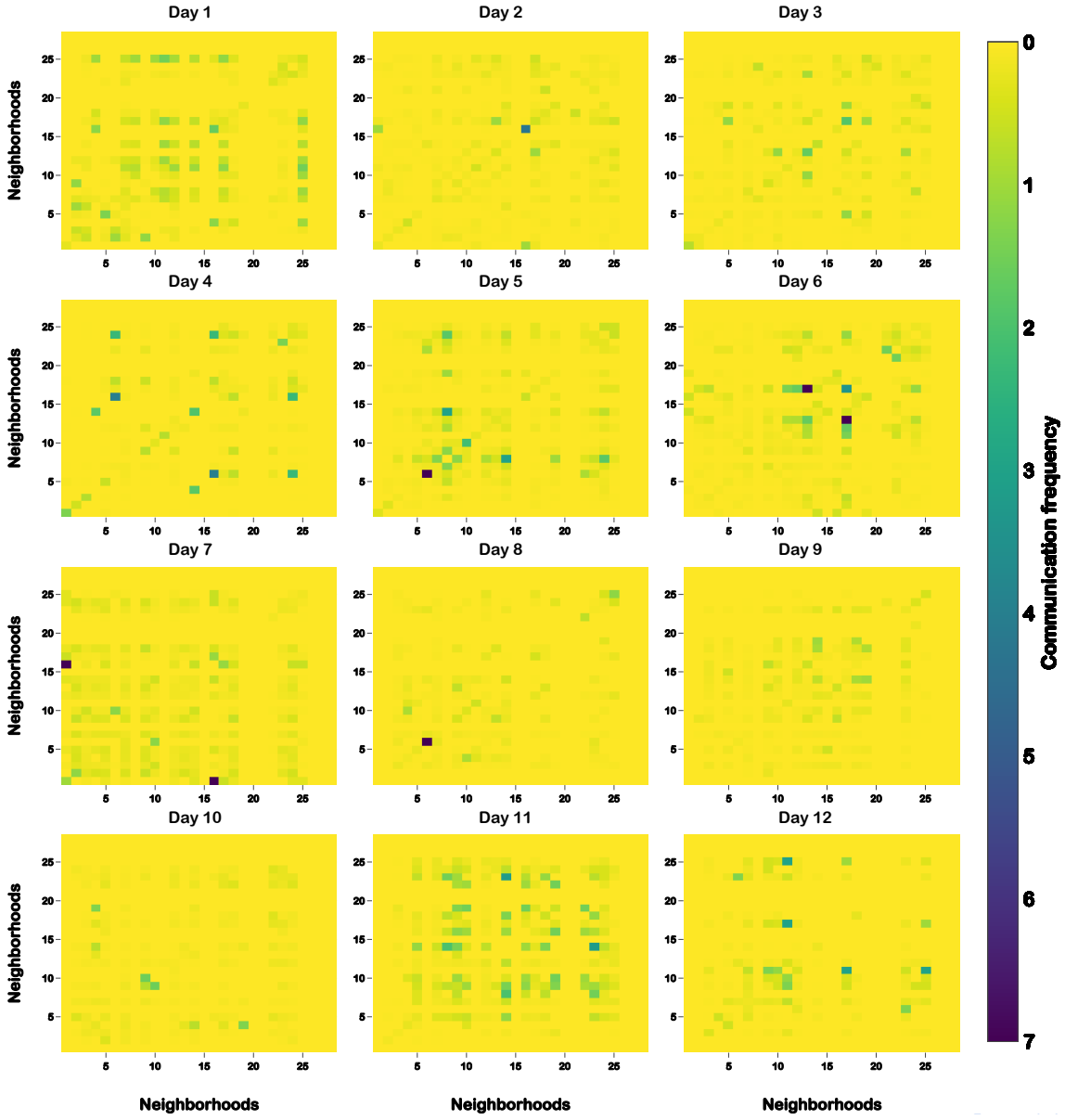

Figure 28 Daily communication frequency between neighborhoods.

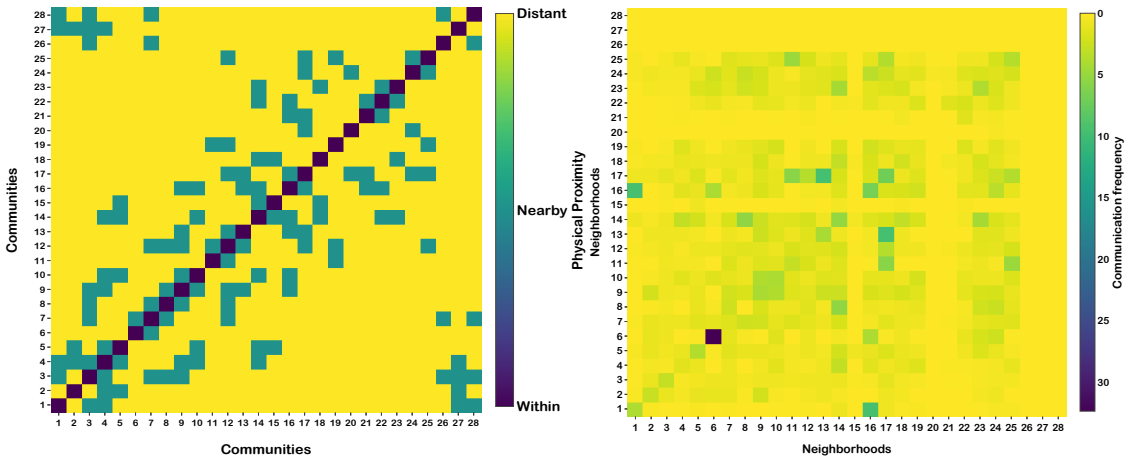

(a) **(b)**

Figure 29 The matrices of physical proximity (a), communication frequency (b) in pair-wise neighborhoods.

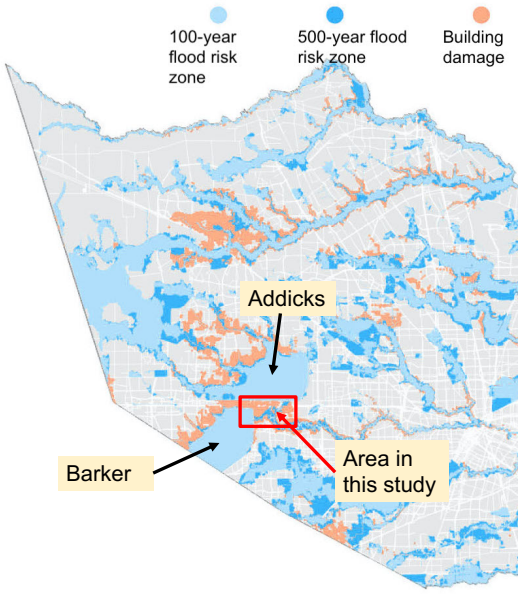

Figure 30 Flood risk zones and building damages for studied area (Bajaj et al., 2017).

Table 4 Primary neighborhood investigated in this study.

No.	# of Users	No.	# of Users
1	167	15	45
2	377	16	66
3	422	17	379
4	115	18	509
5	652	19	77
6	18	20	17
7	811	21	48
8	16	22	125
9	200	23	321
10	226	24	114
11	211	25	461
12	841	26	21
13	84	27	19
14	444	28	13

Table 5 Definitions and Examples of Thematic Content Codes.

Content Theme	Theme Definition and Post Example
Housing and properties	Refers to posts that contain information about damages of housing (e.g., roofs, walls, windows, and houses), loss of properties (e.g., car, bike, TV and table), and casualty
	"*Our home backyard fence is already under water on one side. Frontyard water is also creeping up (half mailbox under water).*"
Infrastructure status	Refers to posts that contain infrastructure facilities (e.g., network, power, water, sewage, communication facilities, grocery stores, gas, roads, airport, reservoir, bayou, dam, school, canal and heating)
	"*Has anyone found a way to get to I10 from south of the bayou? I am at Eldridge and Enclave.*"
Evacuation/Shelter	Refers to posts that contain information about pre-evacuations, mandatory evacuations, and sheltering information
	"*I just received an email from my apartment complex strongly urging us to evacuate.*"
Disaster descriptions	Refers to posts that contain descriptions of the disaster itself, such as locations or containment, and/or descriptions of the disaster scales, such as damaged areas and weather conditions.
	"*The weather is improving and they are expecting 1-2" of rain on our end of town today and tonight so fingers crossed the water levels will remain or possibly start to go down slowly.*"

Table 5 Continued.

Relief/Advisory information	Refers to posts that contain relief information, such as phone numbers, websites, locations, and service of help facility sites, insurance, law and preparedness, response and recovery tips
	"*The Harris County Office of Homeland Security & Emergency Management invites residents affected by Hurricane Harvey to a recovery fair this weekend*."
Request for help	Refers to posts that request for neighbors' on-site help
	"*Does anyone have a canoe/boat/float of some sort to use tomorrow morning to get to our homes on Ivy Wall and Silvergate? XXX_1 and XXX_2 were one of the many wonderful men in our neighborhood helping with rescuing many of our neighbors. XXX_1 had 3 blowup kayaks that are gone now after rescue efforts. If anyone can help us we would be so grateful. Please call or text XXX.XXX.XXXX or XXX.XXX.XXXX.* *Thank you to the XXX's and all of our amazing neighbors who have helped everyone during this time of need. XXX*"
Volunteer	Refers to posts that contain information about volunteering, such as websites, phone numbers or locations of volunteer facilities, donation or providing individual help to neighbors
	"*For my amazing neighbors affected by the flood. Please let me know if you need some baby food. We just outgrew this stage. God bless*"
Off Topic	Refers to posts that are not within the scope of disaster-related topics

Note: personal information such as name and phone numbers appearing in the examples are replaced with "XXX" or deleted.

Table 6 Basic information about social networks and activity foci detection.

Days	# of nodes	# of edges	Modularity	# of activity foci
1	230	1704	0.590	15
2	440	4428	0.685	21
3	427	2790	0.730	21
4	440	3711	0.799	32
5	479	4927	0.742	23
6	367	2085	0.630	25
7	295	3354	0.490	14
8	282	1799	0.730	16
9	251	1299	0.679	25
10	224	1161	0.777	20
11	254	2715	0.573	19
12	161	945	0.733	19

Table 7 Number of nodes (N) and edges (E) in each activity foci during the hurricane and flooding.

Activity foci	Day 1		Day 2		Day 3		Day 4		Day 5		Day 6	
	N	E	N	E	N	E	N	E	N	E	N	E
1	44	621	61	1659	66	314	65	325	105	651	81	619
2	41	229	58	283	58	536	53	1378	84	2051	58	199
3	39	143	44	573	48	337	37	105	65	337	51	228
4	24	92	37	162	48	176	34	376	36	630	34	132
5	19	91	32	124	46	235	33	157	35	121	25	256
6	16	120	31	147	34	209	27	351	30	294	24	97
7	12	38	30	92	33	123	27	242	23	181	22	82
8	9	36	25	95	22	77	25	111	22	121	14	43
9	7	21	19	82	18	153	25	102	14	91	7	21
10	5	10	19	105	11	55	18	111	11	31	7	16
11	5	7	14	79	11	41	12	48	10	19	6	15
12	3	3	12	42	6	15	10	25	8	13	4	6
13	2	1	12	35	4	6	8	28	5	10	4	6
14	2	1	11	28	4	6	8	18	5	6	4	6
15	2	1	6	15	4	6	7	16	4	6	3	3
16			5	10	4	6	6	9	4	6	3	3
17			4	6	2	1	4	6	3	3	3	3
18			3	3	2	1	4	6	3	3	3	3
19			3	3	2	1	4	6	3	3	2	1
20			2	1	2	1	4	6	3	3	2	1
21			2	1	2	1	4	6	2	1	2	1
22							3	3	2	1	2	1
23							3	3	2	1	2	1
24							3	3			2	1
25							2	1			2	1
26							2	1				
27							2	1				
28							2	1				
29							2	1				
30							2	1				
31							2	1				
32							2	1				

Table 7 Continued.

Activity foci	Day 7		Day 8		Day 9		Day 10		Day 11		Day 12	
	N	**E**	**N**	**E**	**N**	**E**	**N**	**E**	**N**	**E**	**N**	**E**
1	68	2020	55	407	37	165	37	164	42	861	29	253
2	57	172	43	465	31	225	28	230	40	571	24	276
3	36	225	33	95	29	90	27	124	40	525	22	90
4	33	225	30	102	23	196	23	104	37	152	18	109
5	29	129	25	102	21	54	23	74	24	75	15	42
6	23	57	25	94	18	153	15	105	18	98	10	45
7	15	105	21	117	18	51	13	58	10	20	4	6
8	14	51	17	45	8	28	10	25	7	21	4	6
9	10	21	10	45	7	21	9	36	7	10	4	6
10	2	1	6	15	7	21	8	28	5	10	4	6
11	2	1	5	10	6	15	6	15	5	10	4	6
12	2	1	3	3	5	10	5	6	4	6	4	6
13	2	1	3	3	5	10	4	4	3	3	4	4
14	2	1	2	1	4	6	3	3	2	1	4	4
~~15~~			2	1	4	6	3	2	2	1	3	3
~~16~~			2	1	4	4	2	1	2	1	2	1
~~17~~					3	3	2	1	2	1	2	1
~~18~~					3	3	2	1	2	1	2	1
~~19~~					3	3	2	1	2	1	2	1
~~20~~					3	3	2	1				
~~21~~					3	3						
~~22~~					3	3						
~~23~~					2	1						
~~24~~					2	1						
~~25~~					2	1						

Table 8 The medians of the weights of social ties in OSNs in each day.

Day	**1**	**2**	**3**	**4**	**5**	**6**	**7**	**8**	**9**	**10**	**11**	**12**
Median weight	2	1	1	1	1	1	1	1	1	1	1	1

Table 9 Number of active users and communications each day before and during the disaster.

Days	-6	-5	-4	-3	-2	-1	0
Number of active users	38	10	29	61	29	77	35
Number of communications	150	13	119	358	101	980	137

Table 9 Continued.

Days	1	2	3	4	5	6	7	8	9	10	11	12
Number of active users	230	440	427	440	479	367	295	282	251	224	254	161
Number of communications	1704	4428	2790	3711	4927	2085	3354	1799	1299	1161	2715	945